

THE UNIVERSITY OF MANITOBA

DIFFRACTION OF PLANE HORIZONTALLY POLARIZED SHEAR (SH)
WAVES IN HALF-SPACES

by

KIN-CHIU WONG

A Thesis

SUBMITTED TO THE FACULTY OF GRADUATE STUDIES
IN PARTIAL FULFILLMENT OF THE REQUIREMENTS FOR THE DEGREE OF
MASTER OF SCIENCE IN CIVIL ENGINEERING

WINNIPEG, MANITOBA

May, 1982

DIFFRACTION OF PLANE HORIZONTALLY POLARIZED SHEAR (SH)
WAVES IN HALF-SPACES

BY

KIN-CHIU WONG

A thesis submitted to the Faculty of Graduate Studies of
the University of Manitoba in partial fulfillment of the requirements
of the degree of

MASTER OF SCIENCE

© 1982

Permission has been granted to the LIBRARY OF THE UNIVERSITY OF MANITOBA to lend or sell copies of this thesis, to the NATIONAL LIBRARY OF CANADA to microfilm this thesis and to lend or sell copies of the film, and UNIVERSITY MICROFILMS to publish an abstract of this thesis.

The author reserves other publication rights, and neither the thesis nor extensive extracts from it may be printed or otherwise reproduced without the author's written permission.

ABSTRACT

The problem of scattering of SH-waves by surface, near surface or embedded inhomogeneities in a semi-infinite medium is studied in this thesis. A combined numerical and analytical technique is used to solve the problem. One of the advantages of the combined technique is that it is applicable to arbitrary shapes of scatterers and multiple scatterers. The results compare well with other available analytical and numerical results.

ACKNOWLEDGEMENTS

The author wishes to express his most sincere appreciation to his advisor, Dr. A.H. Shah, for his extensive guidance, encouragement and assistance throughout this thesis work. Without all the help he offered, the thesis work would have not been possible.

Special appreciation goes to Dr. D.W. Trim and Dr. E.Z. Lajtai for their careful reading of the thesis and their invaluable suggestions.

The author wishes to thank Mrs. Valerie Ring for her excellent work in typing the thesis.

Finally, the author is deeply indebted to his mother, Y.Y. Lai, who has been a constant source of support and encouragement.

TABLE OF CONTENTS

	PAGE
ABSTRACT	i
ACKNOWLEDGEMENTS	ii
TABLE OF CONTENTS	iii
LIST OF FIGURES	v
LIST OF TABLES	vii
ABBREVIATIONS	viii
CHAPTER	
1 INTRODUCTION	1
1.1 PREVIOUS WORKS	1
1.2 PRESENT WORKS	3
2 SCATTERING OF SH-WAVES BY SURFACE OR NEAR SURFACE DEFECTS	5
2.1 METHOD OF ANALYSIS	6
2.1.1 Numerical-Analytical Technique	6
(i) Interior Region	6
(ii) Exterior Region	8
(a) Integral Equation Method	9
(b) Wave Function Expansion Method	11
2.1.2 Matched-Asymptotic Expansion	13
2.2 NUMERICAL RESULTS AND DISCUSSION	14
2.2.1 Surface Canyons	14
(i) Semi-Circular Canyon	14
(ii) Triangular Canyon	15
(iii) Multiple Scattering	15
2.2.2 Edge Cracks	17
(i) Within Isotropic Material	17
(ii) Within Anisotropic Material	18
3 SCATTERING OF SH-WAVES BY EMBEDDED DEFECTS	21
3.1 METHOD OF ANALYSIS	21
3.1.1 Interior Region	21
3.1.2 Exterior Region	22
3.2 NUMERICAL RESULTS AND DISCUSSION	25
4 SUMMARY AND CONCLUSIONS	29
BIBLIOGRAPHY	31
APPENDICES	33

	PAGE
APPENDIX A RESULTS OF THE ANALYSIS OF MATCHED-ASYMPTOTIC EXPANSIONS (up to $O(\varepsilon^4)$)	34
APPENDIX B TABLES	38
APPENDIX C FIGURES	41
APPENDIX D LISTINGS OF COMPUTER PROGRAMS	76

LIST OF FIGURES

FIGURE	PAGE
1. Geometry of a Surface Canyon Showing the Inner and Outer Regions	42
2. Geometry of an Edge Crack Showing the Inner and Outer Regions	43
3. Geometry of an Embedded Circular Canyon or Embedded Crack Showing the Inner and Outer Regions	44
4. Crack-tip Elements	45
5. Finite Element Subdivision of the Inner Region	46
6. Comparison for Real Part of $w^{(s)}$ ($\eta = 0.1/\pi$)	47
7. Comparison for Imaginary Part of $w^{(s)}$ ($\eta = 0.1/\pi$)	48
8. Displacement Amplitude at the Surface of a Triangular Canyon with 45° Slopes, With and Without Buried Cavity. ($\eta = 0.25$ and $\gamma = 90^\circ$)	49
9. Displacement Amplitude at the Surface of a Triangular Canyon with 45° Slopes, With and Without Buried Cavity. ($\eta = 0.25$ and $\gamma = 45^\circ$)	50
10. Displacement Amplitude at the Surface of a Triangular Canyon with 45° Slopes, With and Without Buried Cavity. ($\eta = 0.25$ and $\gamma = 0^\circ$)	51
11. Geometry of a Triangular Canyon With Buried Circular Cavity	52
12. Displacement Amplitude at the Surface of a Triangular Canyon With Buried Cavity. ($\eta = 0.25$)	53
13. COD at the Base of a Normal Crack	54
14. COD Along a Normal Crack for Grazing Incidence	55
15. COD Along a Normal Crack for 45° Incidence	56
16. COD Along a 45° Canted Crack for Grazing Incidence	57
17. COD Along a Normal Crack for Different Incidence Angles	58
18. COD Along a Normal Crack for Different Incidence Angles	59

FIGURE	PAGE
19. COD Along a 45° Canted Crack for Different Incidence Angles	60
20. COD Along a 45° Canted Crack for different incidence Angles	61
21. Magnitude of the Scattered Field Due to a Normal Crack Along the Free Surface	62
22. Comparison of the Far Field Scattered Displacement Amplitudes Obtained by MAE and Numerical Techniques	63
23. Far Field Scattered Displacement Amplitude Due to a 45° Canted Crack	64
24. Phase of the Far Field Scattered Displacement Due to a Normal Crack	65
25. Phase of the Far Field Scattered Displacement Due to a 45° Crack	66
26. Scattered Displacement Amplitudes on the Free Surface Due to a Buried Circular Cavity and a Vertical Crack	67
27. Scattered Displacement Amplitudes on the Free Surface Due to a Vertical Crack Embedded at Different Depths	68
28. Scattered Displacement Amplitudes Due to Buried Cracks of Different Orientations	69
29. Scattered Displacement Amplitudes Due to Buried Cracks of Different Orientations and for Different Angles of Incidence	70
30. Comparison of the Back Scattered Displacement Amplitudes Due to a Buried Crack and a Circular Cavity, and an Edge Crack	71
31. Comparison of the Back Scattered Displacement Amplitudes Due to a Buried Vertical Crack and a Vertical Edge Crack	72
32. Scattered Displacement Amplitudes on $y = 0$ for a Buried Circular Cavity for Various Angles of Incidence	73
33. Scattered Displacement Amplitudes on $y = 0$ for Different Wave Numbers Due to a Buried Circular Cavity	74
34. Displacement of the Cavity Wall.	75

LIST OF TABLES

TABLE	PAGE
1 Comparison of Results with Analytical Solution, Semi-Cylindrical Canyon of Radius a. $(\gamma = 30^\circ)$	39
2 Scattered Displacement Amplitudes at the Surface of the Half-space Due to a Buried Circular Cavity. Comparison of MAE and FEM. $(\gamma = 0^\circ)$	40

ABBREVIATIONS

A_n, B_n, E_n	constants
D_n, F_n, G_n	
a	length of a scatterer
B, B_1	boundary of a region
b	the radius of semi-circle B
COD	Crack Opening Displacement
CST	Constant Strain Triangle
c_2	the shear wave speed in the (parent) homogeneous isotropic medium
FEM	Finite Element Method
H_n	Hankel functions of the first kind of order n
$H_o^{(2)}$	Hankel functions of the second kind of order zero
$H_n^{(2)}$	Hankel functions of the second kind of order n
h	depth from the free surface
k_1, k_2	wave number of region R_1 and R_2 , respectively
$L_j(x, y)$	shape functions
ℓ	the maximum length of the element
MAE	Matched Asymptotic Expansions
N_I	number of nodes in R_2 , excluding nodes on boundary B
N_B	number of nodes on boundary B
n	the outward normal to the contours B_1 and B_2

n_o	the outward normal to the contour c
R_1	the unbounded interior region
R_2	the unbounded exterior region
R_c	the region of the plane outside contour c
r_1	the distance of point $Q(x_o, y_o)$ to $P(x, y)$
r_2	the distance from P to the image point of Q with coordinate $(x_o, -y_o)$
SH	Horizontally polarized Shear
s	the arc length along c
w_j	the nodal values
$w^{(1)}, w^{(2)}$	the displacement in z -direction in Region R_1 and R_2 , respectively
$w^{(o)}$	the total incident field near the scatterer
$w^{(i)}$	the excitation of the half-space
$w^{(r)}$	the reflected wave
$w^{(s)}$	the scattered field
β	the angle of inclination of crack from the horizontal
γ	the angle of incident of plane SH-wave
η	the ratio of radius of the canyon to one-half wave-length of incident waves
$\bar{\gamma}$	the Euler's constant
λ	the incident wave-length
$\mu^{(1)}, \mu^{(2)}$	the shear modulus of the material occupying region R_1 and R_2 , respectively

$\rho^{(1)}$ $\rho^{(2)}$ the mass density of the material occupying region R_1 and R_2 , respectively

ω the circular frequency

CHAPTER 1

INTRODUCTION

In the past ten years, the subject of two-dimensional scattering of incident SH-waves by inhomogeneities has received considerable attention of researchers in earthquake engineering. However, most of these studies have dealt with the case of an infinite medium. Only recently has the problem of scattering in a semi-infinite medium been given adequate attention. The presence of the free boundary of the half-space influences the scattered field in a significant manner. Previous works on the scattering of plane SH-wave in half-space will be summarized in the next section.

1.1 PREVIOUS WORKS

In the study of the effects of surface structure interaction, analytical solutions for interaction of a shear wall with the soil for incident SH-waves have been obtained [1,2]. Luco [1] obtained the closed-form solution for the dynamic interaction of a shear wall with an isotropic, homogeneous and elastic half-space for vertically incident SH-waves. Later, Trifunac [2] generalized Luco's results to arbitrary incidence of SH-waves. The studies showed that waves scattered from a rigid foundation contribute significantly to the surface ground motion near and away from the shear wall.

In the study of the effects of surface topography on ground motion, analytical solutions for semi-cylindrical [3], and semi-elliptical canyons [4] under incident SH waves have been obtained by Trifunac. He

solved the two problems by the method of separation of variables. The solutions were in the form of infinite series whose coefficients were determined directly from the boundary conditions on the surfaces of the canyons. It is indicated that the nature of ground motion depends on two principle parameters: (1) the angle of incidence, and (2) the ratio of the canyons width to the wave length of incident SH-waves. The solutions of the two problems provide a check on the validity of other analytical or numerical approaches. Using the method of asymptotic expansions, expressions for the diffracted field of the surface irregularity of arbitrary slope have been obtained by Sabin and Willis [5]. The expressions are restricted to low frequency. Another approach uses numerical solutions of integral equations to describe the effect of topography on ground motion under low frequency incident waves [6]. It assumes periodicity of surface shape and uses discretized integral equations to describe the movement in the neighbourhood of topographic irregularities with small slopes. The SH-wave diffraction problem has also been formulated in terms of Fredholm integral equations of second kind [7], and of first kind [8,9] to study the topographic effect. Wong and Jennings [7] formulated the problem in terms of singular integral equations to solve the scattering and diffraction of SH-waves by canyons of arbitrarily shaped cross-section. Sánchez-Sesma et al. [8,9] formulated the same problem in terms of a system of Fredholm integral equations of the first kind with the integration paths defined outside the boundary in order to get regular kernels.

Diffraction of SH-waves by an edge crack in a semi-infinite, homogeneous elastic medium has become a subject of considerable interest in

the area of non-destructive testing. Analytical results [10] were obtained when the crack was oriented at an arbitrary angle to the free surface. The analysis was confined to the case of long wave-lengths. A numerical technique, [11], based on an integral equations formulation has been applied to study the case of normal cracks in a homogeneous half-space for both long and short wave-lengths.

In recent years, several studies dealing with scattering of plane SH-waves by embedded cavities in a semi-infinite elastic medium have appeared in the literature [12,13]. Diffraction of SH-waves by an elliptic elastic cylindrical inclusion has been solved using the method of matched asymptotic expansions [12]. The near and far field distributions of the displacement were reported. The solution for a buried circular cavity in a half space has also been obtained in terms of integral equations [13].

Each technique mentioned in the review is restricted to solve only one type of scatterer after formulation, and the elastic material surrounding the scatterer is limited to isotropic and homogeneous materials. For multiple scatterer these techniques will be very difficult, if not impossible, to apply. It is the aim of this thesis to present a single technique which will investigate scattering of plane SH-waves by inhomogeneities which are either near the surface or embedded in it.

1.2 PRESENT WORK

Scattering of elastic waves by surface canyons, edge cracks, embedded cavities or cracks is investigated in this thesis (see Figures 1, 2 and 3). Solutions to these problems are obtained by a combined numerical and analytical technique. In this technique, media inhomogene-

ties are enclosed inside a contour. The interior region so defined is bounded and is represented by finite elements. For the exterior region, two approaches are considered:

1) In the first approach, wave function expansion is used in the region outside the contour. Continuity conditions for the field and its derivative are imposed at a finite number of points on the contour.

2) In the second approach, an integral equation is formulated in the exterior region using half-space Green's function. The field on the contour may be interpreted as a boundary condition for the interior region and as an equivalent source distribution for the integral equation. Thus, the integral equation is taken as a constraint.

This thesis will be separated into two parts. Scattering of SH-waves by surface or near surface inhomogeneities will be discussed in Chapter 2, while scattering by embedded inhomogeneities will be investigated in Chapter 3. The final chapter summarizes and concludes the thesis.

CHAPTER 2

SCATTERING OF SH-WAVES BY SURFACE OR NEAR SURFACE DEFECTS

Scattering of horizontally polarized shear (SH) waves by arbitrarily shaped canyons and cracks, located near the surface, is studied in this chapter, using a combined finite element and analytical technique. Attention is focused here in the long to medium wave lengths.

Two approaches of the proposed techniques, namely, the combined finite element and integral equation, and, the combined finite element and wave function expansions, are used in solving the scattering problems of arbitrarily shaped canyons. Surrounding materials are assumed to be homogeneous and isotropic. To gauge the accuracy and the applicability of these two methods, numerical results are compared with the analytical solution [3] for the semi-circular canyon. Then the results for triangular canyon are presented in comparison with other available numerical solutions [8]. In order to demonstrate the versatility of the methods, a problem of multiple scattering is studied. The effect of a near surface buried circular tunnel on the surface displacements at a triangular canyon is studied for different angles of incidence. It is found that the result obtained by the wave function expansion method has better agreement than the integral equation method with the solutions given in [3,8].

The problem of scattering by an edge crack of length ℓ at different orientations relative to the free surface of the half-space is studied next using the wave function expansion method. Owing to the stress singularity at the crack tip, six-node isoparametric triangular quarter point

elements [14,15], (see Figure 4) were used for the region around the crack tip. Then seven-node isoparametric quadrilateral transitional elements [16] were used between the crack tip elements and the constant strain triangular elements, which were used in the rest of the region R_2 . A typical finite element mesh is shown in Figure 5. Numerical results are presented for crack opening displacements and scattered fields on the surface when the medium is homogeneous, or when the crack is located in an insert with different material properties. In order to ascertain the accuracy, comparison has been made between the results of this numerical technique and the method of matched asymptotic expansions (MAE), which is valid when the wave-length is long compared to the dimensions of the scatterer. Application of MAE to solve scattering problems in bounded and unbounded media has been demonstrated in some published papers [10,12,13].

2.1 METHOD OF ANALYSIS

2.1.1 Numerical-Analytical Technique

Figures 1 and 2 show a portion of the xy -plane and the r,θ -coordinates. A bounded region R_2 is contained within the boundary $B + B_1$, and the unbounded exterior region is denoted by R_1 . The surface defects and the non-homogeneity are contained within R_2 . In the following formulation region R_2 is assumed to consist of isotropic material.

i) Interior Region

For the propagation of harmonic polarized SH-waves in region R_2 , the displacement in the z -direction, $w^{(2)}$, satisfies the Helmholtz equation

$$\frac{\partial^2 w^{(2)}}{\partial x^2} + \frac{\partial^2 w^{(2)}}{\partial y^2} + k^2 w^{(2)} = 0 , \dots \dots \dots \quad (2.1)$$

where $k^2 = \frac{\rho^{(2)} \omega^2}{\mu^{(2)}}$, $\rho^{(2)}$ and $\mu^{(2)}$ are the mass density and shear modulus of the region R_2 and ω the circular frequency of the materials in the region R_2 .

The boundary conditions on $w^{(2)}$ are

$$\frac{\partial w^{(2)}}{\partial y} = 0 , \quad y = 0$$

$$\frac{\partial w^{(2)}}{\partial n} = 0 , \quad r \in B_1 , B_2 , \dots \dots \dots \quad (2.2)$$

where n is the outward normal to the contour B_1 and B_2 (see Figures 1 and 2), B_2 has been taken to be the surface of a canyon or a crack.

The variational formulation for the solution $w^{(2)}$ in the region R_2 is the minimization of the quadratic functional.

$$F = \int_{R_2} (\nabla w^{(2)} \cdot \bar{\nabla w}^{(2)} - k^2 w^{(2)} \bar{w}^{(2)}) dx dy , \dots \dots \dots \quad (2.3)$$

where $\nabla w^{(2)} \cdot \bar{\nabla w}^{(2)} = |\nabla w^{(2)}|^2$. The overbar denotes complex conjugate.

R_2 is sub-divided into finite elements having $N_I + N_B$ nodes, where N_I and N_B are the numbers of interior nodes and nodes on B , respectively. The displacement field within each element is represented in terms of shape functions $L_j(x,y)$ and nodal values w_j as

$$w^{(2)}(x,y) = \sum L_j w_j . \dots \dots \dots \quad (2.4)$$

The subscript j refers to the node position, some internal (subscripted I) and some on the boundary B (subscripted B). Then the Equation (2.4) may be written as

$$w^{(2)}(x,y) = \{L_I\}^T \{w_I\} + \{L_B\}^T \{w_B\} , \dots \dots \dots \quad (2.5)$$

where $\{L\}$, $\{W\}$ are column vectors and superscript T represents transpose.

Defining the matrices S_{II} , S_{IB} , S_{BI} and S_{BB} as

$$S_{MN} = \int_{R_2} [\{\nabla L_M\}^T \{\nabla L_N\} - k^2 \{L_M\}^T \{L_N\}] dx dy , \quad \dots \dots \dots \quad (2.6)$$

the functional F of (2.3) can be rewritten as

$$\begin{aligned} F = & \{\bar{W}_I\}^T [S_{II}] \{W_I\} + \{\bar{W}_I\}^T [S_{IB}] \{W_B\} \\ & + \{\bar{W}_B\}^T [S_{BI}] \{W_I\} + \{\bar{W}_B\}^T [S_{BB}] \{W_B\} . \quad \dots \dots \dots \end{aligned} \quad (2.7)$$

Taking the boundary conditions $\{W_B\}$ as known (Dirichlet boundary condition), but yet unspecified, and taking the variation $\frac{\partial F}{\partial \bar{W}_I} = 0$, it is found that W_I is related to W_B by the equation

$$[S_{II}] \{W_I\} = - [S_{IB}] \{W_B\} . \quad \dots \dots \dots \quad (2.8)$$

ii) Exterior Region

In region R_1 , the displacement $w^{(1)}$ in the z -direction is composed of two parts

$$w^{(1)} = w^{(o)} + w^{(s)} , \quad \dots \dots \dots \quad (2.9)$$

where $w^{(o)}$ is the free-field displacement and $w^{(s)}$ the contribution of the scattered waves. The excitation of the half-space, $w^{(i)}$, is assumed to consist of an infinite train of plane SH-waves with frequency ω given by

$$w^{(i)} = \exp[i\omega t - ik_1 \sin \gamma x + ik_1 \cos \gamma y] , \quad \dots \dots \dots \quad (2.10)$$

where γ is the angle of incidence (shown in Figures 1 and 2), $k_1^2 = \rho^{(1)}$ $\omega^2/\mu^{(1)}$, $\rho^{(1)}$ and $\mu^{(1)}$ are the mass density and shear modulus of the material occupying R_1 . R_1 is assumed homogeneous and linearly elastic. To

satisfy the free boundary conditions at $y = 0$, a reflected wave must be given by

$$w^{(r)} = \exp[i\omega t - ik_1 \sin \gamma x - ik_1 \cos \gamma y] . \dots \dots \dots \quad (2.11)$$

The free-field solution $w^{(o)} = w^{(i)} + w^{(r)}$ may be written as

$$w^{(o)} = 2\cos(k_1 \cos \gamma y) \exp[i\omega t - ik_1 \sin \gamma x] . \dots \dots \dots \quad (2.12)$$

The total field $w^{(1)}$ and the scattered field $w^{(s)}$ satisfy the Helmholtz equation in R_1 ,

$$\frac{\partial^2 w^{(s)}}{\partial x^2} + \frac{\partial^2 w^{(s)}}{\partial y^2} + k_1^2 w^{(s)} = 0 . \dots \dots \dots \quad (2.13)$$

(a) Integral Euation Method

A contour c is introduced as shown in Figure 1. The region of the plane outside c is called R_c and it is stipulated that the region of overlap between R_c and R_2 be homogeneous and isotropic having material properties of R_1 . The overlap region precludes evaluation of the integral equation at a source point, thus avoiding the Green's function singularities.

In the region R_c the Helmholtz Equation (2.13) holds. The scattered solution satisfying the stress-free boundary condition at $y = 0$ can be written in integral form [8] as

$$w^{(s)}(P) = \int_c [w^{(s)}(Q) \frac{\partial G}{\partial n_O}(P, Q) - G(P, Q) \frac{\partial w^{(s)}}{\partial n_O}(Q)] ds , \quad (2.14)$$

where

$$G(P, Q) = \frac{i}{4} [H_0^{(2)}(k_1 r_1) + H_0^{(2)}(k_1 r_2)] \dots \dots \dots \quad (2.15)$$

$i = \sqrt{-1}$, $H_0^{(2)}$ is Hankel function of the second kind and order zero, $r_1 = [(x - x_o)^2 + (y - y_o)^2]^{1/2}$ is the distance point from $Q(x_o, y_o)$ to $P(x, y)$, $r_2 = [(x - x_o)^2 + (y + y_o)^2]^{1/2}$ is the distance from P to the image point of Q with coordinate $(x_o, -y_o)$, s is arc length along c , and n_o is the outward normal to the contour c . In equation (2.15) Hankel function represents cylindrical SH-waves propagating outwards to infinity with speed ω/k_1 and satisfies Sommerfeld's radiation condition.

Equation (2.14) can also be written in terms of the total field as

$$w^{(s)}(P) = \int_c [w^{(1)}(Q) \frac{\partial G}{\partial n_o}(P, Q) - G(P, Q) \frac{\partial w^{(1)}}{\partial n_o}(Q)] ds . \quad (2.16)$$

Since $w^{(1)} = w^{(2)}$ on c , field quantities on c in Equation (2.16) may be represented by the node functions and displacements given by Equation (2.5) as

$$\begin{aligned} w^{(s)}(P) &= \left[\int_c (\{L_I\}^T \frac{\partial G}{\partial n_o} - G \{\frac{\partial L_I}{\partial n_o}\}^T) ds \right] \{W_I\} \\ &+ \left[\int_c (\{L_B\}^T \frac{\partial G}{\partial n_o} - G \{\frac{\partial L_B}{\partial n_o}\}^T) ds \right] \{W_B\} . \quad \dots \dots \quad (2.17) \end{aligned}$$

Evaluating the integrals at all N_B node points on the boundary B , and collecting terms, the constraint equation can be written in terms of scattered field in the matrix form as

$$\{W_B^{(s)}\} = [M]\{W_I\} , \quad \dots \dots \quad (2.18)$$

or in terms of total field

$$\{W_B^{(1)}\} = [M]\{W_I\} + \{W^{(o)}\} , \quad \dots \dots \quad (2.19)$$

where $\{W^{(o)}\}$ is the value of $w^{(o)}$ at the node points on B . Equations

(2.8) and (2.19) can be solved to yield

$$\begin{aligned} & \left[[S_{II}] + [S_{IB}][M] \right] \{W_I\} = - [S_{IB}] \{W^{(o)}\} \\ & \{W_I\} = - \left[[S_{II}] + [S_{IB}][M] \right]^{-1} [S_{IB}] \{W^{(o)}\} , \end{aligned} \quad (2.20)$$

Substituting Equation (2.20) into Equation (2.19), $\{W_B\}$ can be evaluated, and substituting these, in turn in Equation (2.17) displacement at any exterior point can be evaluated.

It may be mentioned here that matrices S_{II} and S_{IB} are real while M is complex. The contour c can be arbitrary. Here it has been chosen circular for convenience.

b) Wave Function Expansion Method

The solution of Equation (2.13), satisfying the stress free boundary condition at $y = 0$, is written in terms of series [3]

$$\begin{aligned} w^{(s)}(r, \theta) = & \sum_{n=1}^{N_B} [A_{2n-1} H_{2(n-1)}^{(2)}(kr) \cos 2(n-1)\theta \\ & + A_{2n} H_{2n-1}^{(2)}(kr) \sin(2n-1)\theta] , \end{aligned} \quad \dots \dots \dots \quad (2.21)$$

where A_n are constants and $H_n^{(2)}$ are Hankel functions of the second kind of order n . It may be noted that only a finite number of terms is kept in Equation (2.21), so that Equation (2.21) represents an approximate solution.

Guided by the expansion Equation (2.21) the interior field can be represented as

$$w^{(2)}(r, \theta) = \sum_{n=1}^{N_B} [D_{2n-1} w_{2n-1}^{(2)}(r, \theta) + D_{2n} w_{2n}^{(2)}(r, \theta)] , \quad \dots \dots \quad (2.22)$$

where D_n are constants and $w_n^{(2)}(r, \theta)$ are unknown functions. From Equation (2.21) and wave function expansion [17] of free-field solution $w^{(o)}(r, \theta)$, we conclude that

$$w^{(2)}(b, \theta) = \sum_{n=1}^{N_B} [D_{2n-1} \cos(2(n-1)\theta) + D_{2n} \sin(2n-1)\theta], \dots \quad (2.23)$$

where b is the radius of semi-circle B.

In order to find $w^{(2)}(r, \theta)$, $w_n^{(2)}(r, \theta)$ at the interior nodal points are determined by assuming that the nodal values of $w_n^{(2)}(b, \theta)$ are given by the values of $\cos(2(n-1)\theta)$ and $\sin(2n-1)\theta$ at the nodes.

Let

$$\{V_B\}_n = \begin{cases} \cos(2(n-1)\theta_B), N = 2(n-1) & n = 1, \dots, N_B \\ \sin(2n-1)\theta_B, N = 2n-1 & \dots \end{cases} \quad (2.24)$$

Using Equation (2.24) in Equation (2.8), $\{V_I\}_N$ are solved. Interior nodal values of V can thus be constructed as

$$\{V_I\}_N = -[S_{II}]^{-1}[S_{IB}]\{V_B\}_N. \quad \dots \quad (2.25)$$

Equation (2.22) can now be written in the matrix form as

$$\{w^{(2)}\} = \sum_{n=1}^{N_B} D_n \{V\}_n = [V]\{D\}, \quad \dots \quad (2.26)$$

where

$$\{V\}_N = \begin{Bmatrix} V_I \\ V_B \end{Bmatrix}_N, \quad [V] = \begin{Bmatrix} [V_I] \\ [V_B] \end{Bmatrix}$$

The next task will be to determine the constants A_n and D_n so that exterior and interior fields can be calculated from Equations (2.21) and (2.26), respectively. To this end, the radial derivatives of $w^{(2)}(r, \theta)$ are first evaluated at the boundary nodes as

$$\{w_B^{(2)}\} = [V_B']\{D\} \quad \dots \quad (2.27)$$

Since the matrix $[V]$ is known from Equations (2.24) and (2.25), the matrix $[V_B']$ can be evaluated from Equation (2.5). Next, the continuity conditions

at the nodes on B are applied

$$w^{(1)}(b, \theta) = w^{(2)}(b, \theta)$$

$$\frac{\partial w^{(1)}}{\partial r} = \frac{\partial w^{(2)}}{\partial r}, \quad r = b. \quad \dots \quad (2.28)$$

This leads to a system of equations

$$\begin{bmatrix} [V_B] & [H] \\ [V'_B] & [H'] \end{bmatrix} \begin{Bmatrix} \{D\} \\ \{A\} \end{Bmatrix} = \begin{Bmatrix} \{W^{(o)}\} \\ \{W'^{(o)}\} \end{Bmatrix}, \quad \dots \quad (2.29)$$

to solve for A_n and D_n . In Equation (2.29) the elements of vector $\{W'^{(o)}\}$ and the diagonal matrices $[H]$ and $[H']$ are given by

$$W_i^{(o)} = \frac{\partial W^{(o)}}{\partial r} \Big|_{r=b}$$

$$H_{ii} = H_{i-1}^{(2)}(k_1 b)$$

$$H'_{ii} = \frac{\partial H_{i-1}^{(2)}}{\partial r} \Big|_{r=b}. \quad \dots \quad (2.30)$$

The matrices $[V_B]$ and $[V'_B]$ are real while $[H]$ and $[H']$ are complex.

2.1.2 Matched-Asymptotic Expansion

It has been shown that if the wave-length is long compared to the dimensions of the scatterer, the scattered field anywhere in the medium can be obtained by matched-asymptotics [10,12,13]. In this technique the scattered field is expanded into two asymptotic series; one valid in an interior region containing the scatterer and the other valid away from the scatterer. The complete solution is obtained by matching these series in some overlap region. A long wave-length analytical solution for the scattered field has been obtained [10] for the case when the region containing

the crack has the same property as the surrounding material. The results of that analysis up to $O(\epsilon^4)$ are reproduced in Appendix A.

2.2 NUMERICAL RESULTS AND DISCUSSION

2.2.1 Surface Canyons

Sufficiently general computer programs were written for the two methods. Isoparametric elements, as well as constant strain triangles (CST), were built in. To gauge the accuracy, range of applicability and versatility of these methods, three illustrative examples are given. In all cases considered, regions R_1 and R_2 have the same material properties, and therefore the wave numbers $k_1 = k_2$ and are designated as k . In all the examples some typical length of a scatterer is designated as "a", and for comparison results are normalized as

$$ka = \eta\pi = \frac{2a\pi}{\lambda}$$

where λ is the incident wave-length.

In the first example a semi-circular canyon is considered, while in the second one a triangular canyon is considered. In the final example a triangular canyon with a buried circular cavity is studied.

i) Semi-Circular Canyon

To gauge the accuracy and range of applicability of the methods, a semi-cylindrical canyon of radius "a" is considered. The analytical results for this case are presented by Triffunac [3]. For this case of simple geometry an automatic mesh-generator program was used. This facilitates the generation of different sizes of elements.

Several runs were made with different combinations of γ , η and k .

For illustration purposes values of real and imaginary parts of the displacement at some points on the canyon are presented in Table 1, for $\gamma = 30^\circ$ and $n = 0.1, 0.5, 0.75$ and 1.5 .

Good agreement was found only up to $n = 1.5$. If the maximum length of the element is denoted as ℓ , then good results were obtained when $a/\ell \geq 5$. The incident angle was not a governing parameter. The above two conditions were sufficient for rapid convergence of the series (2.21).

ii) Triangular Canyon

Real and imaginary parts of scattered field at the surface of a triangular canyon for two different depths, incidence angle $\gamma = -45^\circ$ and $n = 0.1/\pi$ are shown in Figures 6 and 7. The solution is compared with the one given in [8]. Both curves show a similar trend. For 45° slope canyon number of elements and nodes taken were 300 and 150, respectively, while for $22\frac{1}{2}^\circ$ slope they were 400 and 200, respectively.

Figures 8-10 show displacement amplitudes at the surface of a triangular canyon with 45° slope with depth "a" for three incidence angles ($\gamma = 90^\circ, 45^\circ, 0^\circ$) and $n = 0.25$. Results are compared with those given in [8]. It is observed that matching is excellent.

iii) Multiple Scattering

To show the versatility of the method, the problem with two scatterers is considered. A 45° slope triangular canyon is taken as before but with a buried circular scatterer as shown in Figure 11. The origin was taken at the surface. Number of elements and nodes taken were 400 and 250, respectively.

Figures 8-10 and 12 show displacement amplitudes at the surface of the triangular canyon obtained by wave function expansion method. From

these figures, it is observed that presence of the circular cavity considerably affects the scattering pattern.

It is seen from Figures 6 and 7 that the results obtained by the wave function expansion method are in good agreement with the solution given in [8]. There is some agreement with the results obtained by the integral equation technique. These methods predict results in good agreement with the analytical solution for the circular canyon. Further comparison of the results obtained by the two methods and those reported in [8] is shown in Figures 8-10 for the displacement on the triangular canyon. It is interesting to note that for incidence angles of 45° and 90° both the methods predict the minimum displacement amplitude at smaller values of x/a than given in [8]. Further, the displacements on the shadow side of the canyon wall are predicted somewhat higher than calculated in [8].

Also depicted in Figures 8-10 are the displacements of the canyon wall in the presence of a nearby circular cavity obtained by the wave function method. It is seen that for grazing incidence the displacement for $x/a < -0.6$ is not affected by the cavity. Beyond this point the displacement of the canyon wall is modified considerably by the presence of the cavity. Amplitudes are magnified for $-0.6 < x/a < 1.0$. The minimum occurs at $x/a = 0.75$, which is a little to the left of the point nearest to the cavity wall. Displacement amplitudes are less magnified as the angle of incidence decreases. It is observed that for vertical incidence the displacement of the canyon wall near the cavity shows deviation from that in the absence of the wall. However, the other side is not affected much by the cavity. Figure 12 shown the effect of different incidence angles. The

displacements on the illuminated side are observed to be amplified more if the wave is incident from the cavity side.

2.2.2 Edge Cracks

Numerical computations were carried out for a range of non-dimensional wave numbers $\epsilon (= k_2 l)$ from 0.0 to 3.0 for the two cases of a normal edge crack ($\beta = 90^\circ$) and when the crack was inclined at 45° . Here the incidence angle γ is measured from the horizontal as shown in Figure 2.

i) Within Isotropic Region

First the whole region R_1 and R_2 was assumed to be homogeneous and isotropic. In this case the results for small ϵ were compared with those of Datta [10]. For large ϵ and $\beta = 90^\circ$ the results were compared with those of Stone et al. [11].

It was found that in the range of $0 \leq \epsilon \leq 3$ good agreement was obtained with 26 terms in the series (2.21). It may be noted that this choice led to 137 and 141 interior nodes for the inclined and normal cracks, respectively. In both cases the number of nodes on the crack face was 13. Thus the crack opening displacements were obtained at seven locations including the crack tip on the crack face. (See Figure 5).

Figure 13 shows the absolute value of the crack opening displacement at the mouth of the crack for $\beta = 90^\circ$ against ϵ for different angles of incidence. It is seen that results compare very well with those of [11].

Figures 14 and 15 show the variation of the absolute value of the crack opening displacement along the crack for different ϵ . Also shown in these figures are the results obtained by the method of matched asymptotic expansions (MAE) [10] and the numerical results of [11]. For values of ϵ up to 0.5 the solution presented here agrees well with those of [10]. It

is interesting to observe that for large ϵ the MAE predicts smaller crack opening displacement (COD) for $\gamma > 45^\circ$ and larger COD for $\gamma < 45^\circ$. It can be seen that the agreement with the solution presented in [11] is quite good.

Figure 16 shows the absolute value of COD for a 45° inclined crack in comparison with the solution obtained by MAE. It is again seen that the comparison is quite good up to $\epsilon = 1$. It is noted from Figures 13-16 that COD increases with ϵ reaching a maximum at around $\epsilon = 1$ and then drops rapidly up to about $\epsilon = 3$. The comparison of the low frequency MAE solution with the numerical solution shows that the former is larger than the latter for cracks with large orientation angles and/or for small angles of incidence.

ii) Within Anisotropic Material

In order to see the changes that may arise in COD of the crack when it is embedded in a material different from the surrounding matrix, a case was considered in which the region R_2 was occupied by an anisotropic material. Computer programs were modified to accommodate anisotropy.

$$\rho_2/\rho_1 = 1.01, \mu_{2x}/\mu_1 = 1.63, \mu_{2y}/\mu_1 = 1.04.$$

The COD's calculated in this case are compared with the predictions for the isotropic case in Figures 17-20. At long wave-lengths the difference between the COD's for the isotropic and anisotropic cases are quite large. At short wave-lengths ($\lambda/l \approx 0.5$), however, there is very little difference. It is also noted that for 45° inclined cracks (Figure 20), COD's do not change appreciably when the incidence angle γ is changed to $180^\circ - \gamma$. This

observation agrees with that in Reference [10]. Figure 21 depicts the variation of the scattered wave amplitude for grazing incidence on $y = 0$ with the distance from the crack for a normal crack. At long wave-lengths the amplitude drops rapidly with the distance from the crack, reaching almost a steady value at around twice the crack length. At short wave-lengths the amplitude oscillates initially and then reaches a steady value at around thrice the crack length. It is interesting to note that at short wave-lengths ($\ell/\lambda \approx 0.3$) the amplitudes of the scattered wave for both isotropic and anisotropic cases reach the same steady value at the same distance.

Figure 22 shows the comparison of the backscattered amplitude on the surface $y = 0$ obtained by the finite element method (FEM) with the long wave-length MAE approximation. It is seen that the long wave-length approximation gives good results as long as the crack length to the wave-length ratio is less than $1/2\pi$. Figure 23 shows the comparison for a 45° inclined crack. It is seen from this figure that at long wave-lengths the back scattered amplitude is almost the same whether the angle of inclination of the crack is β or $\pi - \beta$. The distinction becomes pronounced if the wave-length to crack-length ratio is less than 4. It is interesting to note, however, that the difference becomes smaller again when this ratio is about 2. It is observed that the amplitude increases more slowly than in the isotropic homogeneous case.

Finally, Figures 24 and 25 depict the variation of the phase of the backscattered field for normal and inclined cracks. Most significant feature of this calculation is that the phase changes linearly with frequency except at very low frequency. It is also seen that the difference

between the phases for the isotropic and anisotropic cases is very small. Figure 25 shows that there are measurable differences between the phases for 45° and 135° inclined cracks, except at very short wave-lengths.

CHAPTER 3

SCATTERING OF SH-WAVES BY EMBEDDED DEFECTS

In this chapter, scattering of plane SH-waves by sub-surface circular cavities and cracks in a semi-infinite elastic medium is studied. The technique of combined finite element and wave function expansion that is useful in the long to intermediate wave-length range is employed here. The results are checked with those obtained by matched asymptotic expansion technique. The results show good agreement for long wave-lengths.

3.1 METHOD OF ANALYSIS

Figure 3 shows a portion of the semi-infinite xy -plane occupied by a homogeneous isotropic elastic material of rigidity modulus μ and density ρ . A cavity (or crack) bounded by the contour C is located in this plane at a depth h from the free surface. The cavity will be assumed to be enclosed by a circle B of radius $b(< h)$. Note that if h is very small, as will be the case when the cavity is very close to or penetrates the free surface, then B may be taken as a semi-circle. This was done in Chapter 2. Although the same could be done in the present case, it would greatly expand the finite-element region, and thus would be far more expensive. If the inhomogeneity is deep inside, it is more economical to enclose it by a circle lying fully inside the semi-infinite region.

3.1.1 Interior Region

The formulation in the interior region for the present case is

the same as that in Chapter 2. Because of the difference in the nature of the problems, the formulation of the exterior region for the present case is described in the following.

3.1.2 Exterior Region

In order now to solve for w at the internal and boundary nodal points, it is necessary to match the solution in R_2 with the solution in the exterior region R_1 . For this purpose the solution for w satisfying equation (2.13) and the boundary conditions on $y = 0$, viz,

$$\frac{\partial w^{(1)}}{\partial y} = 0 \quad \text{on } y = 0 , \quad \dots \dots \dots \quad (3.1)$$

will have to be found. This solution can be formally written as

$$w^{(1)} = w^{(0)} + w^{(s)} , \quad \dots \dots \dots \quad (3.2)$$

where $w^{(0)}$ is the total incident field near the cavity and $w^{(s)}$ is the scattered field.

The solution $w^{(s)}$ can be written as

$$\begin{aligned} w^{(s)} = & \sum_{n=0}^{\infty} [A_n(H_n(kr)\cos n\theta + H_n(kR)\cos n\theta) \\ & + B_n(H_n(kr)\sin n\theta + H_n(kR)\sin n\theta)] , \quad \dots \dots \dots \quad (3.3) \end{aligned}$$

where H_n is the Hankel function of the first kind and the coordinates (r,θ) and (R,θ) are shown in Figure 3. Since

$$\begin{aligned} H_n(kR)\cos n\theta &= H_n(2kh) + \sum_{m=1}^{\infty} \{H_{n+m}(2kh) + (-1)^m H_{n-m}(2kh)\} \times J_m(kr)\cos m\theta \\ H_n(kR)\sin n\theta &= \sum_{m=1}^{\infty} \{H_{n+m}(2kh) - (-1)^m H_{n-m}(2kh)\} \times J_m(kr)\sin m\theta , \quad \dots \quad (3.4) \end{aligned}$$

Equation (3.3) can be rewritten as

$$w^{(s)} = \sum_{m=0}^{\infty} [F_m \cos m\theta + G_m \sin m\theta] , \dots \quad (3.5)$$

where

$$F_m = \begin{cases} A_m H_m(kr) + \sum_{n=0}^{\infty} A_n \{H_{n+m}(2kh) + (-1)^m H_{n-m}(2kh)\} J_m(kr), & m \neq 0 \\ A_0 H_0(kr) + \sum_{n=0}^{\infty} A_n H_n(2kh), & m = 0 \end{cases}$$

and

$$G_m = B_m H_m(kr) + \sum_{n=0}^{\infty} B_n \{H_{n+m}(2kh) - (-1)^m H_{n-m}(2kh)\} J_m(kr) .$$

For the purpose of numerical solution only a finite number of terms of the series will be kept. Choosing the number of nodes, N_B , on the boundary B to be even, Equation (3.5) will be written as

$$w^{(s)} = \sum_{m=0}^{\frac{1}{2}N_B-1} F_m \cos m\theta + \sum_{m=1}^{\frac{1}{2}N_B} G_m \sin m\theta , \dots \quad (3.6)$$

with

$$F_m = \begin{cases} A_m H_m(kr) + \sum_{n=0}^{\frac{1}{2}N_B-1} A_n \{H_{n+m}(2kh) + (-1)^m H_{n-m}(2kh)\} J_m(kr), & m \neq 0 \\ A_0 H_0(kr) + \sum_{n=0}^{\frac{1}{2}N_B-1} A_n H_n(2kh) , & m = 0 \end{cases}$$

$$G_m = B_m H_m(kr) + \sum_{n=1}^{\frac{1}{2}N_B} B_n \{H_{n+m}(2kh) - (-1)^m H_{n-m}(2kh)\} J_m(kr) .$$

Thus there are N_B unknown constants A_n and B_n .

Guided by the expansion (3.5), we assume that the interior field can be written in the form

$$w^{(2)}(r, \theta) = \sum_{n=0}^{\frac{1}{2}N_B-1} D_n u_n^{(2)}(r, \theta) + \sum_{n=1}^{\frac{1}{2}N_B} E_n v_n^{(2)}(r, \theta), \dots \quad (3.7)$$

where D_n , E_n are unknown constants and, $u_n^{(2)}$ and $v_n^{(2)}$ are unknown functions. Continuity conditions require that on $r=b$,

$$w^{(2)}(b, \theta) = \sum_{n=0}^{\frac{1}{2}N_B-1} D_n \cos n\theta + \sum_{n=1}^{\frac{1}{2}N_B} E_n \sin n\theta. \dots \quad (3.8)$$

In order to find $w^{(2)}(r, \theta)$, $u_n^{(2)}(r, \theta)$ and $v_n^{(2)}(r, \theta)$ are first solved at the interior nodal points by assuming that the nodal values of $u_n^{(2)}(b, \theta)$ and $v_n^{(2)}(b, \theta)$ are given by the values of $\cos n\theta$ and $\sin n\theta$, respectively, at the boundary nodes.

Let

$$\begin{aligned} \{U_B\}_n &= \cos n\theta_B, \quad n = 0, \dots, \frac{1}{2}N_B-1 \\ \{V_B\}_n &= \sin n\theta_B, \quad n = 1, \dots, \frac{1}{2}N_B. \end{aligned} \quad \dots \quad (3.9)$$

Using Equation (3.9) in Equation (2.8) we solve for $\{U_I\}_n$ and $\{V_I\}_n$. Then two $N_I \times \frac{1}{2}N_B$ matrices can be constructed with the nodal values of U and V in the interior, viz.,

$$[U_I] = - [S_{II}]^{-1} [S_{IB}] [U_B], \quad [V_I] = - [S_{II}]^{-1} [S_{IB}] [V_B]. \quad (3.10)$$

Equation (3.6) can now be written in matrix form as

$$\{w^{(2)}\} = [W] \{D\}, \quad \dots \quad (3.11)$$

where $\{w^{(2)}\}$ is a $(N_I + N_B) \times 1$ column matrix, $[W]$ is a $(N_I + N_B) \times N_B$ matrix and $\{D\}$ is a $N_B \times 1$ column matrix. Note that

$$[W] = \begin{pmatrix} U_I & V_I \\ U_B & V_B \end{pmatrix}, \quad \{D\} = \begin{Bmatrix} D_n \\ E_N \end{Bmatrix}.$$

The next task is to determine the $2N_B$ unknown constants A_n , B_n , D_n , and E_n . To this end the normal derivatives of $w^{(2)}(r, \theta)$ at the boundary nodes are calculated as

$$\{w'_B^{(2)}\} = [W'_B] \{D\}. \quad \dots \dots \dots \quad (3.12)$$

Since the matrix $[W]$ is known, $[W'_B]$ can be obtained from Equation (2.5).

The continuity conditions

$$w^{(1)}(b, \theta) = w^{(2)}(b, \theta), \quad \frac{\partial w^{(1)}}{\partial r}(b, \theta) = \frac{\partial w^{(2)}}{\partial r}(b, \theta), \quad \dots \dots \quad (3.13)$$

are now used to obtain a system of $2N_B$ equations in the $2N_B$ unknown constants. The interior and boundary nodal values of $w^{(2)}$ are then found from Equation (3.11) and the scattered field in the exterior region is given by Equation (3.3). The results of these computations are discussed in the next section, along with those obtained by the method of matched asymptotic expansion (MAE) [13].

3.2 NUMERICAL RESULTS AND DISCUSSION

The displacement w at the nodal points within and on B were computed by the method outlined in the last section. Also, the coefficients A_n and B_n in the series expansion (3.3) were found. This enabled the computation of w at all points outside B . Particular attention was focused on the distribution of w on the surface $y=0$ for various angles of incidence γ as well as for different orientations of the crack. The wave number k was varied in the range $0 < k \leq 7.0$. For the embedded crack

the radius of the circle B was chosen to be $5/3$ times the half crack-length ($a = \ell/2$). Total number of nodes on B was 32 and the number of nodes within B was 144. Near the crack tips six-node isoparametric triangular quarter point elements [14,15] were chosen to obtain the correct square root singularity at the tips. These were surrounded by a layer of seven-node transitional elements [16]. Constant strain triangular elements were used elsewhere. For the embedded circular cavity the ratio of the cavity radius to the radius of the circle B was taken as 1.5. The total number of boundary and interior elements were 40 and 160, respectively. Only constant strain triangular elements were used in this case. The incidence angle γ is measured from the horizontal as shown in Figure 3.

Scattered displacement fields on the free surface $y=0$ for grazing incidence, due to an embedded vertical crack and a circular cavity are compared in Figure 26. Note that θ represents the angle between the radius from the center of the cavity (or crack) to the observation point and the vertical line. It is observed that the backscattered signal in the region $-40^\circ \leq \theta \leq 0^\circ$ due to a circular cavity is much larger than a crack. The difference between the backscattered signals of two different incident waves are also appreciable in this region. For the cracks, however, large differences are observed in regions somewhat farther away from the origin. It is also of interest to note the marked differences between the backscattered signals from cracks and cavities.

Figure 27 shows the scattered field on $y=0$ due to a vertical crack at two different depths. It is seen that the signals are not much different as long as the cracks are fairly deep.

The scattered signals from a vertical crack are compared with those from a 45° -inclined crack in Figure 28. This figure brings out the marked differences between the signals received from cracks of different orientations. The most noticeable distinction is that for a 45° -inclined crack in which most of the energy is scattered in the forward direction, whereas for a vertical crack the energy is scattered much more uniformly in both directions.

Figure 29 depicts the scattered signals from cracks of different orientations for various incidence angles. As in Figure 28, it is seen that scattered signals are significantly influenced by the orientations of the crack. As observed in Figure 28, most of the scattered energy, due to a 45° -inclined crack, is confined in the acute angled region formed by the crack and the free surface. It is interesting to observe that the scattered fields, due to 45° and 135° incidences, are nearly the same.

Comparison of the backscattered fields from deeply embedded cracks and cavities, and edge cracks (from previous Chapter) is made in Figure 30. It is found that the backscattered signals from the circular cavity increase more rapidly with frequency than those from either the edge crack or the deep crack. Also, the maximum amplitude is attained at a lower frequency for a circular cavity than either for an edge crack or for a deep crack. Figure 31 shows the maximum backscattered amplitudes for an edge crack and a deep crack. It is quite interesting to note that the backscattered amplitude for a deep crack increases more slowly with frequency, but reaches almost twice the maximum value for an edge crack at a frequency, which is also twice that for an edge crack. Note that ℓ is the length of the crack.

Figures 32 and 33 depict the scattered displacement fields on $y = 0$ for a deep circular cavity. It is seen from these figures that the field is strongly dependent on the incidence angle, as well as on the frequency. The displacement distribution on the cavity wall is shown in Figure 34. It is noted that the displacement amplitudes are somewhat higher on the side of the cavity nearer the free surface than that on the far side. It is also noticed that the distribution of the local maxima occur on the illumination side of the cavity wall and local minima are on the shadow side.

Finally, the comparison between the predictions for the scattered displacement amplitudes on $y = 0$ by MAE and FEM techniques for a buried circular cavity is included in Table 2. It may be seen that values of $\epsilon^2 W_1$, which is the scattered field correct to $O(\epsilon^2)$, agree quite well with FEM calculations, except when ϵ becomes $O(1)$.

CHAPTER 4

SUMMARY AND CONCLUSION

A combined finite element and analytical method has been investigated in this thesis for studying the diffraction of horizontally polarized shear (SH) waves by surface or embedded inhomogeneities in semi-infinite elastic media. Solutions of the study are obtained by combining finite element techniques, which are valid in the neighborhood of the inhomogeneities, with analytical solutions, which are valid in the far field. The results compare well with other available analytical and numerical results.

In Chapter 2, the problem of scattering of SH-waves by surface depressions (canyons) and edge cracks was considered. Two combined numerical and analytical methods of solution have been presented for studying the scattering of SH-wave by arbitrarily shaped canyons. Both methods are quite versatile in that they can be used to study scattering by more than one defect. As an illustrative example, the problem of scattering by a triangular canyon in the presence of a circular cavity has been solved. The combined finite element and wave function expansion method has been used in the same chapter to solve the problem of diffraction of SH-waves by edge cracks in isotropic, as well as anisotropic elastic media. It is shown that the numerical predictions agree closely with the numerical technique of matched asymptotic expansion (MAE).

The combined numerical and analytical technique is again used in

Chapter 3 to study scattering of SH-waves by deeply embedded cracks and circular cavities in a half-space. Comparison has been made between the prediction of this numerical technique and the method of matched asymptotic expansions. The comparison is found to be favorable as long as the wave-length is long.

The advantage of this combined numerical and analytical technique investigated here is that it is applicable to arbitrarily shaped scatterers. It makes very efficient use of computer time in calculating scattering for various incident waves since most of the computations do not involve the incident fields. Moreover, the artificial contour B can be placed anywhere to bound all the inhomogeneities within the interior region, and the interior and exterior regions are solved separately. However, the limitation of the technique is that at very short wave-lengths, it would become quite expensive to implement.

Part of this work has been accepted for publication [18].

BIBLIOGRAPHY

1. Luco, J.E., "Dynamic Interaction of a Shear Wall with the Soil." *J. Engg. Mech. Div., ASCE*, 95, 333-346 (1969).
2. Trifunac, M.D., "Interaction of a Shear Wall with the Soil for Incident Plane SH-Waves," *Bull. Seism. Soc. Amer.*, 62, 63-83 (1972).
3. Trifunac, M.D., "Scattering of Plane SH-Waves by a Semi-Cylindrical Canyon," *Intl. J. Earthquake Eng. and Struct. Dyn.*, 1, 267-281 (1973).
4. Wong, H.L., and Trifunac, M.D., "Scattering of Plane SH-Waves by a Semi-Elliptical Canyon," *Intl. J. Earthquake Eng. and Struct. Dyn.*, 3, 157-169 (1974).
5. Sabin, F.J., and Willis, J.R., "Scattering of SH-Waves by a Rough Half-Space of Arbitrary Slope," *Geophys. J.R. Astr. Soc.*, 42, 685-703 (1975).
6. Bouchon, M., "Effect of Topography on Surface Motion," *Bull. Seism. Soc. Am.*, 63, 615-632 (1973).
7. Wong, H.L., and Jennings, P.C., "Effects of Canyon Topography on Strong Ground Motion," *Bull. Seism. Soc. Am.*, 65, 1239-1257 (1975).
8. Sánchez-Sesma, F.J., and Rosenblueth, E., "Ground Motion at Canyons of Arbitrary Shape Under Incident SH-Waves," *Intl. J. Earthquake Eng. and Struct. Dyn.*, 7, 441-450 (1979).
9. Sánchez-Sesma, F.J., and Esquivel, J.A., "Ground Motion of Alluvial Valleys Under Incident Plane SH-Waves," *Bull. Seism. Soc. Am.*, 69, 1107-1120 (1979).
10. Datta, S.K., "Diffraction of SH-Waves by an Edge Crack," *J. Appl. Mech.*, 46, 101-106 (1979).
11. Stone, S.F., Ghosh, M.L. and Mal, A.K., "Diffraction of Antiplane Shear Waves by an Edge Crack," *J. Appl. Mech.*, 47, 359-362 (1980).
12. Datta, S.K., "Diffraction of SH-Waves by an Elliptic Elastic Cylinder," *Int. J. Solids Structures*, 10, 123-133 (1974).
13. Datta, S.K., and El-Akily, N., "Diffraction of Elastic Waves by Cylindrical Cavity in a Half-Space," *J. Acoust. Soc. Am.*, 64, 1692-1699 (1978).
14. Barsoum, R.S., "On the Use of Isoparametric Finite Elements in Linear Fracture Mechanics," *Int. J. Num. Methods Engg.*, 10, 25-38, (1976).

15. Barsoum, R.S., "Triangular Quarter-point Elements as Elastic and Perfectly Plastic Crack Tip Elements," *Int. J. Num. Methods Engg.*, 11, 85-98 (1977).
16. Lynn, P.P. and Ingraffia, A.R., "Transition Elements to be Used with Quarter-point Crack-tip Elements," *Int. J. Num. Methods Engg.*, 12, 1031-1036 (1978).
17. Pao, Y.H., and Mow, C.C., "Diffraction of Elastic Waves and Dynamic Stress Concentration," The Rand Corporation, New York, 1973.
18. Shah, A.H., Wong, K.C., and Datta, S.K., "Diffraction of Plane Sh-Waves in a Half-space," to be published in *Intl. J. Earthquake Engng. and Struct. Dyn.*

A P P E N D I C E S

A P P E N D I X A

RESULTS OF THE ANALYSIS OF MATCHED-ASYMPTOTIC EXPANSIONS
(UP TO $O(\epsilon^4)$)

APPENDIX A

For the purpose of completeness the long wave-length solution for an edge crack is given here. (Refer Figure 2). The solution w^S can be expressed in two different series, one valid near the crack and the other away from the crack. In the latter region we have

$$\begin{aligned} w^S = & \varepsilon^2 [a_{11} H_1(\varepsilon \bar{r}) \cos \theta_1 + \varepsilon (a_{21} H_1 \cos \theta_1 + a_{22} H_2 \cos 2\theta_1) \\ & + \varepsilon^2 \ln \varepsilon a_{31} H_1 \cos \theta_1 + \varepsilon^2 (a_{41} H_1 \cos \theta_1 + a_{42} H_2 \cos 2\theta_1 \\ & + a_{43} H_3 \cos 3\theta_1)] + O(\varepsilon^5), \end{aligned} \quad (A1)$$

where

$$\begin{aligned} a_{11} &= -\frac{1}{2} \beta(1-\beta/\pi) \cos \gamma e^{-2z}, \quad a_{21} = -\frac{i}{6} \beta(1-\beta/\pi)(1-2\beta/\pi) \cos 2\gamma e^{-2z} \\ a_{22} &= -\frac{1}{6} \beta(1-\beta/\pi)(1-2\beta/\pi) \cos \gamma e^{-3z}, \quad a_{31} = \frac{1}{8\pi} \beta^2 (1-\beta/\pi)^2 \cos \gamma e^{-4z} \\ a_{41} &= -\frac{1}{2} \beta(1-\beta/\pi) \cos \gamma (A - \frac{1}{16\pi} \beta(1-\beta/\pi) e^{-2z}) e^{-2z} \\ &\quad + \frac{1}{192} \beta(1-\beta/\pi)(2-3\beta/\pi)(1-3\beta/\pi) \cos 3\gamma e^{-4z} \\ a_{42} &= \frac{-i}{16} \beta(1-\beta/\pi)(1-2\beta/\pi)^2 \cos 2\gamma e^{-4z} \\ a_{43} &= -\frac{1}{64} \beta(1-\beta/\pi)(2-3\beta/\pi)(1-3\beta/\pi) \cos \gamma e^{-4z} \\ A &= \frac{i}{4} \beta(1-\beta/\pi) e^{-2z} [\frac{1}{2} + \frac{i}{\pi} (\bar{\gamma} - \ln 2 - 1/2) + \frac{i}{2\pi} (2\bar{\gamma} - \frac{1}{2} - 2z + \pi \cot \beta \\ &\quad + 2\psi(\beta/\pi)) - \frac{1}{48} (2-3\beta/\pi)(1-3\beta/\pi)(1-4 \sin^2 \gamma) e^{-4z}] \\ z &= \frac{\beta}{\pi} \ln \frac{\beta}{\pi} + (1-\beta/\pi) \ln(1-\beta/\pi) \end{aligned}$$

The crack opening displacement $[w]$ has an expansion of the form

$$[w] = \varepsilon \{w_1 + \varepsilon w_2 + \varepsilon^2 \ln \varepsilon w_3 + \varepsilon^2 w_4 + \varepsilon^3 \ln \varepsilon w_5 + \varepsilon^3 w_6\} + O(\varepsilon^5). \quad (A2)$$

where

$$w_1 = 2i \sin\beta \cos\gamma K_N(-1) \left[\frac{1}{\beta} + \frac{1}{\pi-\beta} + \sum_{k=1}^{\infty} \left\{ \frac{r^{-k\pi/\beta}}{\beta(1-k\pi/\beta) K_N(-k\pi/\beta)} \right. \right.$$

$$\left. \left. + (\pi-\beta)(1 - \frac{k\pi}{\pi-\beta}) K_N(\frac{-k\pi}{\pi-\beta}) \right\} \right]$$

$$w_2 = -\frac{1}{2} \sin 2\beta \cos 2\gamma K_N(-2) \left[\frac{1}{2\beta} + \frac{1}{2(\pi-\beta)} + \sum_{k=1}^{\infty} \left\{ \frac{r^{-k\pi/\beta}}{(2 - \frac{k\pi}{\beta}) \beta K_N(\frac{-k\pi}{\beta})} \right. \right.$$

$$\left. \left. + \frac{r^{-k\pi/(\pi-\beta)}}{(2 - \frac{k\pi}{\pi-\beta})(\pi-\beta) K_N(-\frac{k\pi}{\pi-\beta})} \right\} \right]$$

$$w_3 = -\frac{\sin^2 \beta K_N(-1)}{4\pi K_P(1)} w_1$$

$$w_4 = Aw_1 - i \sin\beta \cos\gamma K_N(-1) \left[r^2 \left(\frac{1}{2\beta} + 2\frac{1}{(\pi-\beta)} \right) \right.$$

$$\left. - \sum_{k=1}^{\infty} \left\{ \left(\frac{\beta(\pi-\beta) \bar{K}_P(1)}{4\pi(1 - \frac{k\pi}{\beta}) K_P(1)} - \frac{(3-4\sin^2\beta)(1-4\sin^2\gamma) \bar{K}_N(-1)}{4(3 - \frac{k\pi}{\beta}) K_N(-1)} \right) \right. \right]$$

$$\times \frac{r^{-k\pi/\beta}}{k\pi \bar{K}_N(2 - \frac{k\pi}{\beta})} + \left(\frac{\beta(\pi-\beta) \bar{K}_P(1)}{4\pi(1 - \frac{k\pi}{\pi-\beta}) K_P(1)} - \frac{(3-4\sin^2\beta)(1-4\sin^2\gamma) \bar{K}_N(-1)}{4(3 - \frac{k\pi}{\pi-\beta}) K_N(-1)} \right)$$

$$\times \frac{r^{-k\pi/(\pi-\beta)}}{k\pi K_N(2 - \frac{k\pi}{\pi-\beta})} + \frac{r^{-2+k\pi/\beta}}{2(k^2\pi^2/\beta^2 - 1) K_N(-k\pi/\beta)}$$

$$+ \frac{r^{-2+k(\pi-\beta)}}{2(k^2\pi^2/(\pi-\beta)^2 - 1) K_N(-k\pi/(\pi-\beta))} \}$$

$$w_5 = -\frac{i \sin\beta \sin 2\beta \cos 2\gamma K_N(-2)}{24\pi K_P(1) \cos\gamma} w_1$$

$$w_6 = -\frac{1}{2} \frac{B}{\cos\gamma} w_1 + \sum_{k=1}^{\infty} \left\{ \left(\frac{\beta(\pi-\beta) \sin 2\beta \cos 2\gamma K_N(-2) \bar{K}_P(1)}{24\pi(1 - \frac{k\pi}{\pi\beta}) K_P(1)} \right. \right.$$

$$\left. \left. - \frac{\sin 4\beta \cos 4\gamma \bar{K}_N(-2)}{24(4 - \frac{k\pi}{\beta})} \right) \frac{r^{-k\pi/\beta}}{k\pi \bar{K}_N(2 - \frac{k\pi}{\beta})} + \left(\frac{\beta(\pi-\beta) \sin 2\beta \cos 2\gamma K_N(-2) \bar{K}_P(1)}{24\pi(1 - \frac{k\pi}{\pi\beta}) K_P(1)} \right. \right.$$

$$\begin{aligned}
 & - \frac{\sin 4\beta \cos 4\gamma \bar{K}_N(-2)}{24(4 - \frac{k\pi}{\pi-\beta})} \frac{-k\pi/(\pi-\beta)}{k\pi \bar{K}_N(2 - \frac{k\pi}{\pi-\beta})} - \frac{K_N(-2) \sin 2\beta \cos 2\gamma}{8} \\
 & \times \left(\frac{-r^2 + k\pi/\beta}{(2 - \frac{k\pi}{\beta})(1 + \frac{k\pi}{\beta}) \beta K_N(-\frac{k\pi}{\beta})} + \frac{-r^2 + k\pi/(\pi-\beta)}{(2 - \frac{k\pi}{\pi-\beta})(1 + \frac{k\pi}{\pi-\beta})(\pi-\beta) K_N(-\frac{k\pi}{\pi-\beta})} \right) \}
 \end{aligned}$$

$$K_N(-1) = \frac{\beta(1-\beta/\pi)}{\sin \beta} e^{-z}, \quad K_p(1) = e^z \sin \beta$$

$$K_N(-2) = \frac{2\beta(1-\beta/\pi)(1-2\beta/\pi)}{\sin 2\beta} e^{-2z}$$

$$\bar{K}_N(-1) = - \frac{\beta(1-\beta/\pi)(2-3\beta/\pi)(1-3\beta/\pi)}{3 \sin 3\beta} e^{-z}$$

$$\bar{K}_p(1) = \frac{1}{\pi} \sin \beta e^z$$

$$\bar{K}_N(-2) = - \frac{\beta(1-\beta/\pi)(3-4\beta/\pi)(2-4\beta/\pi)(1-4\beta/\pi)}{8 \sin 4\beta} e^{-2z}$$

$$K_N(1 - \frac{k\pi}{\beta}) = \frac{\Gamma(1+k)\Gamma(1-k+k\pi/\beta)}{\Gamma(1+k\pi/\beta)} e^{-\frac{k\pi}{\beta} z}$$

$$\bar{K}_N(2 - \frac{k\pi}{\beta}) = - \frac{k\pi/\beta - 1}{(k\pi/\beta)^2} e^{2z} K_N(-k\pi/\beta)$$

$$\begin{aligned}
 B &= - \frac{i}{12} \sin \beta \sin 2\beta \cos 2\gamma \left(\frac{1}{2} + \frac{i}{\pi} (\bar{\gamma} - \ln 2 - 1/2) \right) \frac{K_N(-2)}{K_p(1)} \\
 &\quad - \frac{\sin \beta \sin 4\beta \cos 4\gamma \bar{K}_N(-2)}{72\beta(\pi-\beta) \bar{K}_p(1)} + \frac{\sin \beta \sin 2\beta \cos 2\gamma \bar{K}_N(-2)}{24\pi K_p(1)} \{ -\frac{1}{3} - 2z \\
 &\quad + 2\gamma + \pi \cot \beta + 2\Psi(\beta/\pi) \}
 \end{aligned}$$

$$\bar{\gamma} = 0.57712157$$

A P P E N D I X B

TABLES

η	x/a	Analytical		Integral Eqn.		Wave Function	
		Real	Imaginary	Real	Imaginary	Real	Imaginary
0.1	-1.0	1.93179	0.78101	1.93048	0.73845	1.93250	0.81346
	-0.5	1.83626	0.46199	1.84397	0.43532	1.83754	0.46775
	0.5	1.78402	-0.20356	1.80065	-0.19691	1.76986	-0.21312
	1.0	1.83179	-0.52272	1.84752	-0.50015	1.82009	-0.53452
0.5	-1.0	1.80366	2.52048	1.85403	2.43898	1.72475	2.59570
	-0.5	0.32537	1.19782	0.44212	1.12894	0.26909	1.21389
	0.5	0.15707	1.11320	0.22535	0.92760	0.17739	1.18900
	1.0	1.32787	-1.14951	1.34911	-1.09398	1.32571	-1.20409
0.75	-1.0	0.66699	3.25134	0.65026	3.11135	0.58280	3.35738
	-0.5	-1.16483	0.08978	-0.93061	+0.18207	-1.30895	0.07356
	0.5	0.18752	2.24114	-0.03565	2.10379	0.14796	2.26704
	1.0	0.52214	-1.99723	0.66629	-1.82064	0.42234	-1.97141
1.5	-1.0	-2.71052	2.07993	-2.50406	1.68840	-3.06495	2.06944
	-0.5	-0.54397	-2.50116	-0.59637	-2.36891	-0.45487	-2.58695
	0.5	-1.45447	0.73688	-1.03997	0.29648	-1.45615	0.74363
	1.0	-1.52016	-0.88486	-1.39943	-1.02369	-1.46272	-0.81358

TABLE 1 - Comparison of Results With Analytical Solution
Semi-Cylindrical Canyon of Radius a. $\gamma = 30^\circ$

$\epsilon=0.1, a/h=0.133$			$\epsilon=0.5, a/h=0.67$			$\epsilon=0.5, a/h = 0.33$			$\epsilon=1.0, a/h=0.67$		
	FEM	MAE	FEM	MAE	FEM	MAE	FEM	MAE	FEM	MAE	
0	.01447	.01211	.5130	.30283	.2358	.20867	.5287	.83466			
80°											
60°	.02321	.01941	.8990	.48536	.3329	.28928	.8493	.11571			
40°											
20°	.01359	.01205	.7709	.30115	.2230	.17289	.1.409	.69157			
0°											
-20°	.0528	.03819	1.354	1.1987	.8426	.83846	2.7806	3.3538			
-40°											
-60°	.06345	.05726	1.417	1.4316	.9300	.99528	2.0026	3.9811			
-80°											
	.03984	.03596	.8640	.89891	.5818	.6338	1.1455	2.5352			

TABLE 2 - Scattered Displacement Amplitudes at the Surface of the Half-Space Due to a Buried Circular Cavity. Comparison of MAE and FEM ($\gamma = 0^\circ$).

A P P E N D I X C

FIGURES

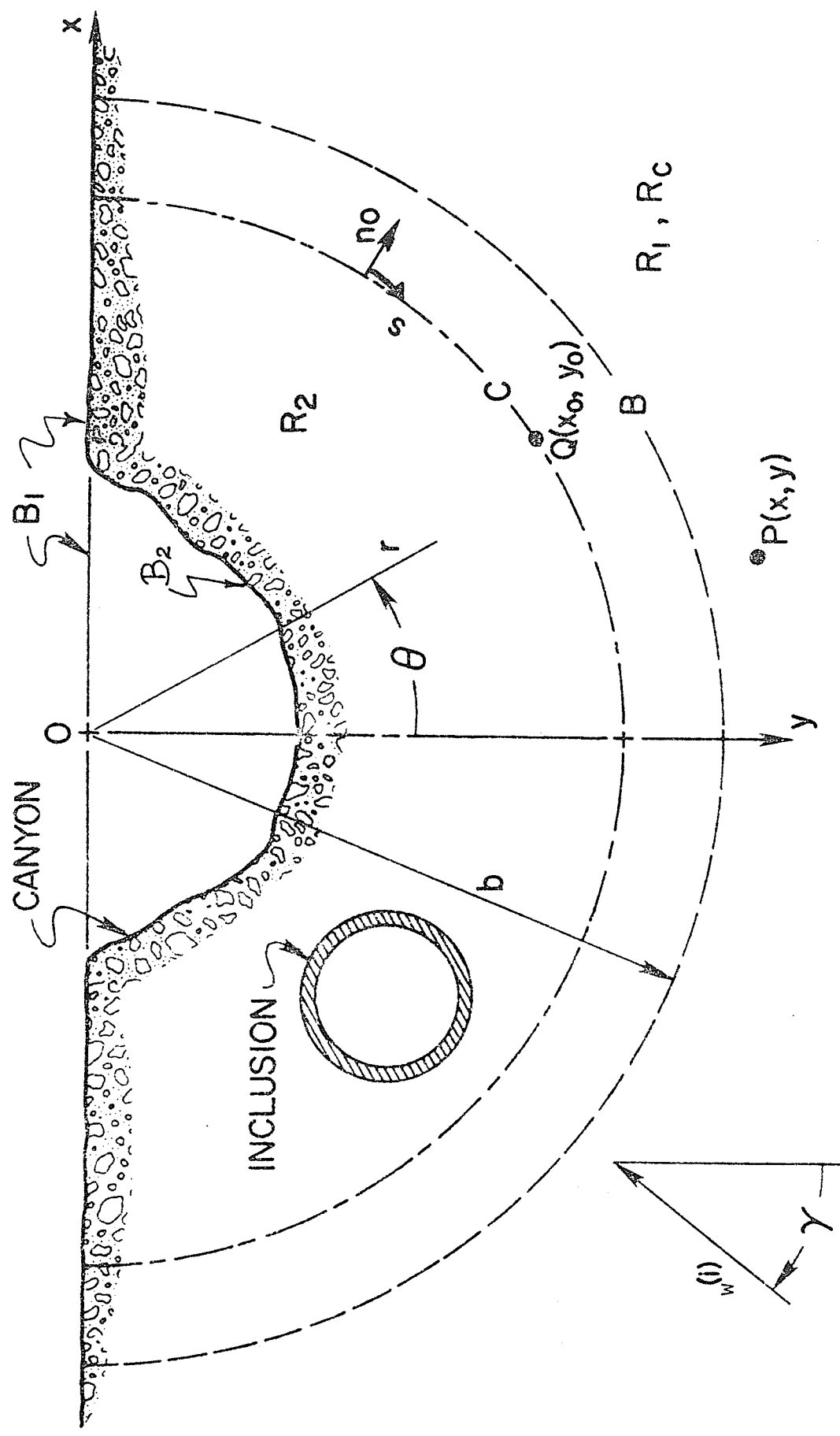


FIGURE 1. Geometry of a Surface Canyon Showing the Inner and Outer Regions.

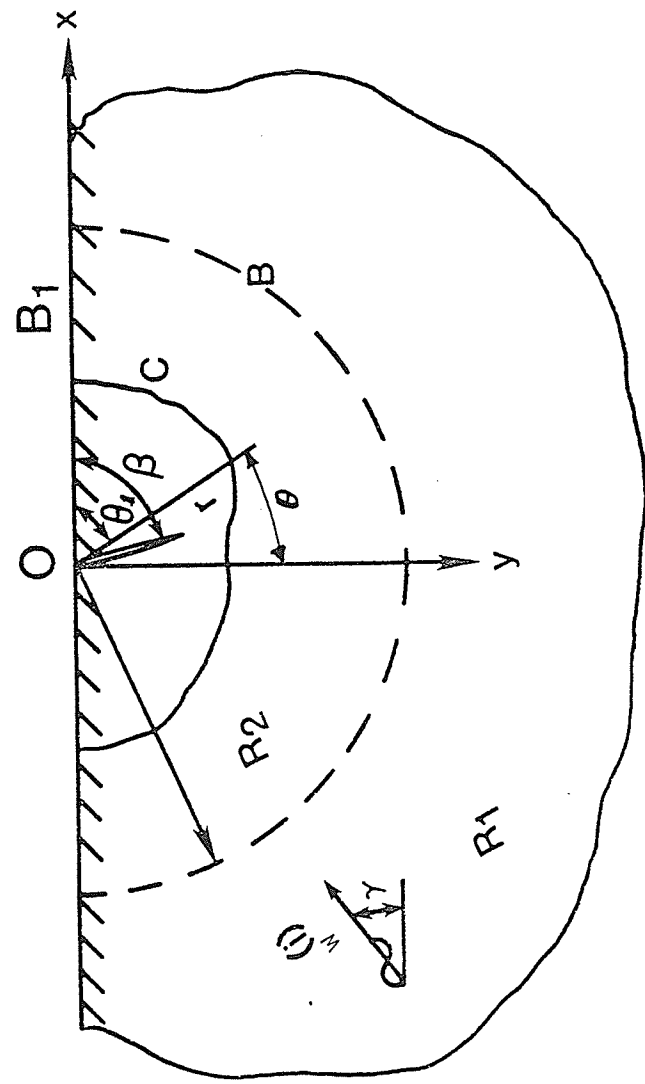


FIGURE 2. Geometry of an Edge Crack showing the
Inner and Outer Regions.

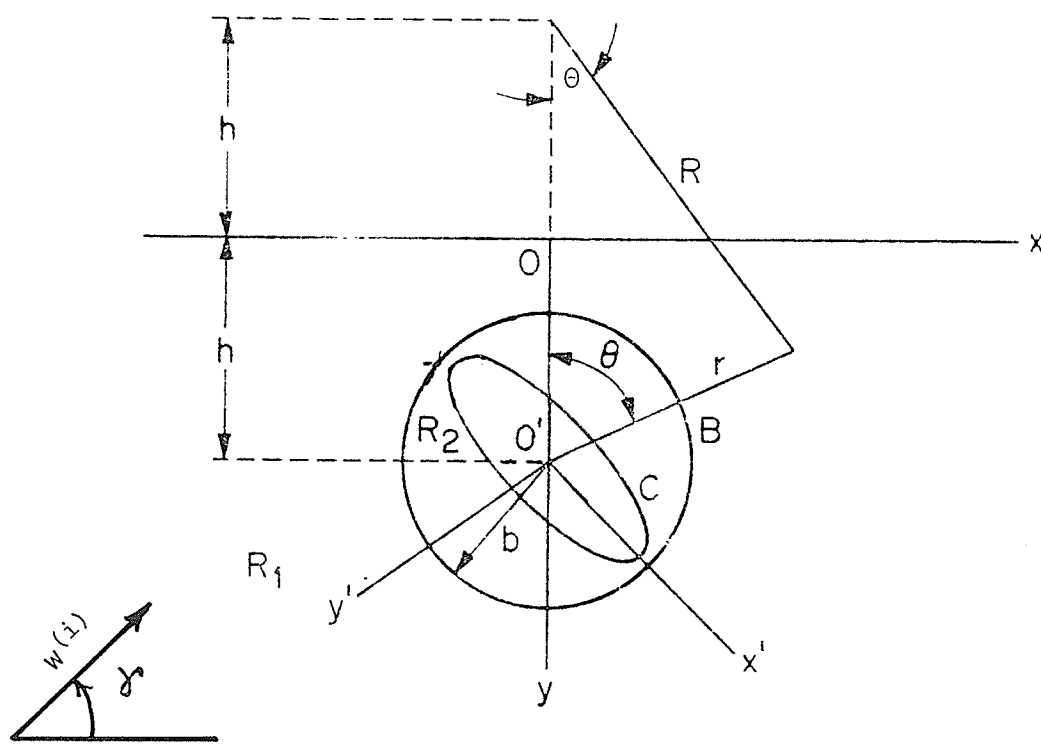


FIGURE 3. Geometry of an Embedded Circular Canyon or Embedded Crack Showing the Inner and Outer Regions.

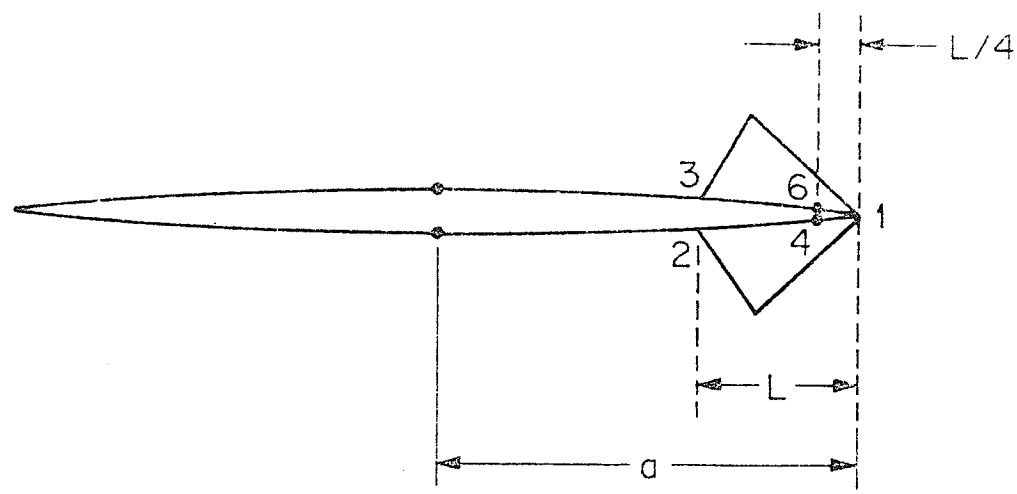


FIGURE 4. Crack-tip Elements.

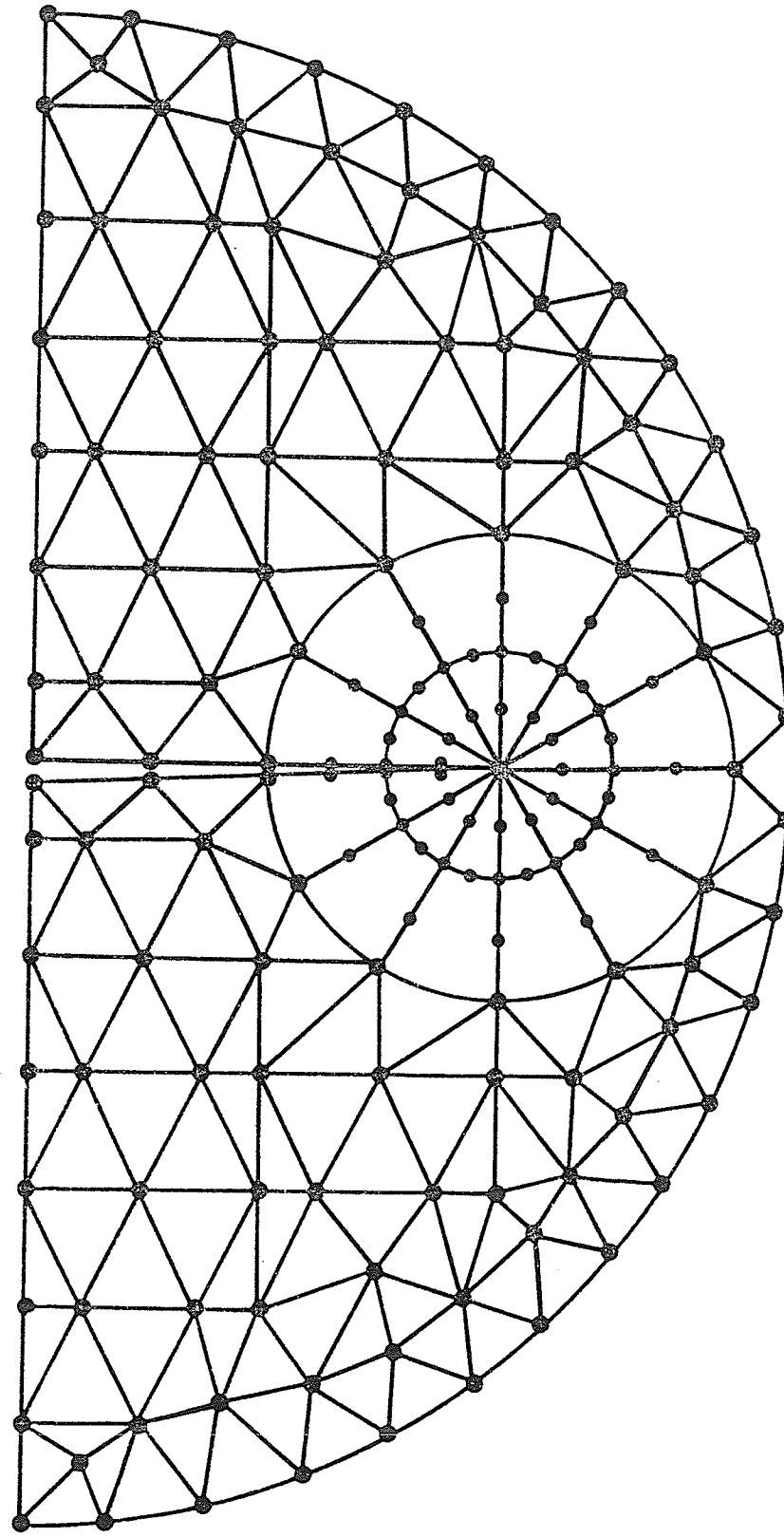


FIGURE 5. Finite Element Subdivision of the Inner Region

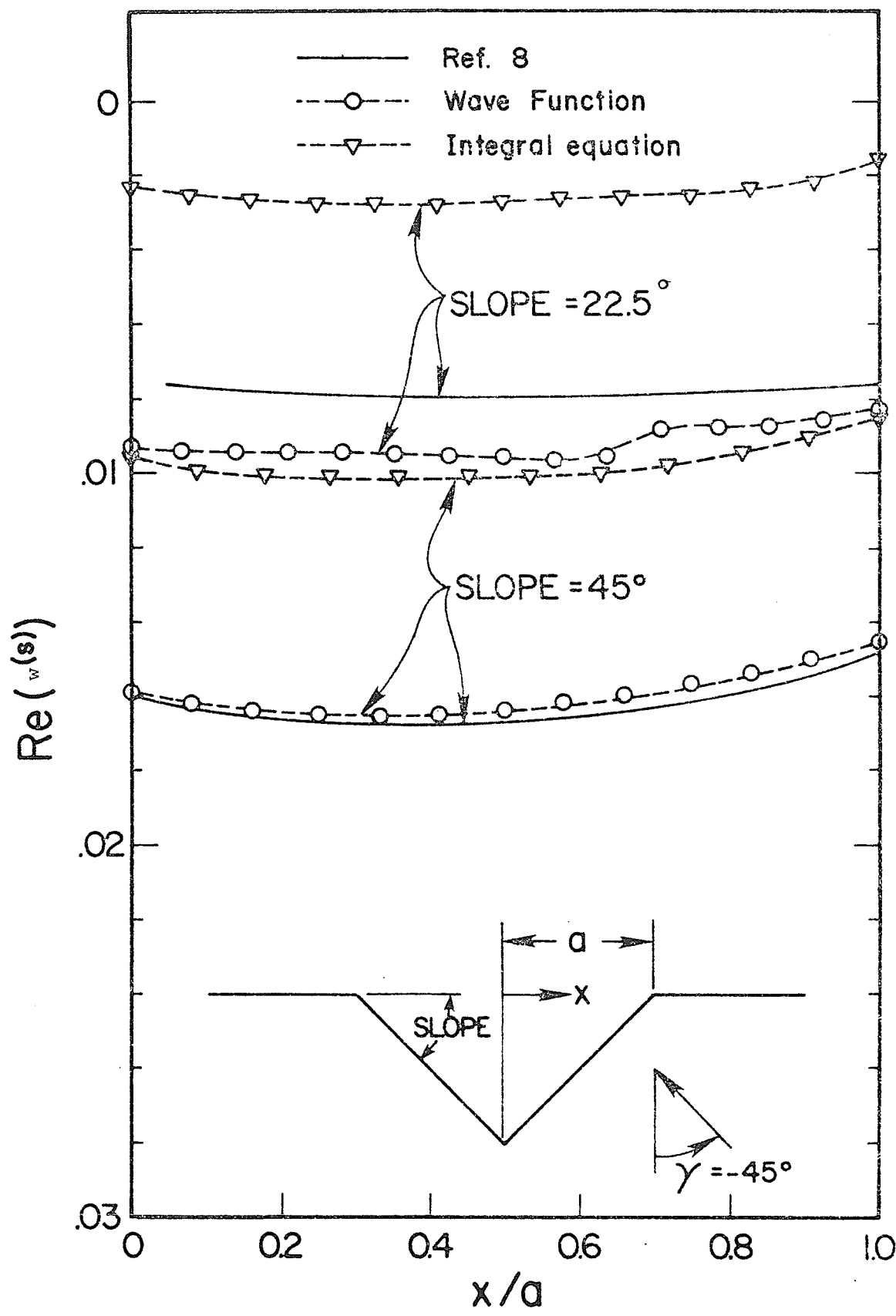


FIGURE 6. Comparison for Real Part of $w^{(s)}$ ($\eta = 0.1/\pi$)

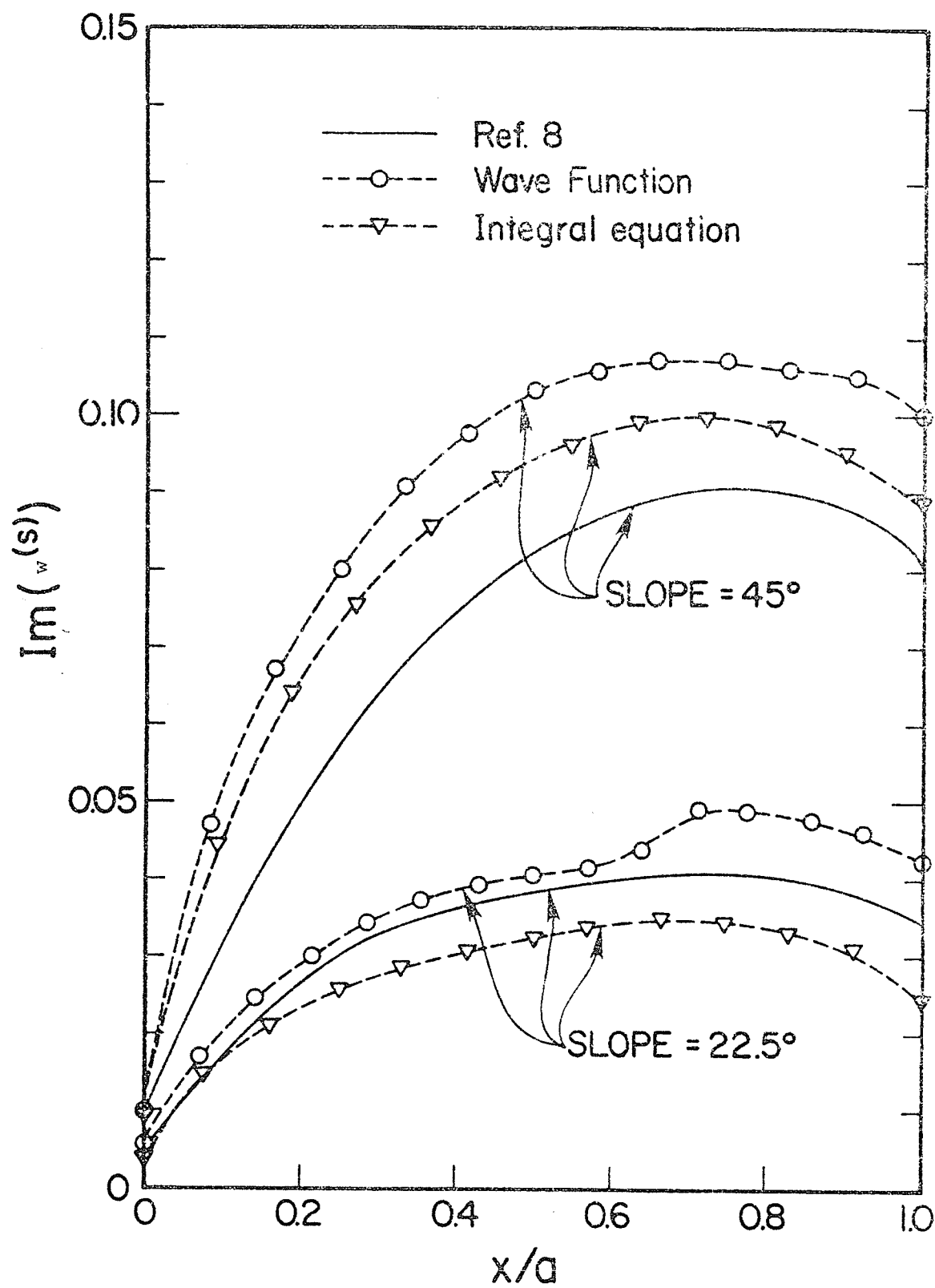


FIGURE 7. Comparison for Imaginary Part of $w^{(s)}$ ($\eta = 0.1/\pi$)

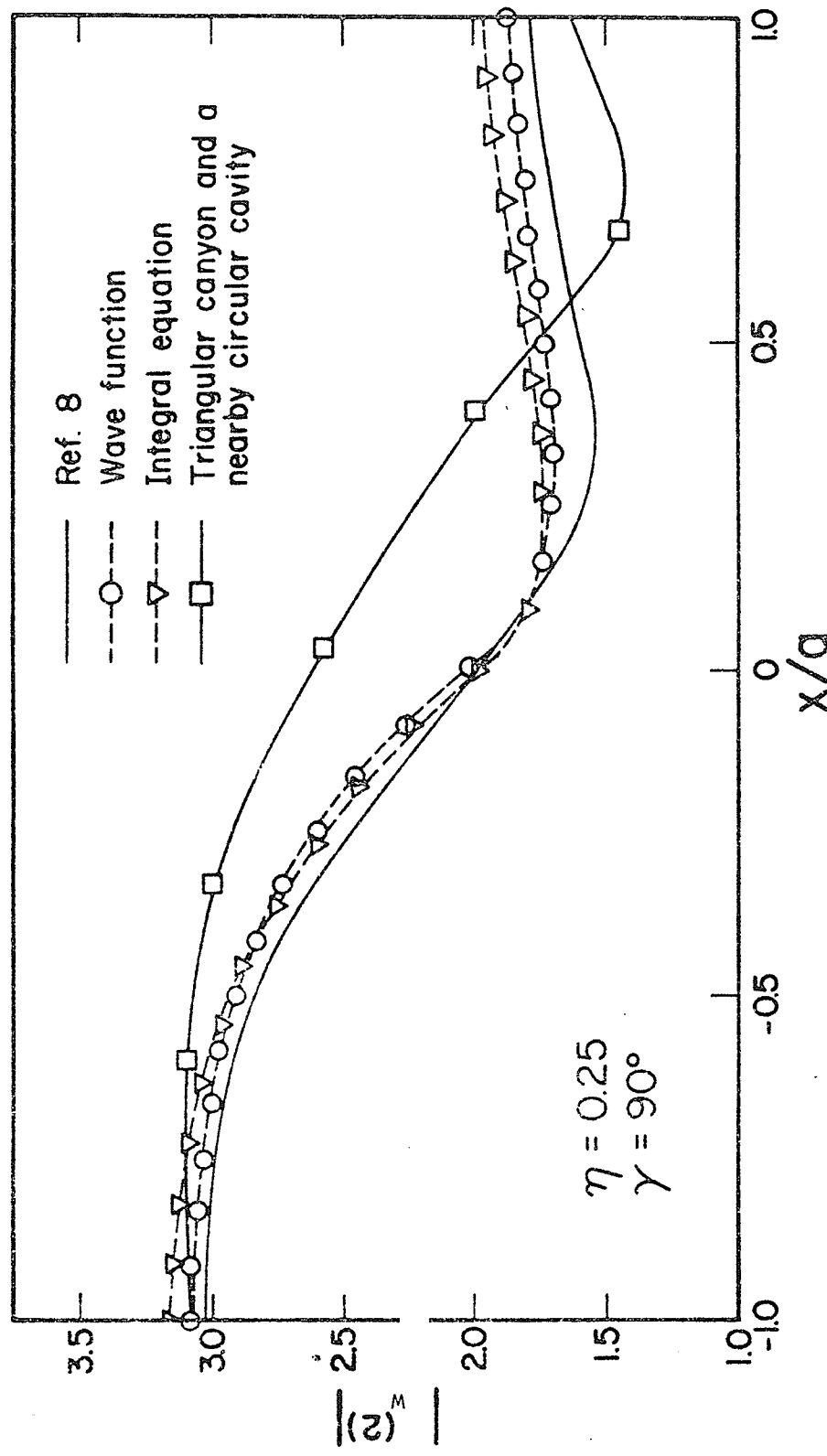


FIGURE 8. Displacement Amplitude at the Surface of a Triangular Canyon With 45° Slopes, With and Without Buried Cavity. ($\eta = 0.25$ and $\gamma = 90^\circ$)

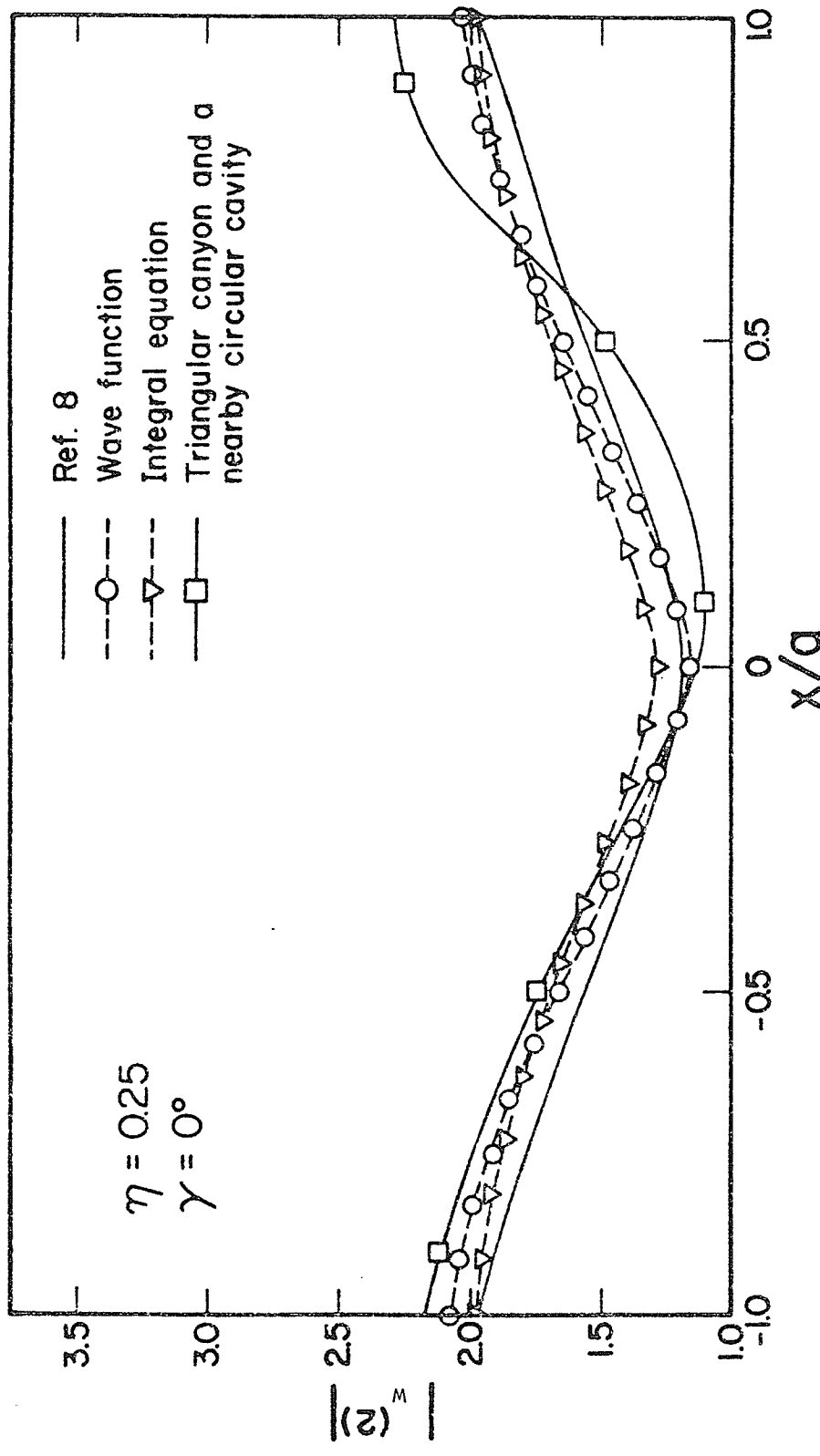


FIGURE 9. Displacement Amplitude at the Surface of a Triangular Canyon With 45° Slopes, With or Without Buried Cavity. ($\eta = 0.25$ and $\gamma = 45^\circ$)

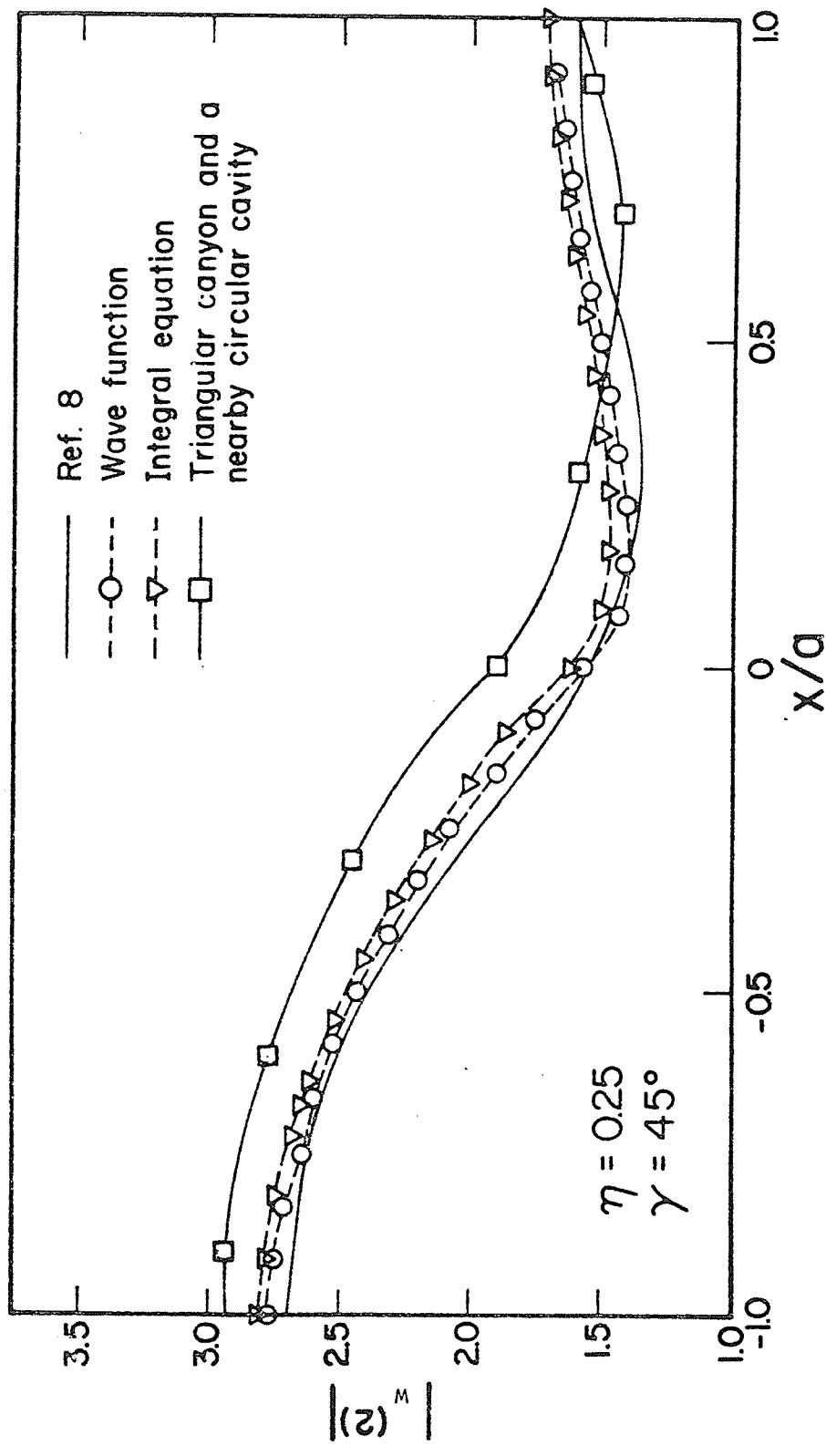


FIGURE 10. Displacement Amplitude at the Surface of a Triangular Canyon With 45° Slopes, With and Without Buried Cavity. ($\eta = 0.25$ and $\gamma = 0^\circ$)

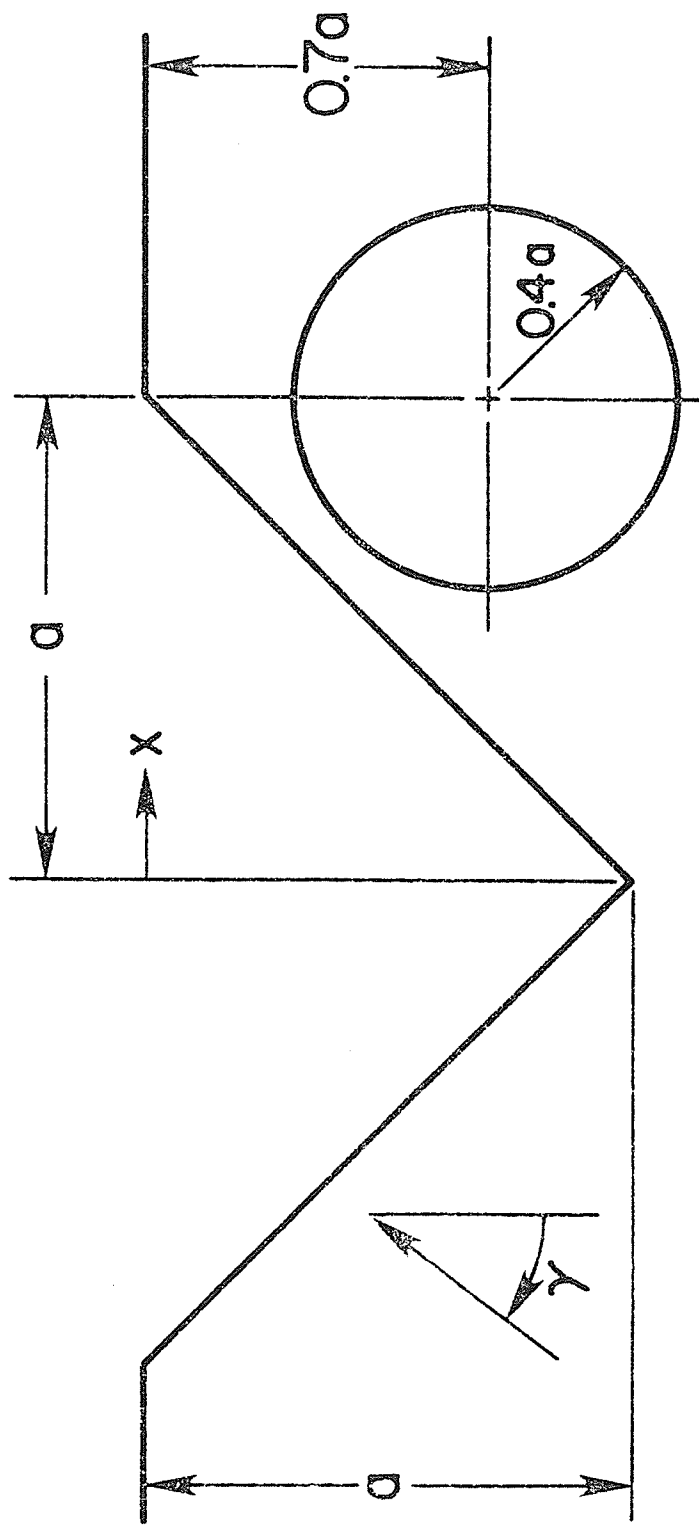


FIGURE 11. Geometry of a Triangular Canyon With Buried Circular Cavity

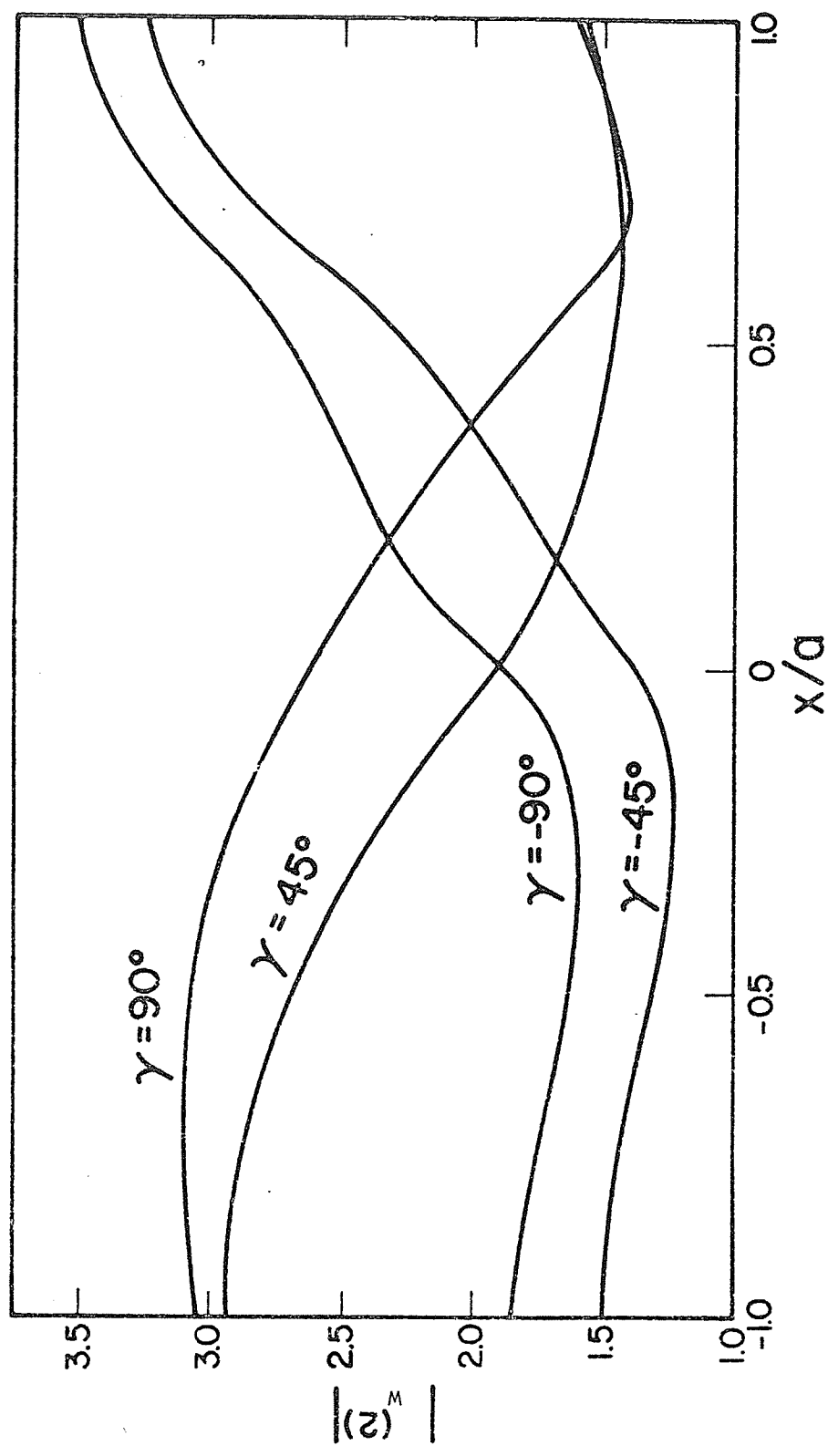


FIGURE 12. Displacement Amplitude at the Surface of a Triangular Canyon With Buried Cavity. ($\eta = 0.25$)

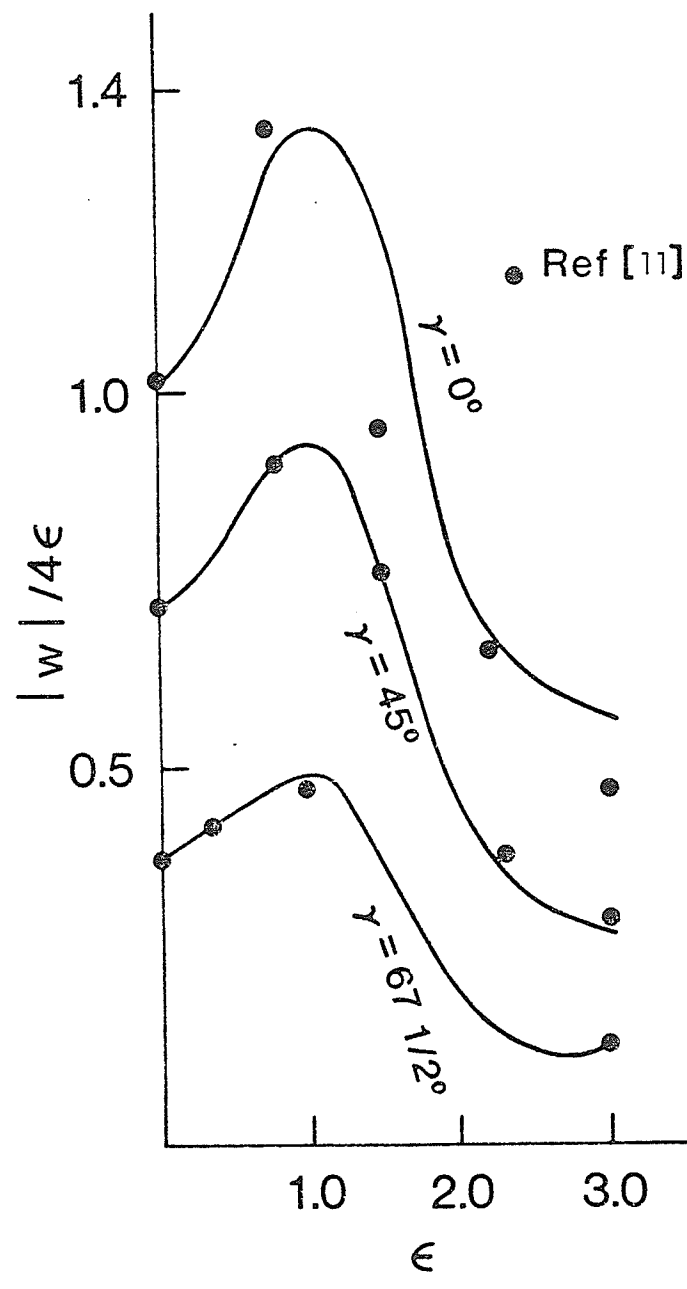


FIGURE 13. COD at the Base of a Normal Crack

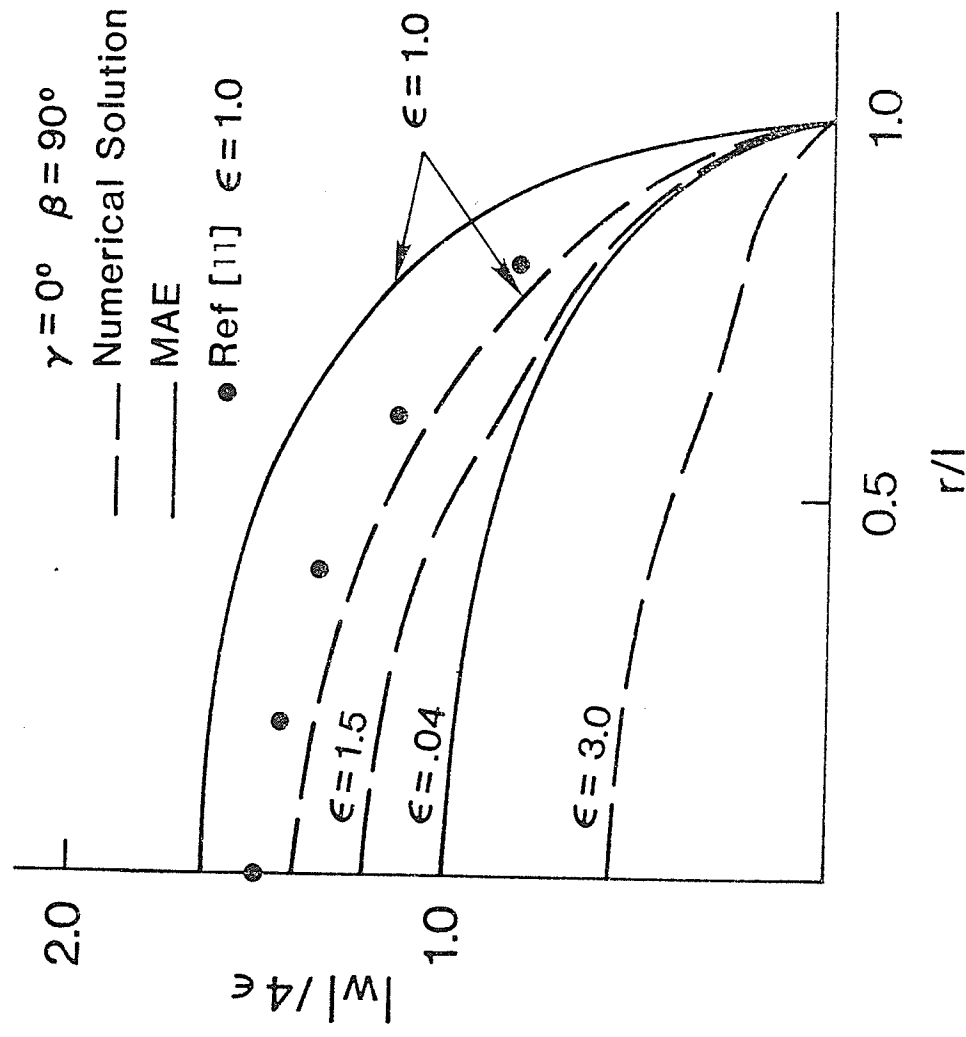


FIGURE 14. COD Along a Normal Crack for Grazing Incidence

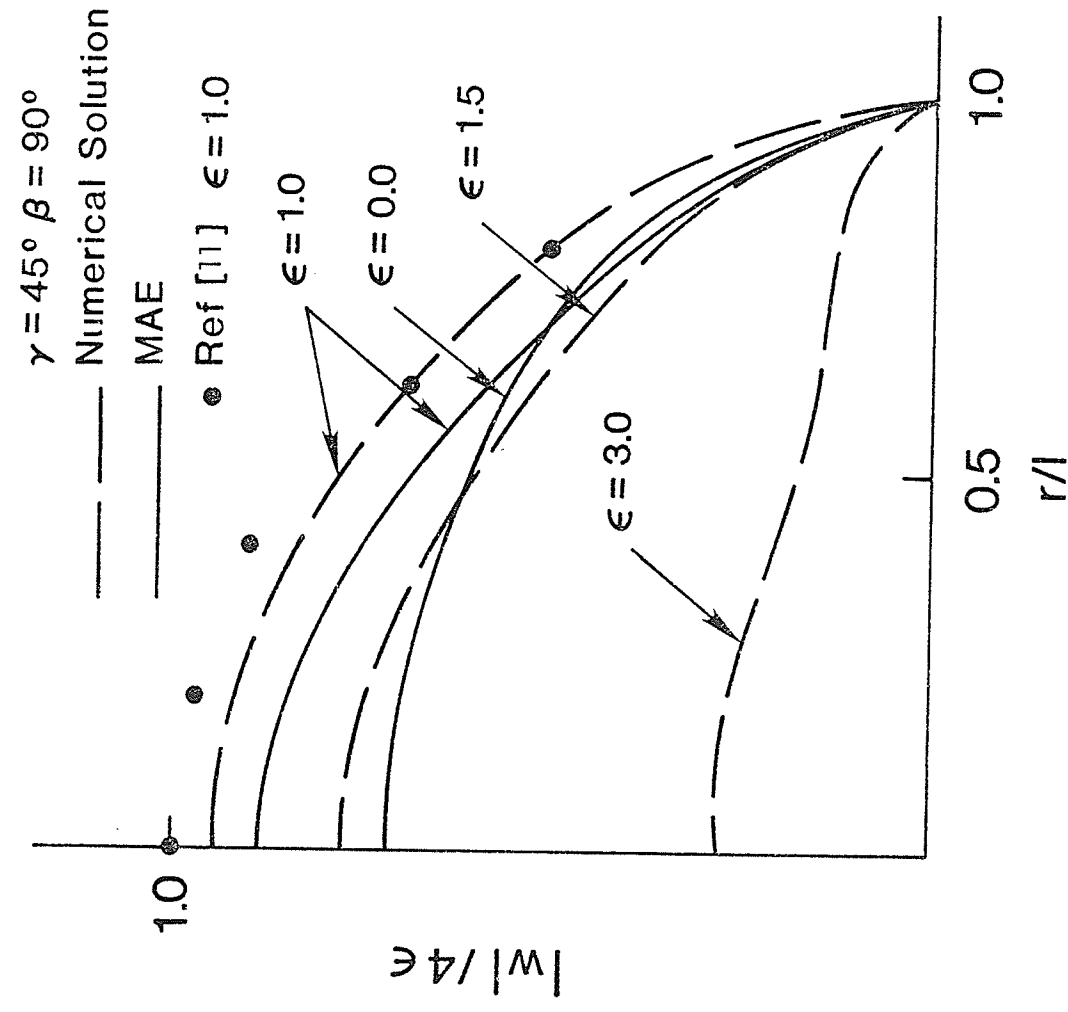


FIGURE 15. COD Along a Normal Crack for 45° Incidence

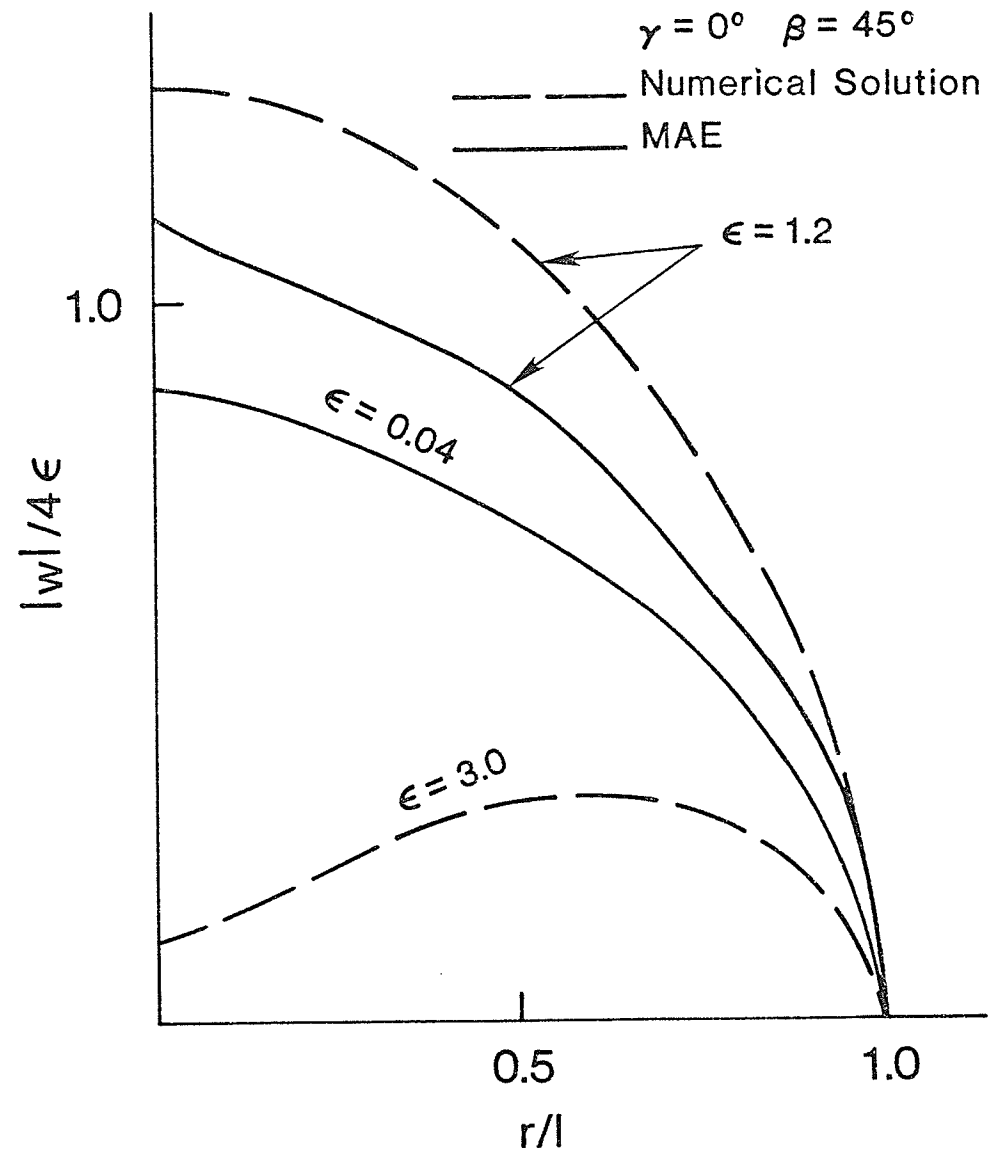


FIGURE 16. COD Along a 45° Canted Crack for Grazing Incidence

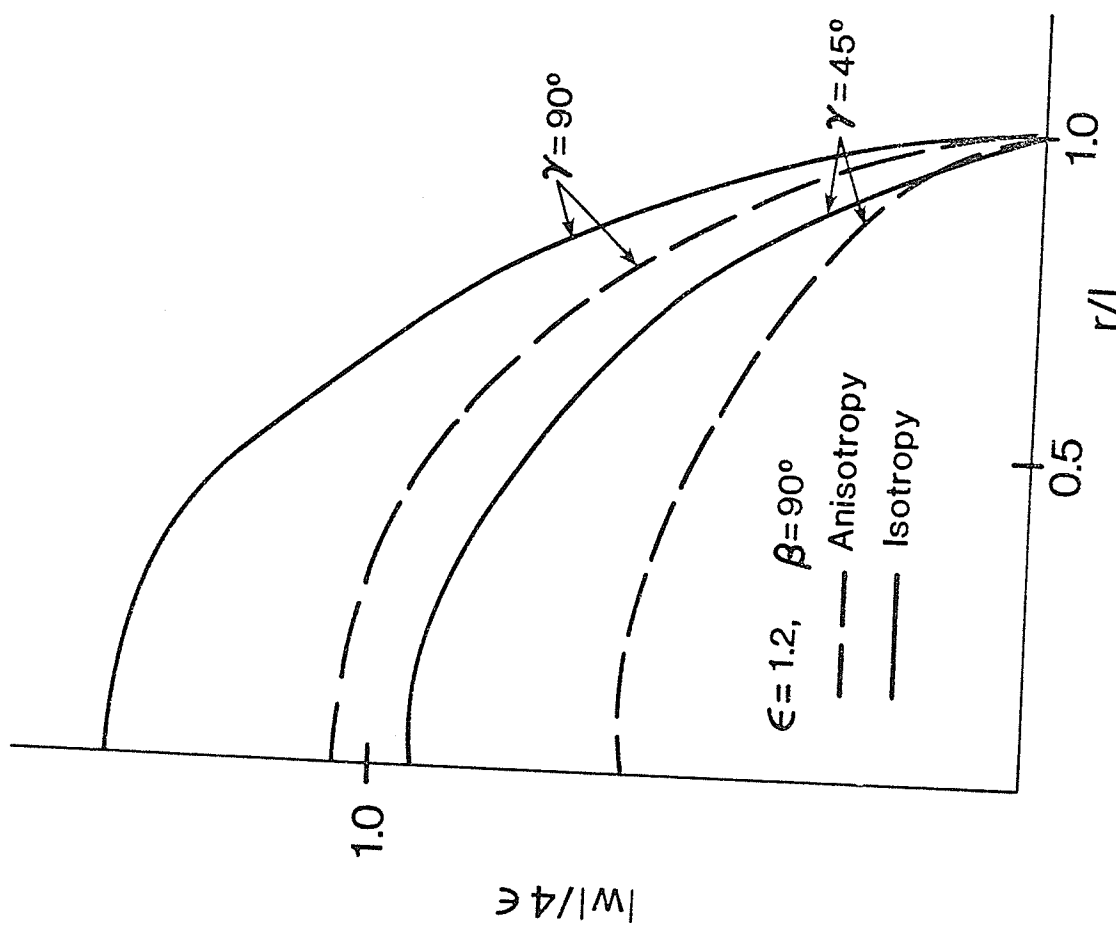


FIGURE 17. COD Along a Normal Crack for Different Incidence Angles

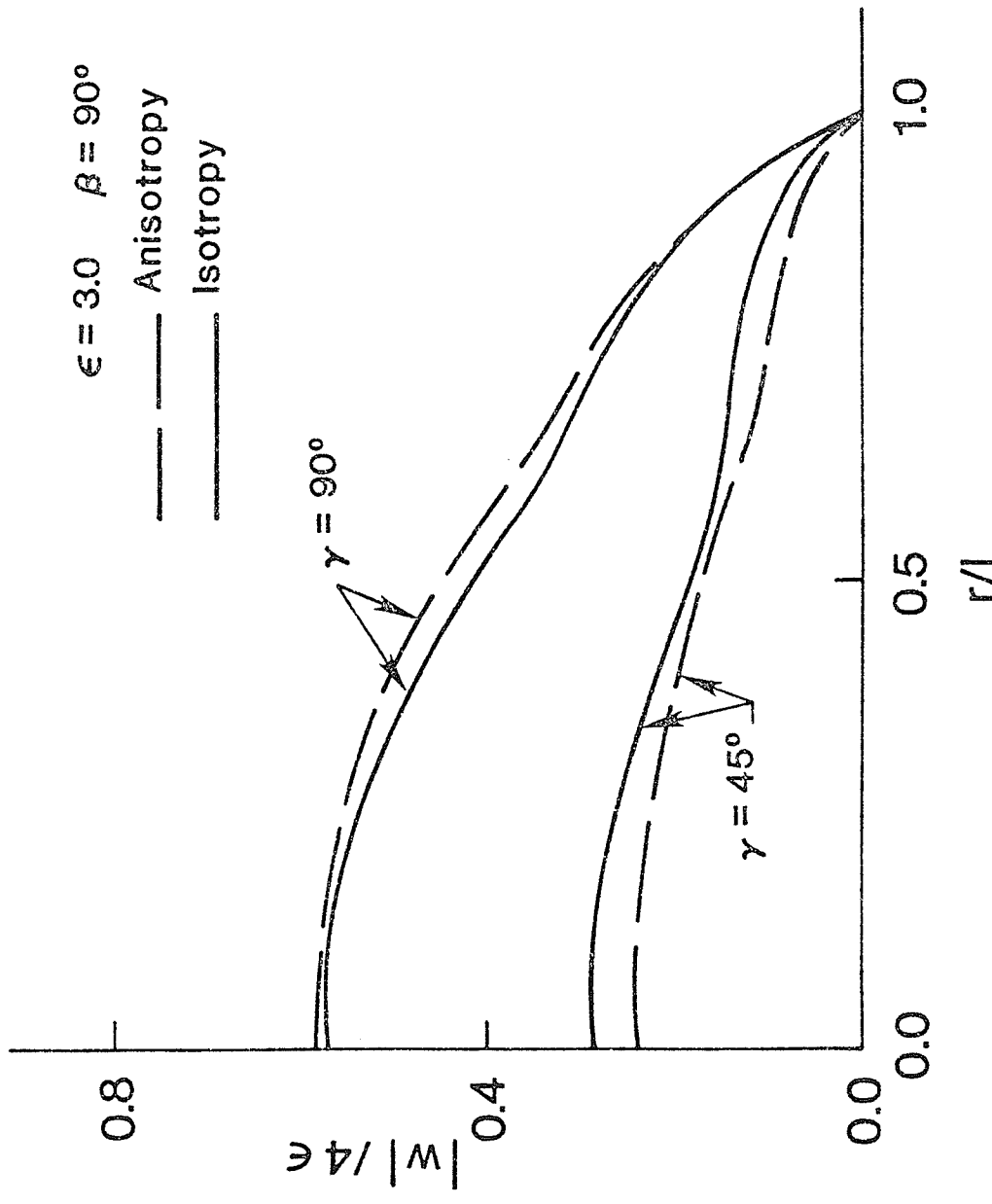


FIGURE 18. COD Along a Normal Crack for Different Incidence Angle

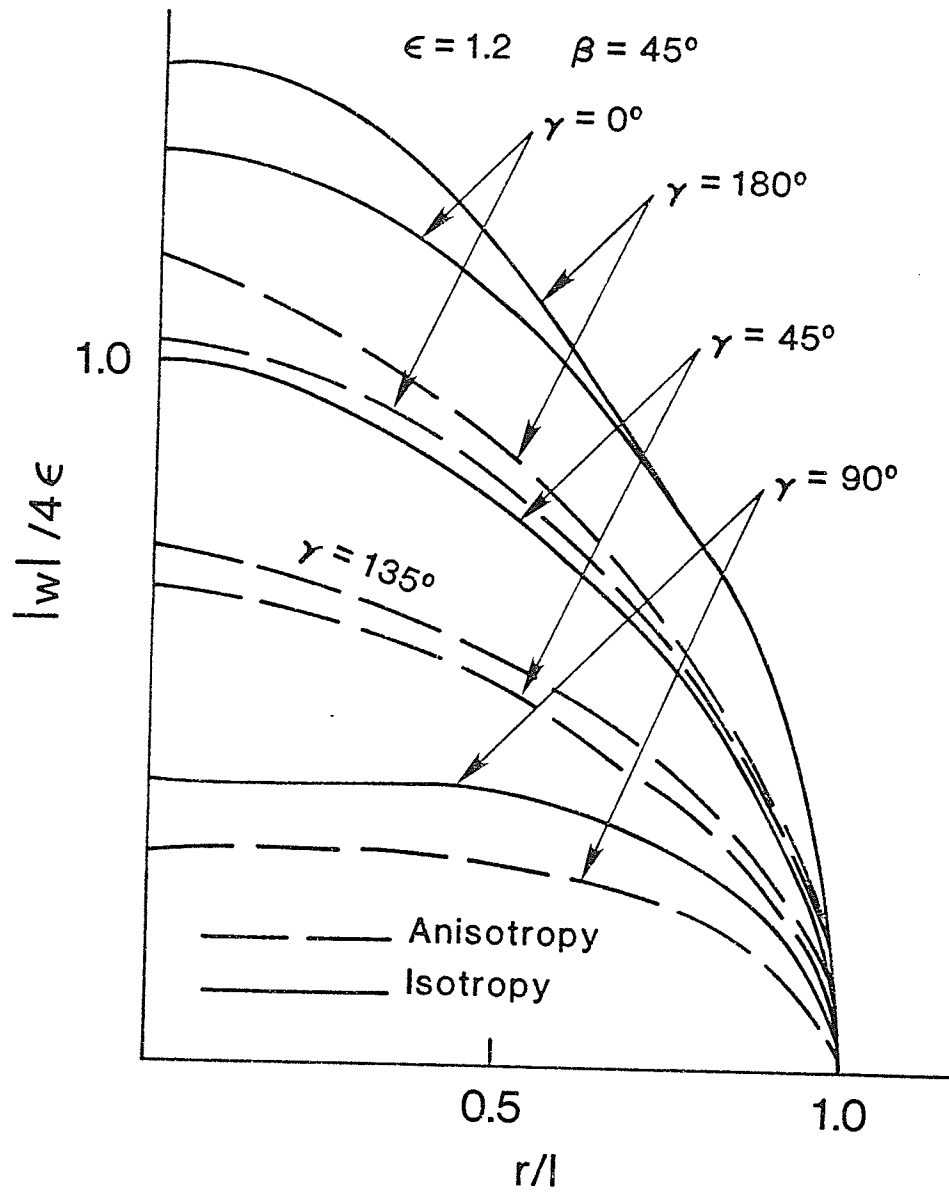


FIGURE 19. COD Along a 45° Canted Crack for Different Incidence Angles

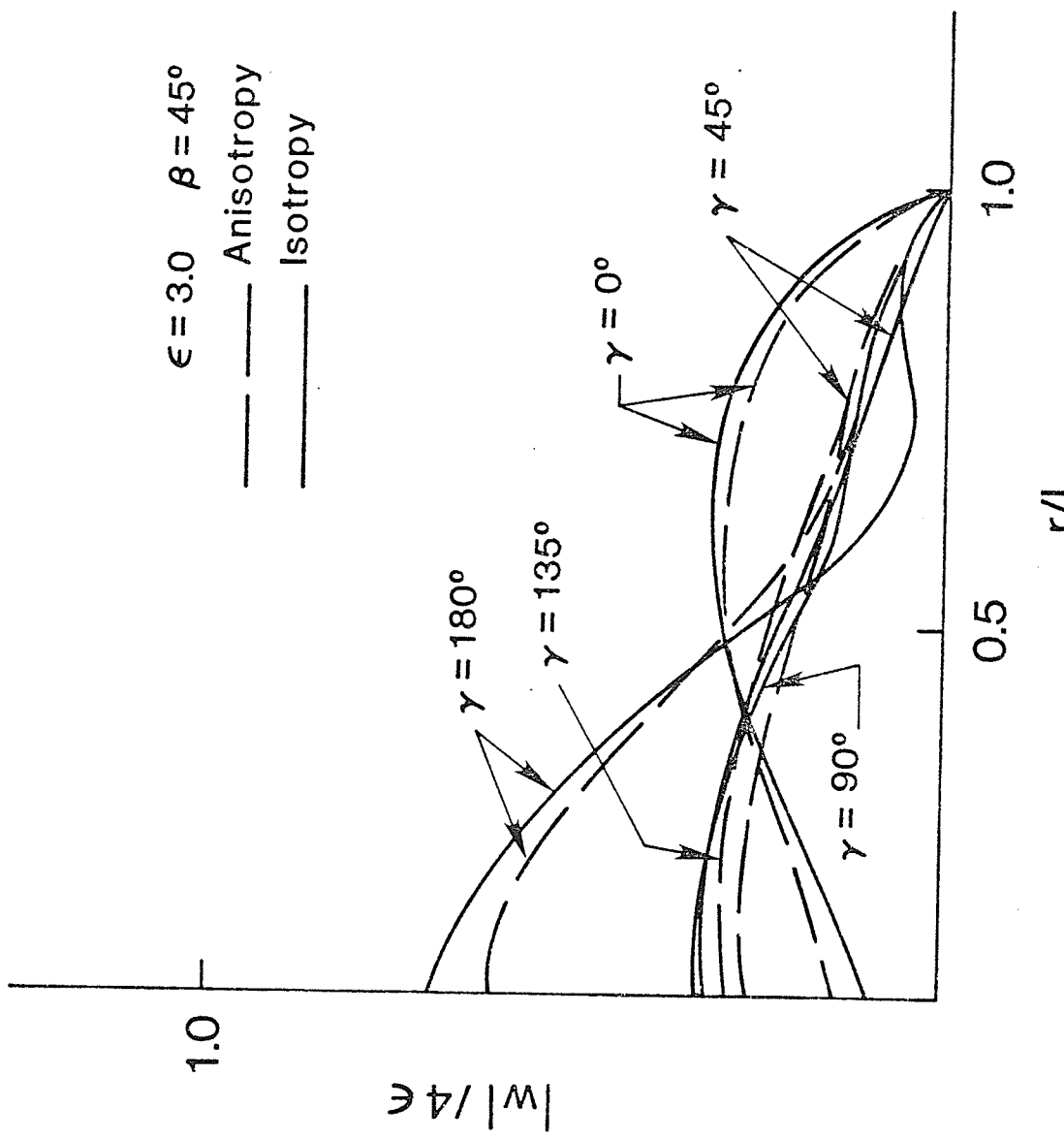


FIGURE 20. COD Along a 45° Canted Crack for Different Angles

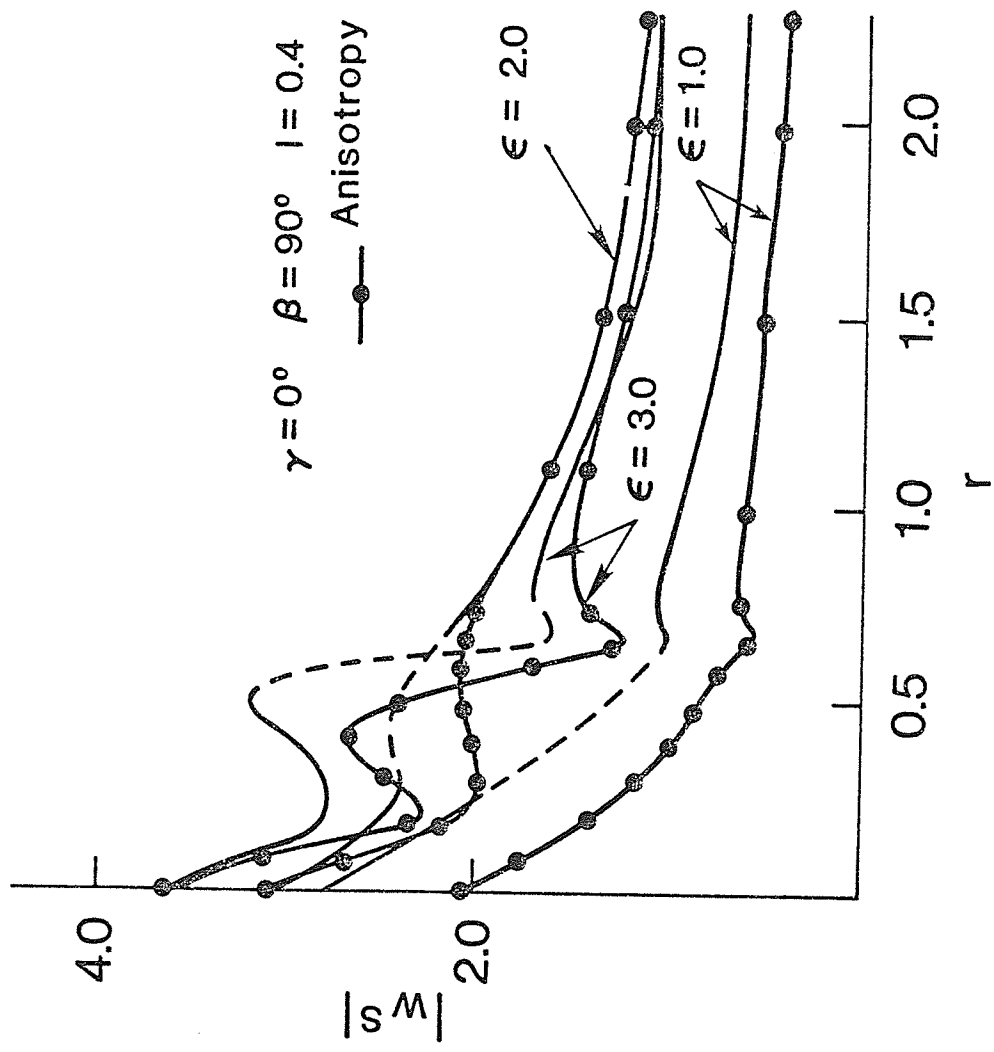


FIGURE 21. Magnitude of the Scattered Field Due to a Normal Crack Along the Free Surface

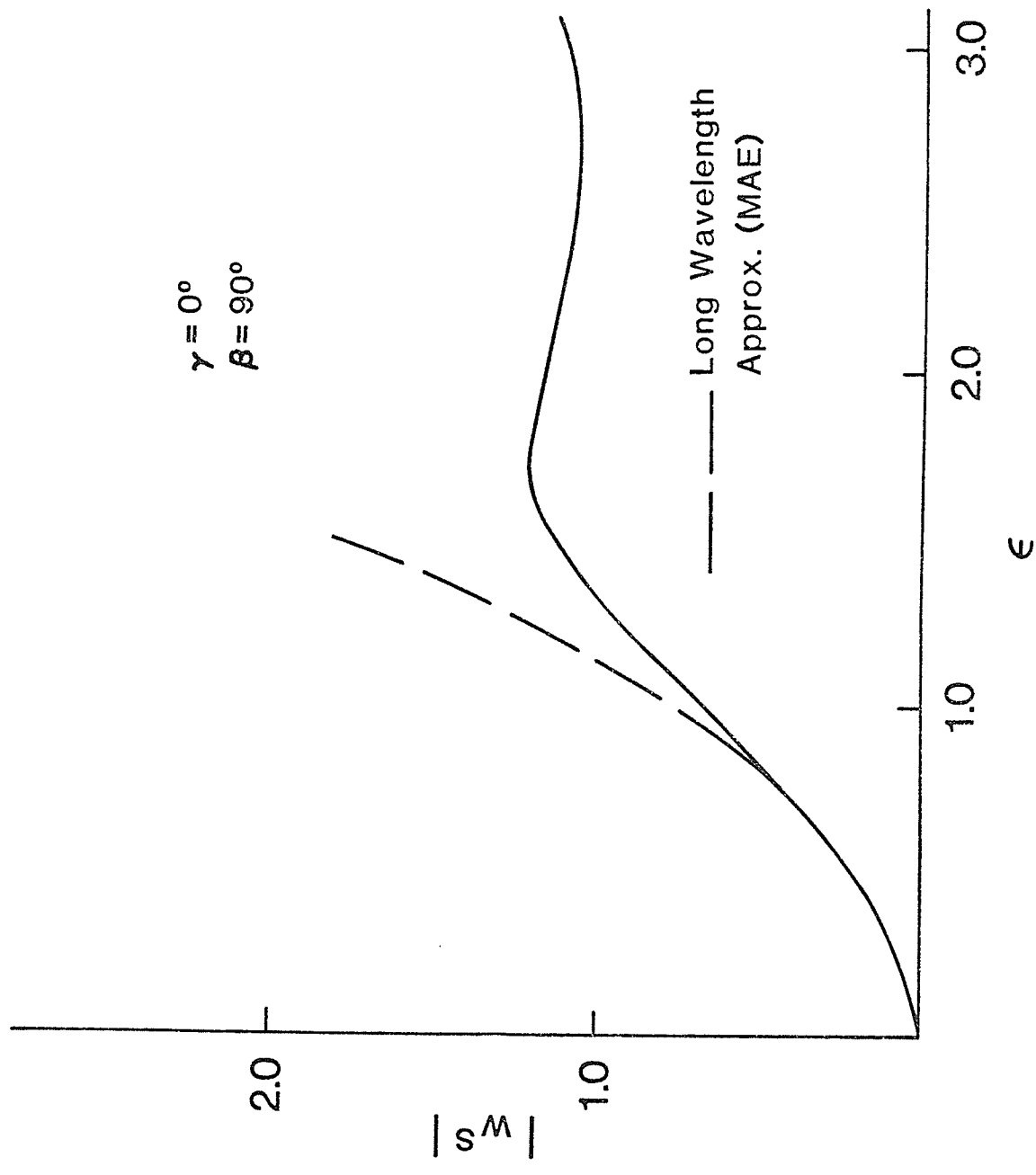


FIGURE 22. Comparison of the Far Field Scattered Displacement Amplitudes obtained by MAE and Numerical Techniques

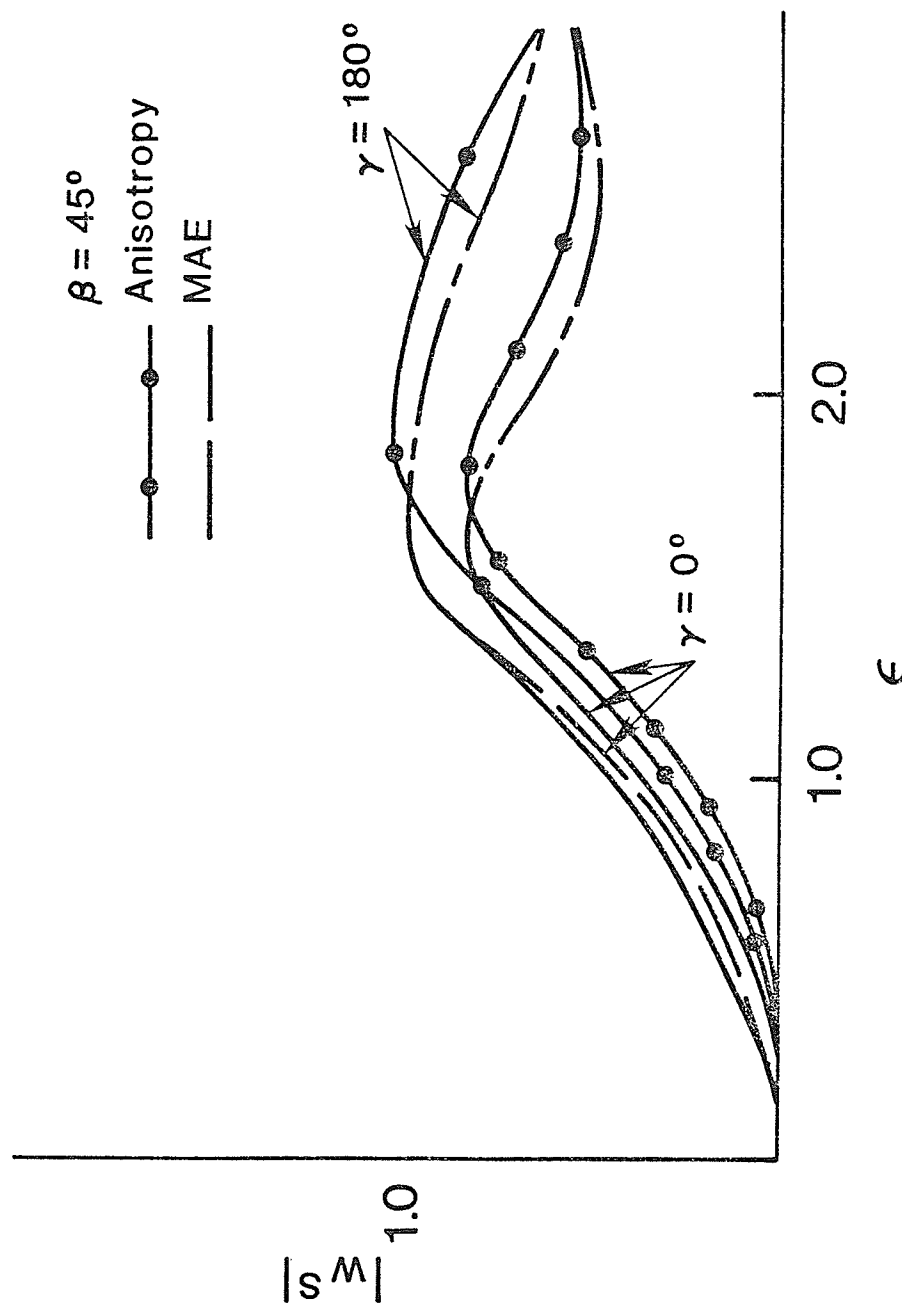


Figure 23. Far Field Scattered Displacement Amplitude Due to a 45° Canted Crack

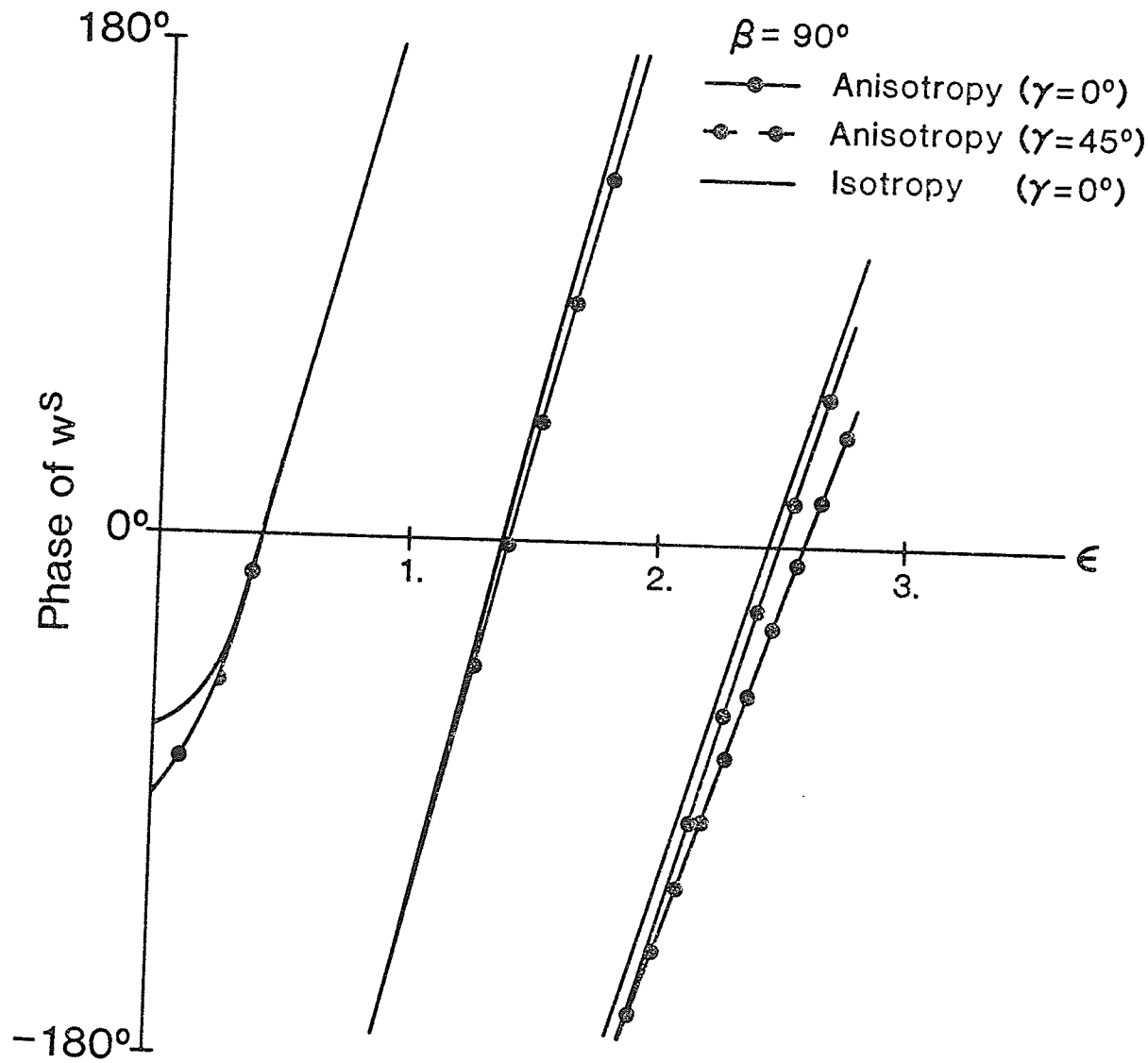


FIGURE 24. Phase of the Far Field Scattered Displacement Due to a Normal Crack.

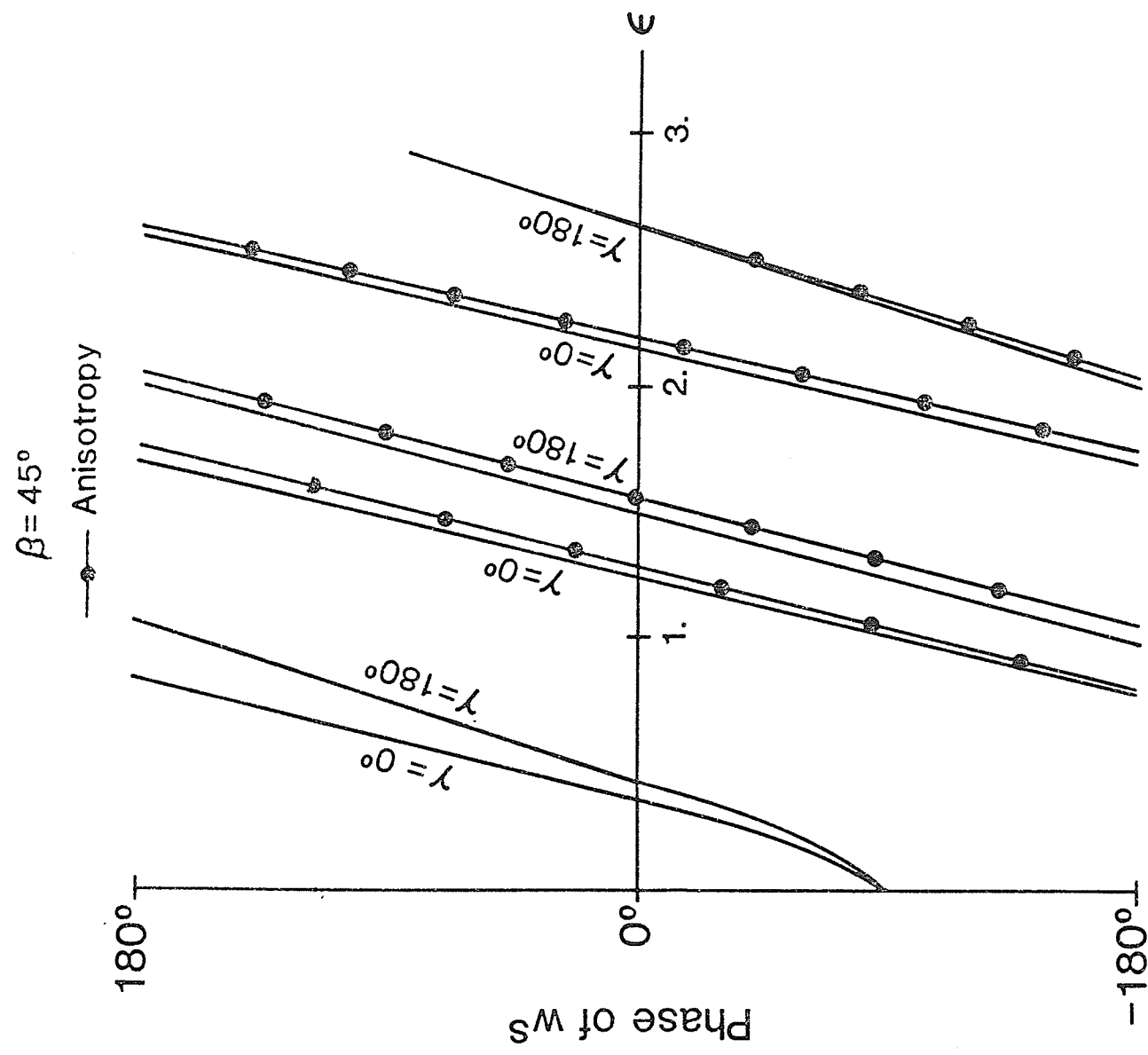


FIGURE 25. Phase of the Far Field Scattered Displacement Due to a 45° Crack

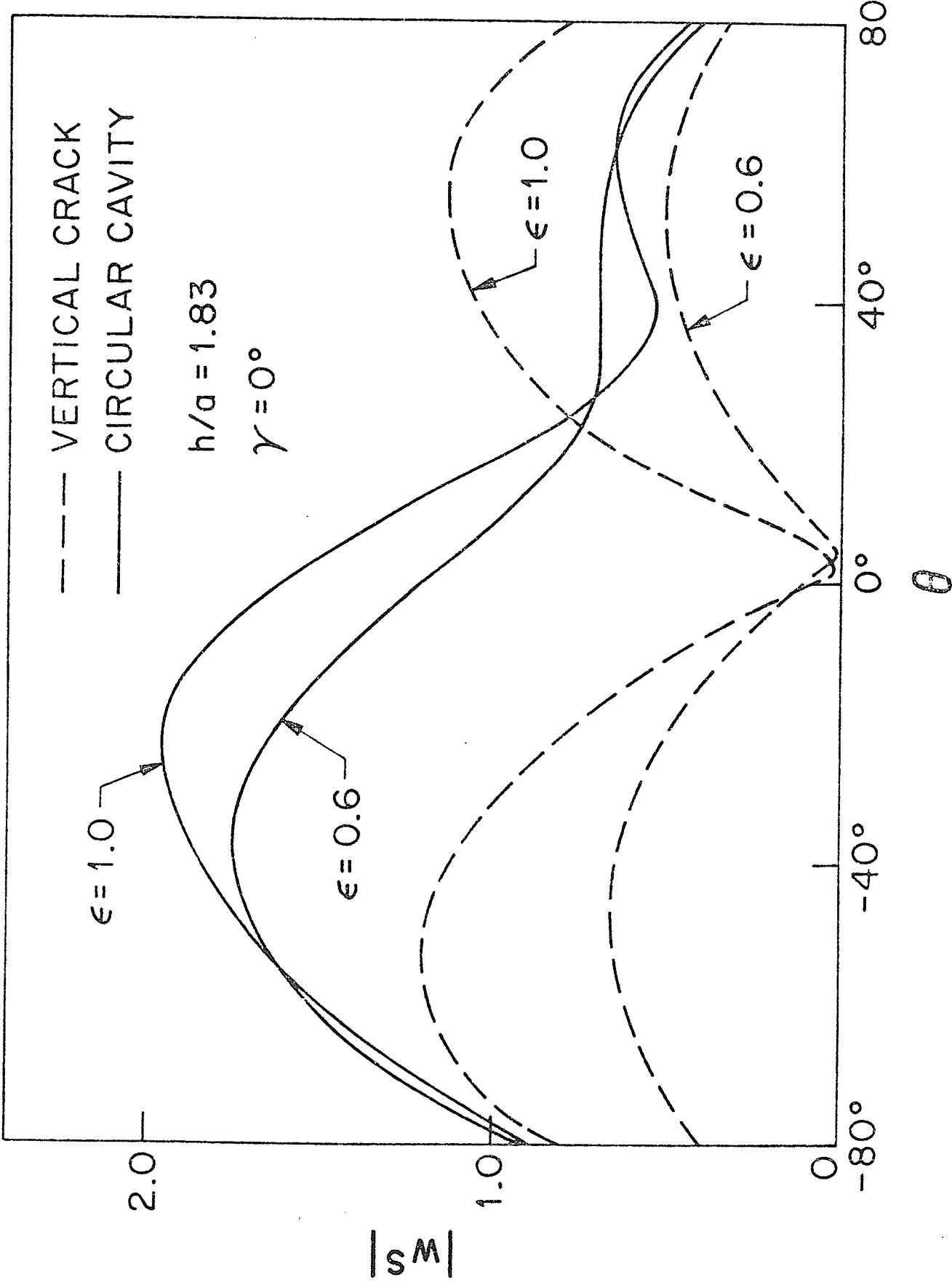


FIGURE 26. Scattered Displacement Amplitudes on the Free Surface Due to a Buried Circular Cavity and a Vertical Crack

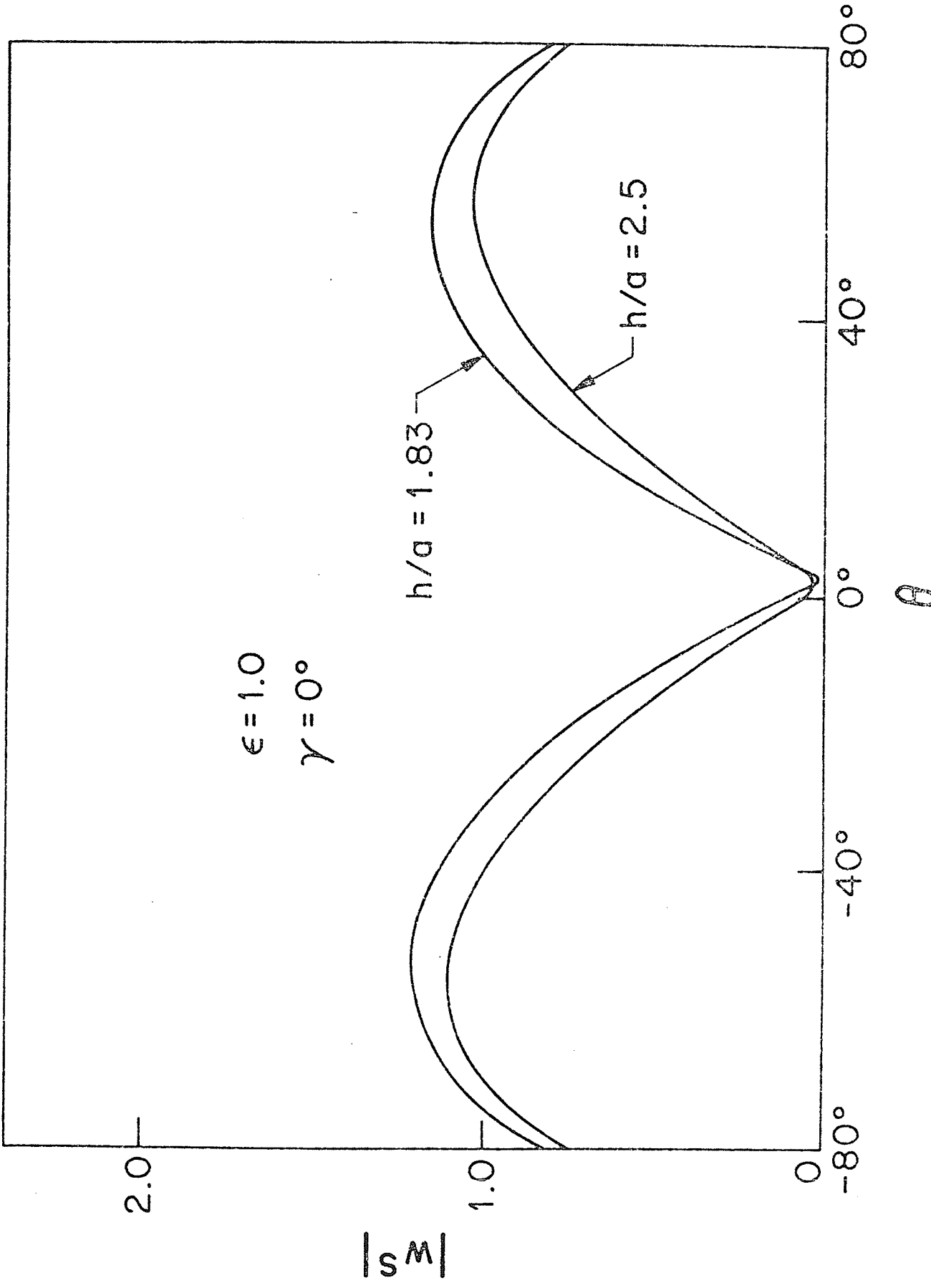


FIGURE 27. Scattered Displacement Amplitudes on the Free Surface Due to a Vertical Crack Embedded at Different Depths

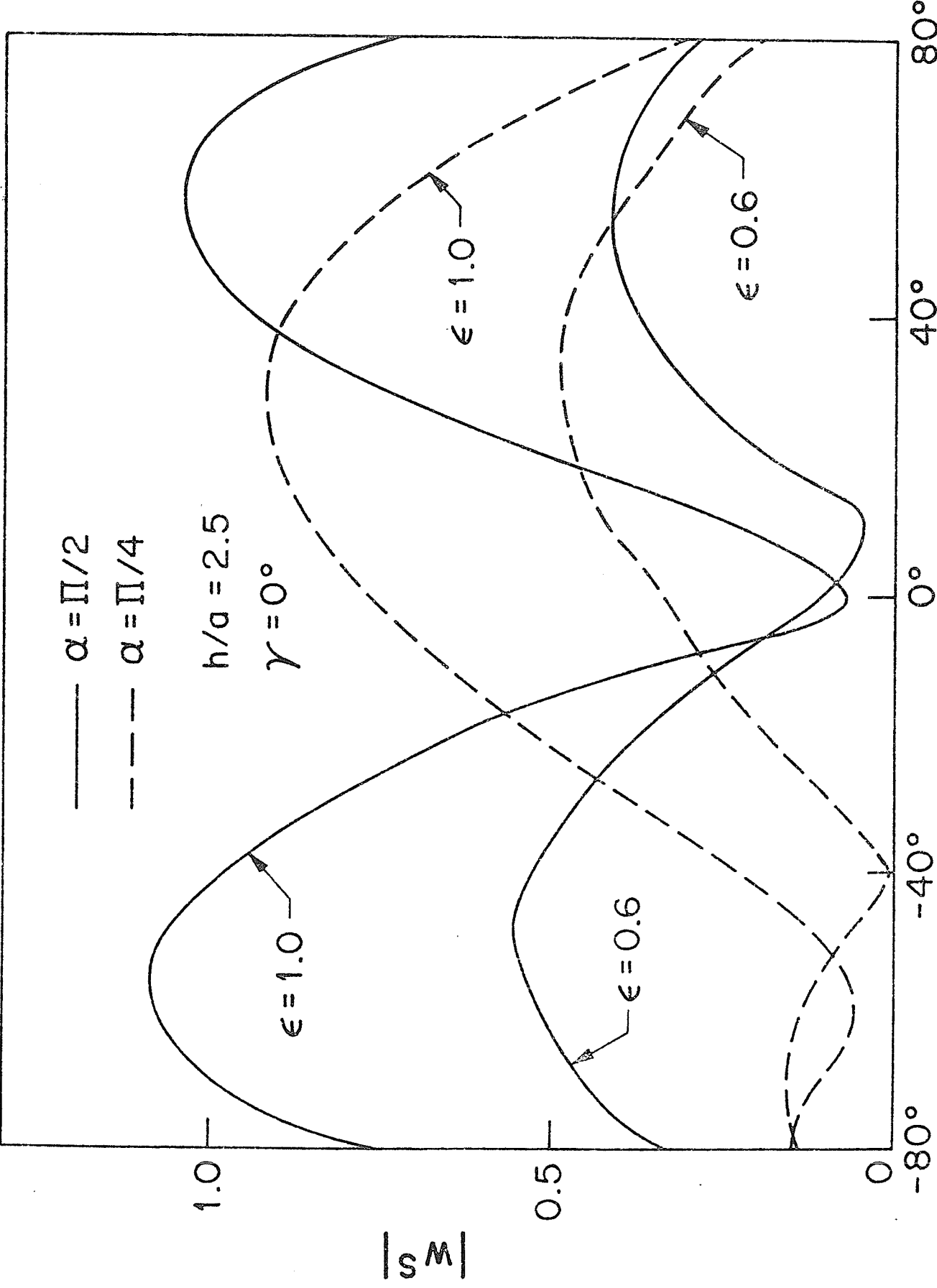


FIGURE 28. Scattered Displacement Amplitudes Due to
Buried Cracks of Different Orientations

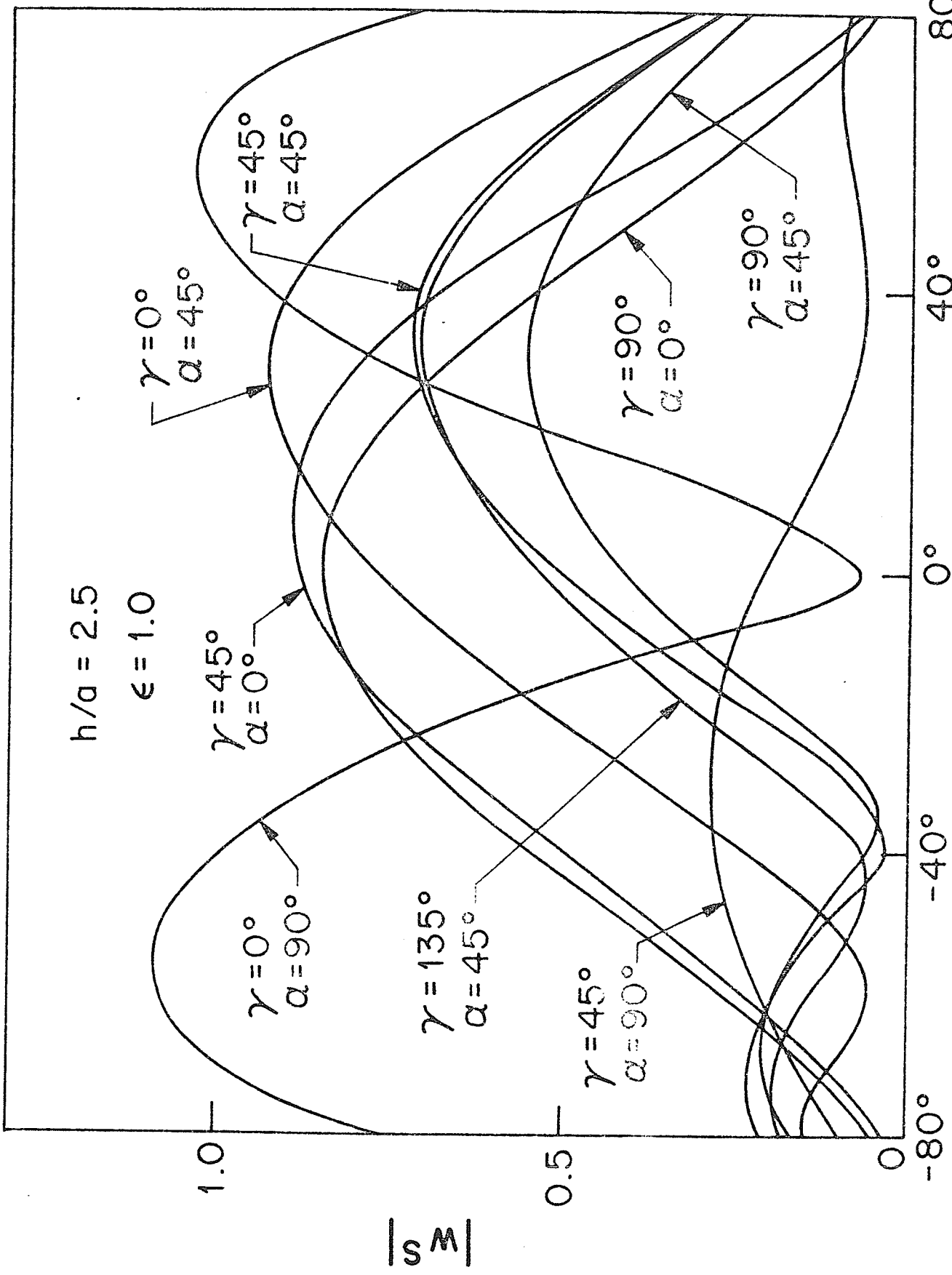


FIGURE 29. Scattered Displacement Amplitudes Due to Buried Cracks of Different Orientations and For Different Angles of Incidence

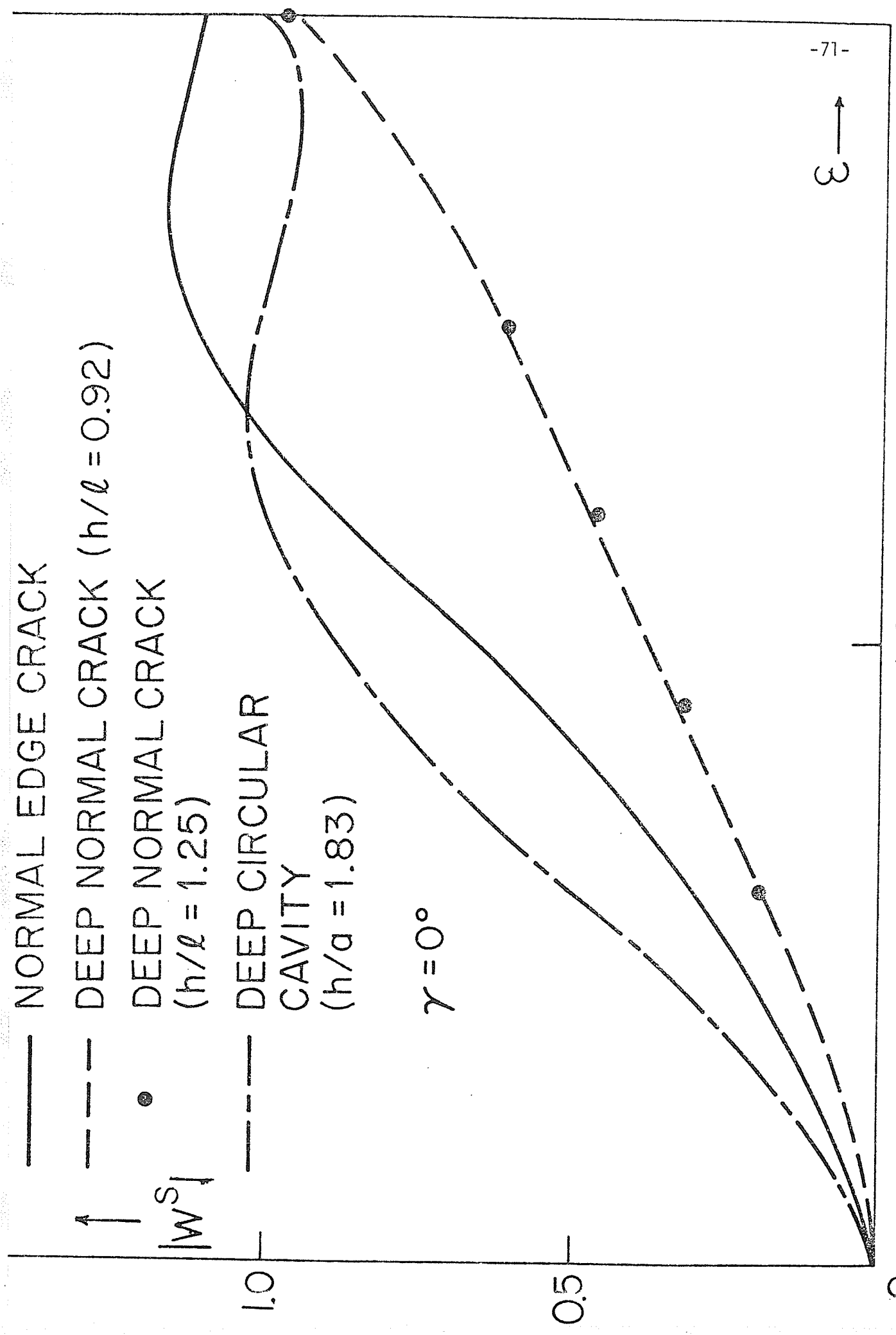


FIGURE 30. Comparison of the Back Scattered Displacement Amplitudes Due to a Buried Crack and a Circular Cavity, and an Edge Crack

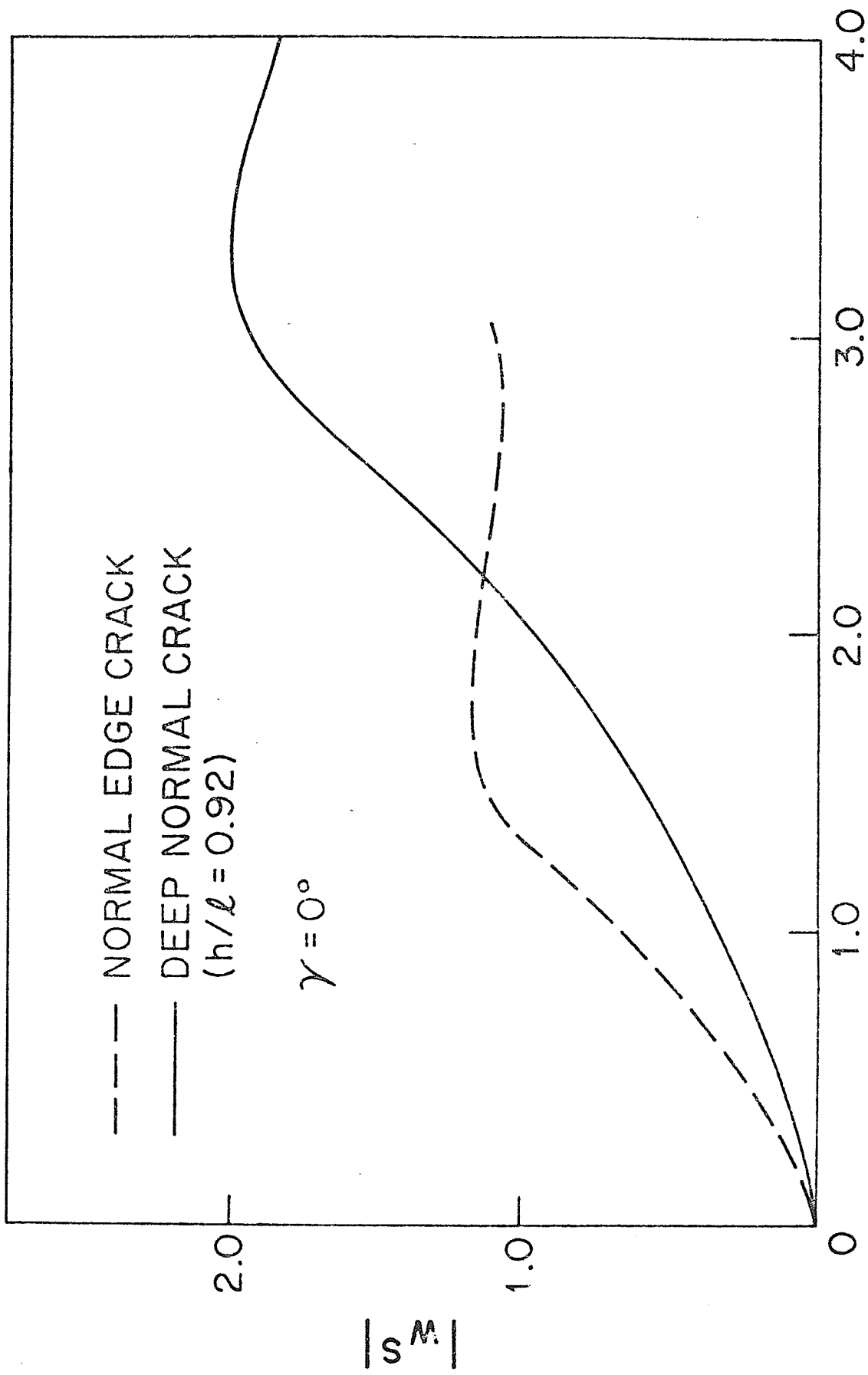


FIGURE 31. Comparison of the Back Scattered Displacement Amplitudes Due to a Buried Vertical Crack and a Vertical Edge Crack

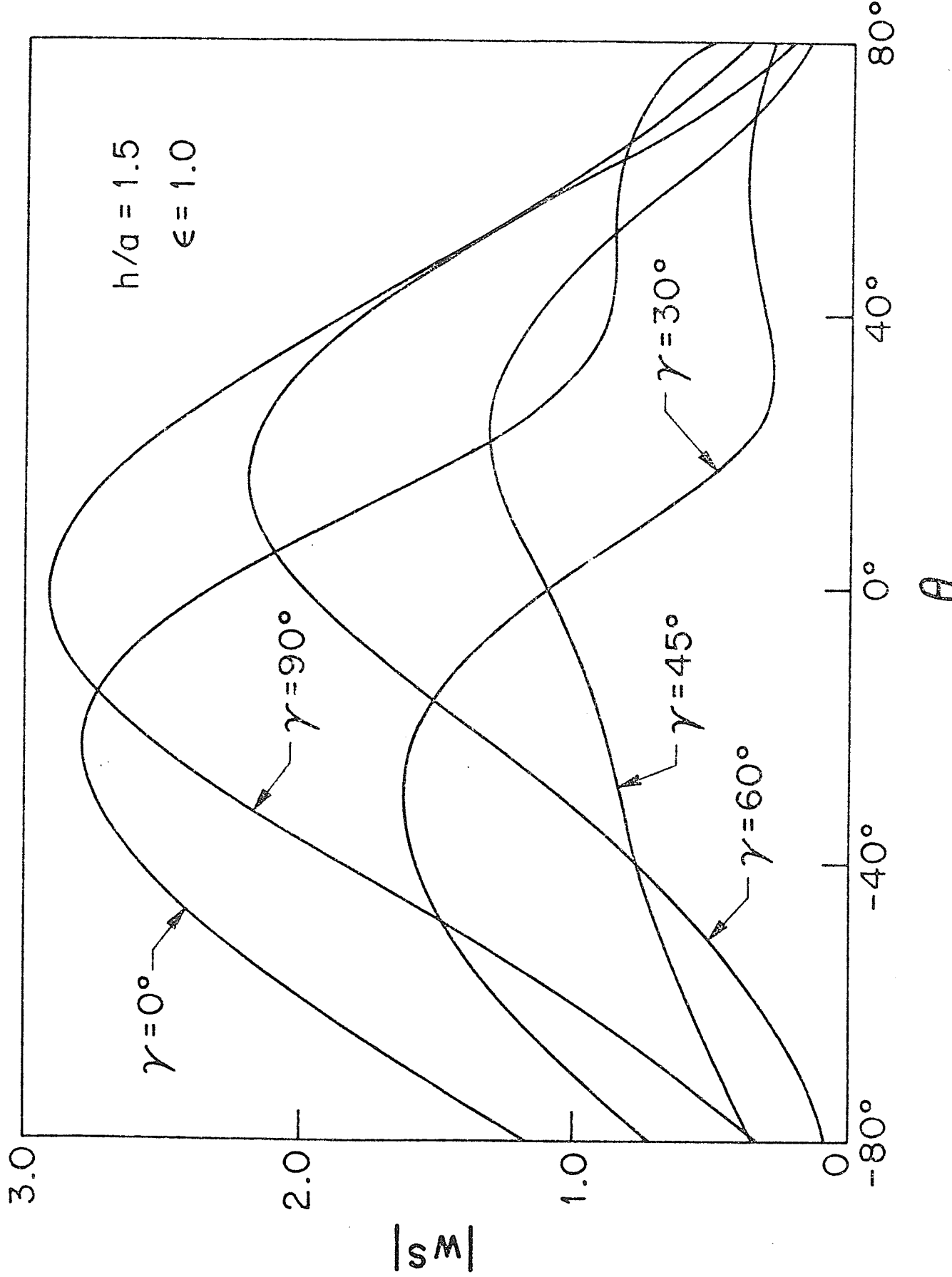


FIGURE 32. Scattered Displacement Amplitudes on $y = 0$ for a Buried Circular Cavity for Various Angles of Incidence

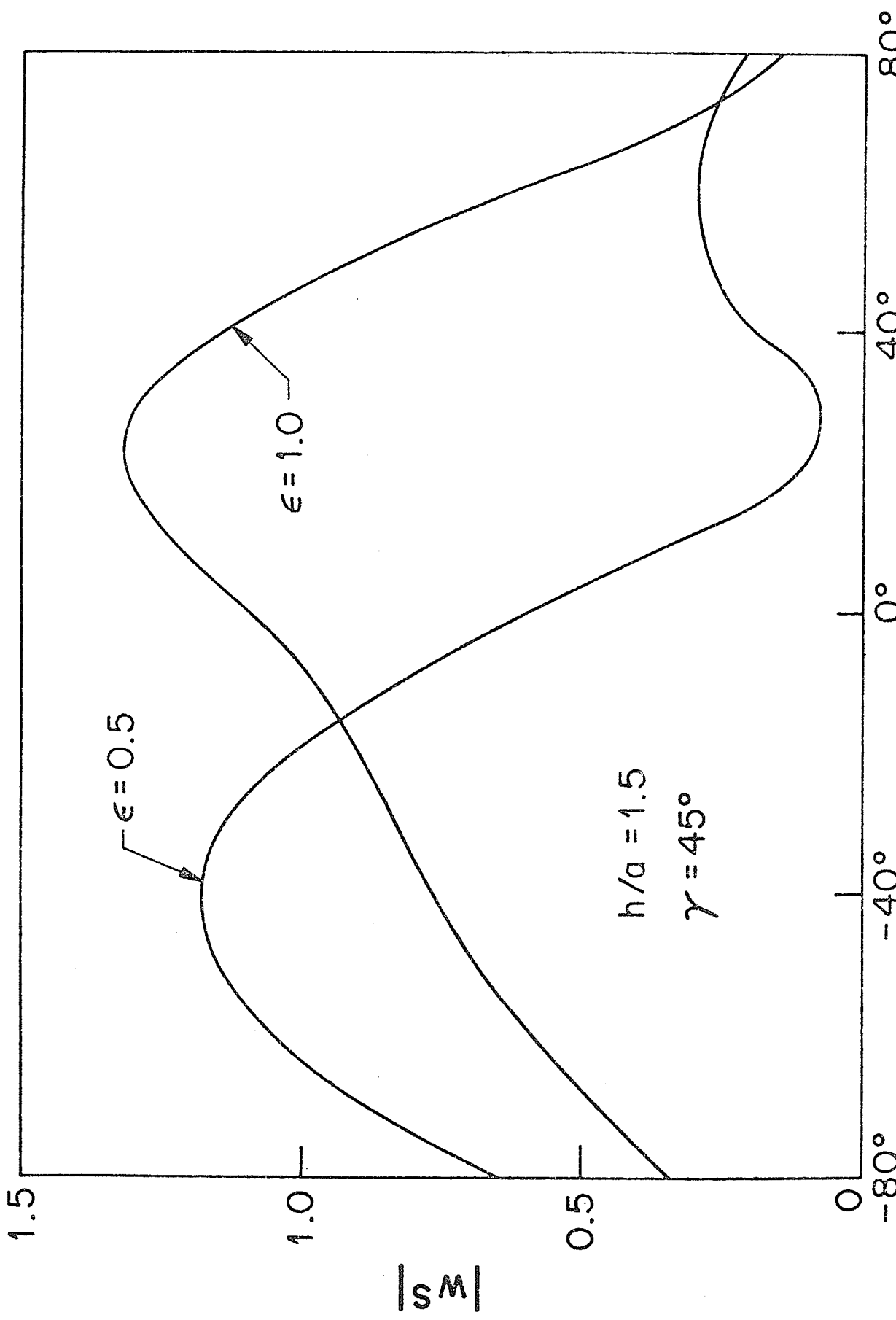


FIGURE 33. Scattered Displacement Amplitudes on $y = 0$ for Different Wave Numbers Due to a Buried Circular Cavity

$\gamma = 0^\circ$, $\epsilon = 1.0$
 $h/a = 1.83$

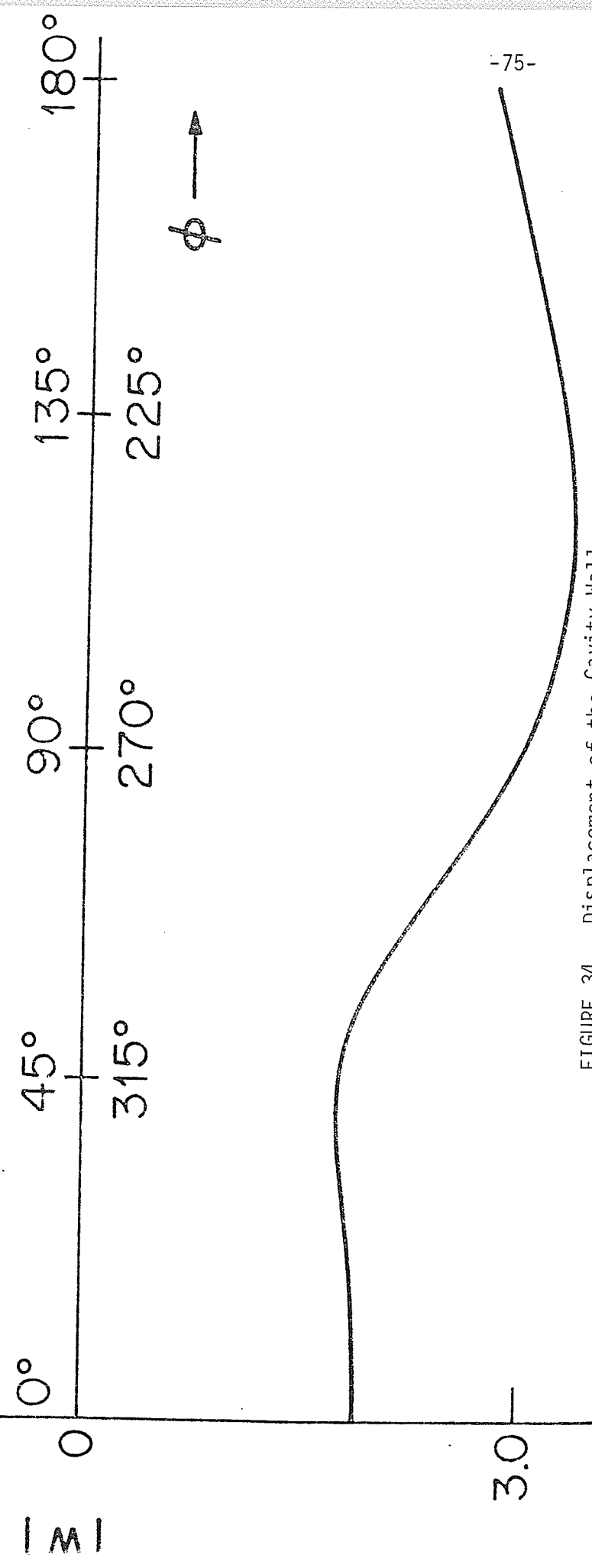


FIGURE 34. Displacement of the Cavity Wall

A P P E N D I X D
LISTING OF THE COMPUTER PROGRAM

C
C PROGRAM WEX
C

```
INTEGER ITFL/123/,ITNP/86/,LAMDA/1/,IELNO1/42/,  
+ IELNO2/61/  
INTEGER IVER(123,3),NPINC,NPINE,NPONS,NPONC,NPONM,NPONB,  
+ ISTA1,IEND1,ISTAR2,IFND2,ISTAR3,IEND3,  
+ ISTAR4,IEND4,ISTAP5,IEND5,ISTAR6,IEND6,  
+ ISNPS,LNPS,ISNPC,LNPC,ISNPM,LNPM,ISNPR,LNPR  
REAL*8 GAMMA/1.047197551/,DFLTA/0.1570796/,  
+ RS/1.0D0/,PC/1.1D0/,RM/1.2D0/,RB/1.3D0/  
REAL*8 X(86),Y(86),RKAPA1,RKAPA2,RK(86,86),ANGLEC(86),  
+ SIE(65,21),ATER,INC  
COMPLEX*16 IMGG,MAT(21,65),TOTHF(21),CP(65),PRODUT(65),  
+ PSIDE(65),LSIDE(65,65),VA(65)  
COMMON/BLK1/ ISNPS,LNPS,ISNPC,LNPC,ISNPM,LNPM,ISNPR,LNPR  
COMMON/BLK2/ ISTA1,IEND1,ISTAP2,IFND2,ISTAR3,IEND3,  
+ ISTA4,IEND4,ISTAP5,IEND5,ISTAR6,IEND6  
COMMON/BLK3/ RKAPA1  
COMMON/BLK4/ RKAPA2  
COMMON/BLK5/ IMGG  
NPINC=22  
NPINP=65  
NPONS=22  
NPONC=21  
NPONM=22  
NPONP=21  
ISNPS=1  
LNPS=22  
ISNPC=23  
LNPC=43  
ISNPM=44  
LNPM=65  
ISNPR=66  
LNPR=86  
ISTA1=1  
IEND1=21  
ISTAR2=22  
IFND2=41  
ISTAR3=42  
IEND3=61  
ISTAR4=62  
IEND4=82  
ISTAP5=83  
IFND5=103  
ISTAR6=104  
IEND6=123  
IMGG=(0.0D0,1.0D0)  
ATER=1.75  
INC=0.25  
C DO 10 J=1,8  
RKAPA1=ATER*3.141592654  
RKAPA2=ATER*3.141692654  
CALL COOR(X,Y,ITNP,RS,PC,RM,RB,NPONS)
```

```

CALL VERCAL(IVER,ITEL)
CALL CALANG(X,Y,ITNP,ANGLEC)
CALL ZANDK(X,Y,ITNP,IVER,ITEL,RK,SIR,NPINE,NPONE)
CALL INCREF(NPINE,X,Y,TOTPF,ITNP,GAMMA,NPONB)
CALL TERM1(ITNP,IVFP,ITEL,LAMDA,X,Y,ANGLEC,RC,DELTA,
+          NPINB,NPONB,MAT,GP)
CALL TERM2(ITNP,ITEL,IELNO1,IFLNO2,IVER,X,Y,RC,ANGLEC,
+          PRODUT,MAT,LAMDA,DELTA,NPINB,NPONB,NPONC)
CALL RIGUT(SIP,TOTHE,RSIDE,NPINB,NPONB)
CALL LEFT(RK,SIR,MAT,NPONE,NPINB,ITNP,LSIDE)
CALL SOLVE(RSIDE,LSIDE,NPINB,NPONB,UA)
C      ATER=ATFR+INC
C10    CONTINUE
      RETURN
      END
      SUBROUTINE COOR(X,Y,ITNP,ES,RC,RM,PP,NPONS)
      INTEGER ITNP,NPONS,ISNPS,LNPS,ISNPC,LNPC,ISNPM,LNPM,
+           ISNPR,LNPR
      REAL*8 X(ITNP),Y(ITNP),RS,RC,RM,RB,PI,DIV,RINC,RINCC
      COMMON/BLK1/ ISNPS,LNPS,ISNPC,LNPC,ISNPM,LNPM,ISNPR,LNPR
      PI=3.141592654
C DIV CHANGED UPON THE PATTERN OF SEPARATING THE REGION
      DIV=NPOONS-2
C COORDINATES OF S CONTOUR
      RINC=PI/DIV
      RINCC=0.0D0
      LNPSM1=LNPS-1
      DO 10 J=ISNPS,LNPS
         IF(J .EQ. ISNPS .OR. J .EQ. LNPSM1)RINC=RINC/2.0D0
         IF(J .NE. ISNPS .AND. J .NE. LNPSM1)RINC=PI/DIV
         X(J)=RS*DCOS(RINCC)
         Y(J)=RS*DSIN(RINCC)
         RINCC=RINCC+RINC
         PRINT 100,J,X(J),Y(J)
100   FORMAT(' ',I4,2F10.3,T50,'NODE ON CONTOUR S')
10    CONTINUE
C COORDINATES OF C CONTOUR
      RINC=PI/DIV
      RINCC=0.0D0
      DO 20 J=ISNPC,LNPC
         X(J)=RC*DCOS(RINCC)
         Y(J)=RC*DSIN(RINCC)
         RINCC=RINCC+RINC
         PRINT 200,J,X(J),Y(J)
200   FORMAT(' ',I4,2F10.3,T50,'NODE ON CONTOUR C')
20    CONTINUE
C COORDINATES OF M CONTOUR
      RINC=PI/DIV
      RINCC=0.0D0
      LNPM1=LNPM-1
      DO 30 J=ISNPM,LNPM
         IF(J .EQ.ISNPM .OR. J .EQ. LNPM1)RINC=RINC/2.0D0
         IF(J .NE.ISNPM .AND. J .NE. LNPM1)RINC=PI/DIV
         X(J)=RM*DCOS(RINCC)

```

```
Y(J)=RM*DSIN(RJNCC)
RJNCC=RJNCC+RINC
PRINT 300,J,X(J),Y(J)
300 FORMAT(' ',I4,2F10.3,T50,'NODE ON CONTOUR M')
30 CONTINUE
C COORDINATES OF R CONTOUR
RINC=PI/DIV
RJNCC=0.0D0
DO 40 J=ISNPR,LNPR
  X(J)=RB*DCOS(RJNCC)
  Y(J)=RB*DSIN(RJNCC)
  RJNCC=RJNCC+RINC
  PRINT 400,J,X(J),Y(J)
400 FORMAT(' ',I4,2F10.3,T50,'NODE ON CONTOUR R')
40 CONTINUE
C ADD IN ORDER TO FIT THE S/R CALANG
Y(LNPS)=0.0D0
Y(LNPC)=0.0D0
Y(LNPM)=0.0D0
Y(LNPR)=0.0D0
RETURN
END
SUBROUTINE VFRCAL(IVFR,ITFL)
INTEGER IVFP(ITFL,3),ITFL,ISNPS,LNPS,LNPC,ISNPM,LNPM,
+      ISNPR,LNPR,ISTAR1,IEND2,ISTAP2,IEND2,ISTAP3,IEND3,
+      ISTAR4,IEND4,ISTAP5,IEND5,ISTAP6,IEND6,K(3)
COMMON/BLK1/ ISNPS,LNPS,ISNPC,LNPC,ISNPM,LNPM,ISNPR,LNPR
COMMON/BLK2/ ISTAP1,IEND1,ISTAP2,IEND2,ISTAP3,IEND3,
+      ISTAR4,IEND4,ISTAP5,IEND5,ISTAP6,IEND6
C CHANGED UPON THE PATTERN OF SEPARATING THE PECTON
K(1)=1
K(2)=ISNPC
K(3)=2
DO 10 M=ISTAP1,IEND1
  DO 11 N=1,3
    IVFP(M,N)=V(N)
    K(N)=K(N)+1
11  CONTINUE
  PRINT 100,M,(IVFR(M,N),N=1,3)
100 FORMAT(' ',I4,3I8)
10  CONTINUE
C
K(1)=2
K(2)=ISNPC
K(3)=ISNPC+1
DO 20 M=ISTAP2,IEND2
  DO 21 N=1,3
    IVFP(M,N)=V(N)
    K(N)=K(N)+1
21  CONTINUE
  PRINT 100,M,(IVFR(M,N),N=1,3)
20  CONTINUE
C
K(1)=ISNPC
```

```
K(2)=ISNPM+1
K(3)=ISNPC+1
DO 30 M=ISTAR3,IEND3
    DO 31 N=1,3
        IVFR(M,N)=K(N)
        K(N)=K(N)+1
31    CONTINUE
    PRINT 100,M,(IVFR(M,N),N=1,3)
30    CONTINUE
C
K(1)=ISNPC
K(2)=ISNPM
K(3)=ISNPM+1
DO 40 M=ISTAR4,IEND4
    DO 41 N=1,3
        IVER(M,N)=V(N)
        K(N)=K(N)+1
41    CONTINUE
    PRINT 100,M,(IVER(M,N),N=1,3)
40    CONTINUE
C
K(1)=ISNPM
K(2)=ISNPB
K(3)=ISNPM+1
DO 50 M=ISTAR5,IEND5
    DO 51 N=1,3
        IVER(M,N)=K(N)
        K(N)=K(N)+1
51    CONTINUE
    PRINT 100,M,(IVER(M,N),N=1,3)
50    CONTINUE
C
K(1)=ISNPM+1
K(2)=ISNPB
K(3)=ISNPB+1
DO 60 M=ISTAR6,IEND6
    DO 61 N=1,3
        IVER(M,N)=K(N)
        K(N)=K(N)+1
61    CONTINUE
    PRINT 100,M,(IVER(M,N),N=1,3)
60    CONTINUE
RETURN
END
SUBROUTINE CALANG(X,Y,ITNP,ANGLEC)
INTEGER ITNP
REAL*8 X(ITNP),Y(ITNP),ANGLEC(ITNP),PI,CE,ACF,ATER,AATER
PI=3.141592654
DO 200 J=1,ITNP
    CE=X(J)
    ATER=Y(J)
    IF(CE)10,20,30
10    IF(ATER)40,50,60
20    ANGLEC(J)=PI/2
```

```

      GO TO 100
30   IF(ATER)70,80,90
40   GO TO 200
50   ANGLEC(J)=1*PI
      GO TO 100
60   AATER=DARS(ATER)
      ACF=DARS(CF)
      ANGLFC(J)=PI-DATAN2(AATER,ACF)
      GO TO 100
70   GO TO 200
80   ANGLFC(J)=0.0
      GO TO 100
90   ANGLEC(J)=DATAN2(ATER,CF)
      GO TO 100
100  CONTINUE
      PRINT 300,J,X(J),Y(J),ANGLEC(J)
300  FORMAT(' ',I4,3G15.3)
200  CONTINUE
      RETURN
      END
      SUBROUTINE ZANDY(X,Y,ITNP,IVER,ITFL,RK,SIR,NPINR,NPONE)
      INTEGER IVER(ITFL,3),IR,IS,IT,IPON,IROW,ICOL,ITNP,ITFL,NPINR,
      +      NPONE
      REAL*8 X(ITNP),Y(ITNP),A(3),B(3),AREA,AREA4,C,D,RKAPAI,
      +      Z(3,3),PR(ITNP,ITNP),SIR(NPINR,NPONE)
      COMMON/RLK3/ RKAPAI
C INITIALIZATION
      DO 10 J=1,ITNP
         DO 11 J=1,ITNP
            PR(J,J)=0.0D0
11      CONTINUE
10      CONTINUE
C ELEMENT MATRIX AND ASSEMBLY MATRIX
      DO 20 J=1,ITFL
         IR=IVER(J,1)
         IS=IVER(J,2)
         IT=IVER(J,3)
         A(1)=X(IT)-X(IS)
         A(2)=X(IR)-X(IT)
         A(3)=X(IS)-X(IR)
         B(1)=Y(IS)-Y(IT)
         B(2)=Y(IT)-Y(IR)
         B(3)=Y(IR)-Y(IS)
         AREA=(A(3)*B(2)-A(2)*B(3))/2.0D0
         AREA4=4*AREA
         C=(RKAPAI**2)*AREA/6.0D0
         DO 21 M=1,3
            IROW=IVER(J,M)
            DO 22 N=1,3
               ICOL=IVER(J,N)
               IF(N .NE. M)D=C/2.0D0
               IF(N .EQ. M)D=C
               Z(M,N)=(B(M)*B(N)+A(M)*A(N))/AREA4-D
               RK(IROW,ICOL)=RK(IROW,ICOL)+Z(M,N)
22      CONTINUE
20      CONTINUE

```

```

22      CONTINUE
21      CONTINUE
20      CONTINUE
C PARTITION RK INTO 4 PARTS
C COPY SIB INTO A NEW MATPIX
    DO 30 M=1,NPINB
        DO 31 N=1,NPONE
            L=N+NPINE
            SIB(M,N)=RK(M,L)
31      CONTINUE
        PRINT 300,M,(SIB(M,N),N=1,NPONE)
300  FORMAT(' ',I4,'SIB',(10G10.3))
30      CONTINUE
C PRINT SII
C     DO 40 M=1,NPINB
C         PRINT 400,M,(RK(M,N),N=1,NPINB)
C400  FORMAT(' ',I4,'SII',(10G10.3))
C40      CONTINUE
        RETURN
        END
SUBROUTINE INCPEF(NPINB,X,Y,TOTHE,ITNP,GAMMA,NPONE)
INTFCER NPINB,ITNP,NPONE
REAL*8 RKAPA1,X(ITNP),Y(ITNP),GAMMA
COMPLEX*16 IMGG,TOTHE(NPONE),TERM1,TERM2,ARC1,ARC2,CONST
COMMON/BLK3/ RKAPA1
COMMON/BLK5/ IMGG
CONST=IMGG*PKAPA1
DO 10 J=1,NPONE
    JJ=J+NPINE
    TERM1=X(JJ)*DCOS(GAMMA)
    TERM2=Y(JJ)*DSIN(GAMMA)
    ARC1=CONST*(TERM1-TERM2)
    ARC2=CONST*(TERM1+TERM2)
    TOTHE(J)=CDEXP(ARC1)+CDEXP(ARC2)
    PRINT 100,J,TOTHE(J)
100  FORMAT(' ',I4,'TOTHE',2G10.3)
10      CONTINUE
        RETURN
        END
SUBROUTINE TERM1(ITNP,IVER,ITEL,LANDA,X,Y,ANGLEC,RC,DELTA,
+          NPINE,NPONE,MAT,GP)
INTEGER ISNPS,LNPS,ISNPC,LNPC,ISNPM,LNPM,ISNPR,LNPR,
+          ITNP,IVER(ITEL,3),LANDA,NPINB,NPONE,ITFL,IO(2),
+          IP(2),IO(2),IW,IS,IT
REAL*8 X(ITNP),Y(ITNP),RC,ANGLEC(ITNP),DELTA,ANGLE,
+          COSINE,SINE,A1,A2,AA1,AA2,B1,P2,RR1,RR2,
+          P1,P2,DR1,DR2,SA2,SA3,SB2,SB3,ARFA,ZZ1,ZZ2,
+          RKAPA1,RKAPA2
COMPLEX*16 IMGG,HANL1,HANL2,HANO,HANI,GP(NPINB),
+          MAT(NPONE,NPINB),TOTAL
COMMON/BLK1/ ISNPS,LNPS,ISNPC,LNPC,ISNPM,LNPM,ISNPP,LNPR
COMMON/BLK3/ RKAPA1
COMMON/BLK4/ RKAPA2
COMMON/BLK5/ IMGG

```

C INITIALIZATION

```

DO 10 M=1,NPONB
    DO 11 N=1,NPINR
        MAT(M,N)=(0.0D0,0.0D0)
11    CONTINUE
10    CONTINUE
DO 20 L=ISNPB,ITNP
    DO 21 J=ISNPC,LNPC
        ANGLE=ANGLEC(J)
        COSINE=DCOS(ANGLE)
        SINE=DSIN(ANGLE)
        A1=X(L)**2+Y(L)**2+RC**2-2*X(L)*RC*COSINE
        A2=2*Y(L)*RC*SINE
        AA1=A1-A2
        AA2=A1+A2
        R1=2*RC-2*X(L)*COSINE
        R2=2*Y(L)*SINE
        RR1=R1-R2
        RR2=R1+R2
        P1=DSORT(AA1)
        P2=DSQRT(AA2)
        DR1=0.5*I/R1*RR1
        DR2=0.5*I/R2*RR2
        ZZ1=PKAPA2*R1
        CALL HANKEL(ZZ1,HANL1,HANL2)
        HANO=HANL2*DR1
        ZZ2=RKAPA2*R2
        CALL HANKEL(ZZ2,HANL1,HANL2)
        HAN1=HANL2*DR2
        GP(J)=(-IMGC/4.0)*PKAPA2*(HANO+I*LAMDA*HAN1)
        IF(J .GT. ISNPB .AND. J .LT. LNPC)CO TO 305
        TOTAL=0.5*PC*DELT*GP(J)
        CO TO 400
305   TOTAL=RC*DELT*GP(J)
400   K1=L-NPINR
        K2=J
        MAT(K1,K2)=MAT(K1,K2)+TOTAL
21    CONTINUE
20    CONTINUE
DO 30 M=1,NPONP
    PRINT 300,M,(MAT(M,N),N=1,NPINR)
300   FORMAT(' ',I4,'MAT',(10C10.3))
30    CONTINUE
RFTUPN
END

SUBROUTINE TERM2(ITNP,ITEL,IEN01,IEN02,IVER,X,Y,PC,ANGLEC,
+                PRODUT,MAT,LAMDA,DELT,APINR,NPONB,NPONC)
INTEGF 100(3),IPP(3),100(3),TRR,ISS,ITT,IV,IS,IT,
+                ITNP,ISNPB,LNPS,ISNPC,LNPC,ISNPM,LNPM,ISNPB,LNPB,
+                LAMDA,IEN01,IEN02,IVER(ITEL,3),ITEL,NPINB,NPONB,
+                NPONC
      RFAL*8 SA22,SA33,SR22,SR33,AREA,ANGLE,COSINE,SINE,
+                A1,A2,AA1,AA2,P1,R2,X(ITNP),Y(ITNP),RC,ANGLEC(ITNP),
+                RKAPA1,ARG1,ARG2,DELTA,ARG,RKAPA2,C

```

```

COMPLEX*16 HANL1,HANL2,HANKO,HANK1,G,PRODUCT(NPINR),
+          TOTAL(3),IMGG,MAT(NPONE,NPINR)
COMMON/BLK1/ ISNPS,LNPS,ISNPC,LNPC,ISNPM,LNPM,ISNPR,LNPR
COMMON/BLK3/ RKAPA1
COMMON/BLK4/ RKAPA2
COMMON/BLK5/ IMGG
DO 10 L=ISNPR,LNPR
    DO 11 J=TELNO1,TLNNO2
        IJK=J
        IOO(1)=IVER(IJK,1)
        IPP(1)=IVER(IJK,2)
        IOO(1)=IVER(IJK,3)
        IOO(2)=IPP(1)
        IPP(2)=IOO(1)
        IOO(2)=IOO(1)
        IOO(3)=IPP(2)
        IPP(3)=IOO(2)
        IOO(3)=IOO(2)
        DO 12 N=1,3
            IRR=IOO(N)
            ISS=IPP(N)
            ITT=IOO(N)
            SA22=X(IRR)-X(ITT)
            SA33=X(ISS)-X(IRR)
            SB22=Y(ITT)-Y(IRR)
            SB33=Y(IPP)-Y(ISS)
            AREA=0.5*(SA33*SB22-SA22*SB33)
CC      PRINT 90,IRR,ISS,ITT,AREA
C90     FORMAT(' ','IRR,ISS,ITT,AREA',3I4,C10.3)
            JJ=IVER(IJK,1)
            JJPI=JJ+1
C      PRINT 91,JJ,JJPI
C91     FORMAT(' ','JJ,JJPI',2I4)
            DO 13 MM=JJ,JJPI
                ANGLE=ANGLEFC(MM)
                COSINE=DCOS(ANGLE)
                SINE=DSIN(ANGLE)
                A1=X(L)**2+Y(L)**2+RC**2-2*X(L)*PC*COSINE
                A2=2.0*Y(L)*RC*SINE
                AA1=A1-A2
                AA2=A1+A2
                P1=DSORT(AA1)
                P2=DSORT(AA2)
                ARG1=RKAPA2*P1
                ARG2=RKAPA2*P2
                CALL HANKFL(ARG1,HANL1,HANL2)
                HANKO=HANL1
                CALL HANKFL(ARG2,HANL1,HANL2)
                HANK1=HANL1
C      PRINT 92,HANKO,HANK1,COSINE,SINE
C92     FORMAT(' ','HANKO,HANK1',4G20.6)
            G=(IMGG/4.0)*(HANKO+LAMDA*HANK1)
C      PRINT 93,G
C93     FORMAT(' ','G',2G20.6)

```

```

C          C=((Y(ISS)-Y(ITT))*COSINE) +
+          ((X(ITT)-X(ISS))*SINE)/(2.0*APFA)
C      PRINT 94,C
C94    FORMAT(' ', 'C', 2G20.6)
         PRODUT(MM)=C*C
13     CONTINUE
         TOTAL(N)=0.5*RC*DELTA*(PRODUT(JJ)+PRODUT(JJP1))
12     CONTINUE
         LL=L-NPINR
         IW=JJ
         IS=JJ+1+NPCNC
         IT=JJ+1
         MAT(LL,IW)=MAT(LL,IW)-TOTAL(1)
         MAT(LL,IS)=MAT(LL,IS)-TOTAL(2)
         MAT(LL,IT)=MAT(LL,IT)-TOTAL(3)
11     CONTINUE
10     CONTINUE
DO 20 M=1,NPONB
         PPINT 200,M,(MAT(M,N),N=1,NPINR)
200   FORMAT(' ',I4,'MAT',(10G10.3))
20     CONTINUE
         PFTURN
         END
SUBROUTINE HANKEL(ARG,HANL1,HANL2)
INTEGER N,IEP
REAL*8 ARG,X,ORDER,JN(2),YN(2),MMBSJ0,MMBSJ1
COMPLEX*16 IMGG,HANL1,HANL2
IMCC=DCMPLX(0.0D0,1.0D0)
ORDER=0.0D0
N=2
X=ARG
JN(1)=MMBSJ0(X,IEP)
JN(2)=MMBSJ1(X,IEP)
CALL MMPSYN(X,ORDER,N,YN,IEP)
HANL1=JN(1)+IMGG*YN(1)
HANL2=JN(2)+IMGG*YN(2)
RETURN
END
SUBROUTINE RIGHT(SIR,TOTHE,RSIDE,NPINR,NPONB)
INTEGER NPINR,NPONB
REAL*8 SIR(NPINR,NPONB)
COMPLEX*16 TOTHE(NPONB),RSIDE(NPINR)
C CONSTRUCT THE RIGHT HAND SIDE MATRIX
DO 10 M=1,NPINR
         RSIDE(M)=(0.0D0,0.0D0)
DO 11 N=1,NPONB
         RSIDE(M)=RSIDE(M)-SIR(M,N)*TOTHE(N)
11     CONTINUE
         PRINT 100,M,RSIDE(M)
100   FORMAT(' ',I4,'RSIDE',2G20.5)
10     CONTINUE
         RETURN
END
SUBROUTINE LEFT(RK,SIR,MAT,NPONB,NPINR,ITNP,LSIDE)

```

```

INTEGER NPONE,NPINB,ITNP
REAL*8 SIR(NPINB,NPONE),RK(ITNP,ITNP)
COMPLEX*16 MAT(NPONE,NPINB),LSIDE(NPINB,NPINB)
C CONSTRUCT SIP*M MATRIX
DO 10 M=1,NPINB
    DO 11 N=1,NPINB
        LSIDE(M,N)=(0.0D0,0.0D0)
    DO 12 L=1,NPONE
        LSIDE(M,N)=LSIDE(M,N)+SIR(M,L)*MAT(L,N)
12    CONTINUE
11    CONTINUE
10    CONTINUE
C CONSTRUCT SII+(SIP*M) MATRIX
DO 20 M=1,NPINB
    DO 21 N=1,NPINB
        LSIDE(M,N)=RK(M,N)+LSIDE(M,N)
21    CONTINUE
        PRINT 200,M,(LSIDE(M,N),N=1,NPINB)
200 FORMAT(' ',I4,'LSIDE',(10G10.3))
20    CONTINUE
    RETURN
END
SUBROUTINE SOLVE(RSIDE,LSIDE,NPINB,NPONE,EA)
INTEGER N,IA,M,IB,IJOB,IFF,NPINB,NPONE
REAL*8 ARTEMP
COMPLEX*16 LSIDE(NPINB,NPINB),RSIDE(NPINB),VA(NPINB),TEMP
N=NPINB
IA=NPINB
M=1
IR=NPINB
IJOB=0
CALL LFOTIC(LSIDE,N,IA,PSIDE,M,IB,IJOB,VA,IFF)
DO 10 J=1,NPINB
    TEMP=RSIDE(J)
    ABTEMP=CDABS(TEMP)
    PRINT 100,J,RSIDE(J),ABTEMP
100 FORMAT(' ',I4,'RSIDE',2G20.6,3X,G15.6)
10    CONTINUE
    RETURN
END

```

```

//WONG JOB ',,,C=0,L=10,T=30','CHOW',MSGLEVEL=(1,1)
// EXEC FORTXCLG,OPT=2,MAP=NOMAP,P=D,AD=DBL4,
//      CSIZE=512K,LSIZE=512K,SIZE=512K,PARM.LKED='SIZF=(512K,124K)'
//FORT.SYSIN DD *
C      PROGRAM SHHALF1(INPUT,OUTPUT,TAPE1,TAPE2)
C      CONTOUR C MUST BE SEMI-CIRCLE AT Y=0.
C      KC MUST BE EVEN NUMBER.
C      NOTATIONS:KI=NODES INSIDE C.ITFL=TOTAL NO.
C      OF ELEMENTS.ISTELC AND IFNFL=STARTING AND ENDING
C      ELEMENT NO. ON C FOR INTEGRATION.NKAPPA=NO. OF
C      KAPPAS CALLED RKAPPA(I).NGAMA=NO. OF INCIDENCE
C      ANGLES CALLED GAMMA(I).IELMAT(L)=MATERIAL PROPERTY
C      OF EACH ELEMENT L.IELND(L)=NEN=NO. OF NODES CONNECTED
C      TO EACH ELEMENT.IVER(L,IELND)=NODE NO. FOR EACH ELEMENT.
C
C      AMU1,AMU2,RHO=MATERIAL PROPERTIES.WN,WI,WC,WO=Z-DISPLACEMENTS
C      TOTAL,INTERIOR,ON C, AND INCIDENCE+REFLECTED.ZK AND PK=
C      ELEMENT AND GLOBAL STIFFNESS MATRICES.ZM AND RM=ELEMENTAL AND
C      GLOBAL MASS MATRICES.UMAT AND VMAT=WINCIDENCE AND ITS DERIVATIVE
C      ON C.IOUTPR=SWITCH FOR PRINTING IN OUTER REGION,IF OUTER=0
C      NO PRINTING,IF IOUTPR.GT.0 READ NO. OF RP(I),THETA(I)
C      WHERE VALUES DESIRED.NTERM=KC+1.NUMAT=NO. OF MATERIAL PROPERTIES.
C
C      FOR INTERIOR WE ARE SOLVING REAL ARITHMETIC
C      PROBLEM WI=-((SII)INVERSE)*SIC*WC
C      S=PK-(KAPPA**2)*RM.ON C WE COLLOCATE TO SOLVE
C          ~*KII KIJ~*~*C~*=~*UMAT~*
C          ~*KJI KJJ~*~*A~*=~*VMAT~*, WHICH NEEDS COMPLEX ALGEBRA.C
C
REAL RKAPPA(20),GAMMA1(20),AMU1(6),AMU2(6),PHOS(6),X(167),Y(167),
ANGLEC(26),SII(141,141),SCC(26,26)
.,SIC(141,26),WC(26,26),WCINV(26,26),WAREA(141),
.WI(167,26),WDER(26,26),R(26),
.RP(24),THETAV(24)
INTEGER IVFR(197,7),IELMAT(197),IELND(197)
INTGFR IPT1(20),IPT2(20)
LOGICAL SWITCH
C
C      NOTES ON READ STATEMENTS:
C      MAIN READS:KI,KC,ITEL,ISTELC,IFNDEL,IOUTPR,NUMAT
C                      RKAPPA1
C                      NGAMA,(GAMMA1(I),I=1,NGAMA)
C      COORD. READS:IELMAT,IELND,IVER
C      MATERL READS:AMU1,AMU2,RHOS
C      IF IOUTPR.GT.0 THEN READ
C      OUTPR :NRPRT,(RP(I),THETAV(I),I=1,NRPRT)
C
READ(1,*) KI,KC,ITEL,ISTELC,IFNDEL,IOUTPR,NUMAT,ISCAT
READ(1,*) RKAPPA1,SWITCH,YLENG,ICOPY,VFRANG
READ(1,*) NGAMA,(GAMMA1(I),I=1,NGAMA)
PRINT 400,KI,KC,ITEL,ISTELC,IFNDEL,IOUTPR,NUMAT
400 FORMAT(' ',2X,'KI = ',I4,2X,'KC = ',I4,2X,'ITEL = ',I4,
.2X,'ISTELC = ',I4,2X,'IFNDEL = ',I4,2X,'IOUTPR = ',
.I4,2X,'NUMAT = ',I4//)

```

```
PRINT 401, RKAPAI
401 FORMAT(' ',2X,'RKAPAI = ',G14.4//)
      PRINT 402, NGAMA,(GAMMA1(I),I=1,NGAMA)
402 FORMAT(' ',2X,'NGAMA = ',I4,2X,'GAMA''S = :',10F9.4//)
      PRINT 404, ISCAT
404 FORMAT(' ',2X,'ISCAT = ',I5//)
      ITNP=KI+KC
      MTERM=KC+1
      CALL COORD(X,Y,ITNP)
      CALL VERCAL(IVER,IELMAT,IELND,ITEL)
      CALL MATRYL(AMU1,AMU2,RHOS,NUMAT)
      CALL CALANG(X,Y,R,ANGLEC,ITNP,KC)
      CALL KANDM(X,Y,ITNP,ITEL,IVER,IELMAT,IELND,
                 AMU1,AMU2,RHOS,NUMAT,SII,SIC,SCC,KI,KC,PKAPAI,SWITCH)
      CALL WCMAT(WC,ANGLEC,WCIINV,KC,WARFA,SCC,SWITCH)
      CALL WIMAT(SII,SIC,WI,WC,KI,KC,ITNP,WARFA,SWITCH)
      G1C=AMU1(1)
      G2C=AMU2(1)
      CALL WDRCI(WI,KI,KC,WDFR,ANGLEC,IVER,X,Y,
                 ITNP,ITEL,ISTELC,IENDEL,G1C,G2C,SWITCH)
      WRITE(2,*) KC,IOUTPR,ISCAT
      WRITE(2,*) RKAPAI,SWITCH,YLFNG,ICOPY,VFRANG
      WRITE(2,*) NGAMA,(GAMMA1(I),I=1,NGAMA)
      WRITE(2,*) ITNP,MTERM
      WRITE(2,*)(X(I),Y(I),I=1,ITNP)
      WRITE(2,*)(ANGLEC(I),R(I),I=1,KC)
      WRITE(2,*)(WC(I,J),WCIINV(I,J),WDFR(I,J),I=1,KC),J=1,KC)
      WRITE(2,*)(WI(I,J),I=1,ITNP),J=1,KC)
      IF (IOUTPR.EQ.0) GO TO 205
      READ(1,*) NPRPT,(RP(I),THETAV(I),I=1,NPRPT)
      PRINT 403,(RP(I),THFTAV(I),I=1,NPRPT)
      WRITE(2,*) NPRPT,(RP(I),THETAV(I),I=1,NPRPT)
205 CONTINUE
      IF(ISCAT.EQ.0) GO TO 221
      READ(1,*) NSCAT,(IPT1(I),IPT2(I),I=1,NSCAT)
      PRINT 405, NSCAT, (IPT1(I),IPT2(I),I=1,NSCAT)
405 FORMAT(' ',2X,'NSCAT = ',I4,2X,'NODE PAIRS: ',20I4//)
      WRITE(2,*) NSCAT, (IPT1(I),IPT2(I),I=1,NSCAT)
221 CONTINUE
403 FORMAT(' ',2X,'$ RP, THFTA ARRAYS :=/(2X,10F9.4))
      STOP
      END
      SUBROUTINE COORD(X,Y,ITNP)
C
C      READS AND PRINTS X, Y, COORDS. OF ALL NODE POINTS.
C
      REAL X(ITNP),Y(ITNP)
      PRINT 200
      DO 10 J=1,ITNP
      READ(1,*) X(J),Y(J)
      PRINT 101, J,X(J),Y(J)
10 CONTINUE
101 FORMAT(' ',4X,I6,2G16.6)
200 FORMAT(' ',4X,'NODE NO.',5X,'X-COORD',10X,'Y-COORD',/)
```

```
PFTURN
END
SUBROUTINE VERCAL(IVER,IELMAT,IELND,ITEL)
C
C      READS AND PRINTS ELEMENT NO. ITS MATERPIAL TYPE AND
C      NO. OF NODES CONNECTED TO EACH ELEMENT
C
      INTEGER  IVER(ITEL,7),IELMAT(ITEL),IELND(ITEL)
      PRINT 200
      DO 10 L=1,ITEL
      READ(1,*) IELMAT(L),IDUM,(IVFR(L,J),J=1,1DUM)
      IELND(L)=IDUM
      PRINT 201,L,IELMAT(L),IELND(L),(IVFR(L,J),J=1,1DUM)
10   CONTINUE
201 FORMAT(' ',4X,I8,8X,I8,8X,I8,8X,7I8)
200 FORMAT(' ',4X,'ELEM NO.',5X,'MATERIAL TYPE',5X,
     .'NODFS PER ELEMENT',20X,'N-O-D-E-S',/)
      RETURN
      END
      SUBROUTINE MATRYL(AMU1,AMU2,RHOS,NUMAT)
C      READS SETS OF MATERIAL PROPERTIES.
      REAL AMU1(NUMAT),AMU2(NUMAT),RHOS(NUMAT)
      PRINT 200
      DO 10 I=1,NUMAT
      READ(1,*) AMU1(I),AMU2(I),RHOS(I)
      PRINT 201,I,AMU1(I),AMU2(I),RHOS(I)
10   CONTINUE
201 FORMAT(' ',5X,I6,3G16.6)
200 FORMAT(' ',2X,'MATERIAL NO.',5X,'G1',15X,'G2',15X,'RHO',/)
      RETURN
      END
      SUBROUTINE CALANG(X,Y,R,ANGLEFC,ITNP,KC)
C
C      CALCULATES R=SORT(X**2+Y**2),ANGLEFC=ARCTAN(X/Y)=THETA
C      AT POINTS ON C ONLY.
      REAL X(ITNP),Y(ITNP),ANGLEC(KC),R(KC)
      DATA PI/3.141592654/
      PRINT 299
      KI=ITNP-KC
      DO 200 I=1,KC
      J=I+KI
      CE=X(J)
      ATER=Y(J)
      IF(X(J).EQ.0..AND.Y(J).EQ.0..) GO TO 80
      R(I)=SQRT(X(J)**2+Y(J)**2)
      IF (CE) 10,20,30
10   IF (ATER) 40,50,60
20   ANGLEC(I)=ATAN2(CE,ATER)
      GO TO 300
50   ANGLEC(I)=PI/2.
      GO TO 300
40   AATER=ABS(ATERN)
      ANGLEC(I)=PI/2.+ATAN2(AATER,CE)
      GO TO 300
```

```

20 IF (ATER) 70,80,90
90 ANGLEC(I)=0.
    GO TO 300
80 R(I)=0.
    ANGLEC(I)=0.
    GO TO 300
70 ANGLFC(I)=PI
    GO TO 300
10 ACE=APS(CE)
    IF (ATER) 100,110,120
120 ANGLFC(I)=-ATAN2(ACE,ATER)
    GO TO 300
110 ANGLEC(I)=-PI/2.
    GO TO 300
100 AATER=ABS(ATR)
    ANGLEC(I)=-PI/2.-ATAN2(AATER,ACE)
300 CONTINUE
    PRINT 201,I,J,X(J),Y(J),R(I),ANGLFC(I)
200 CONTINUE
201 FORMAT(' ',5X,I6,5X,I6,4G16.6)
299 FORMAT(' ',2X,'SERIAL NO.',5X,'NODE NO.',8X,'X-COORD',
.'Y-COORD',12X,'R',10X,'THETA',/)
RETURN
END
SUBROUTINE KANDM(X,Y,ITNP,ITEL,IVER,IELMAT,IELND,AMU1,
.AMU2,RHOS,NUMAT,SII,SIC,SCC,KI,KC,RKAPA1,SWITCH)
C
C      CALCULATES INDIVIDUAL ELEMENT STIFFNESS ZK AND MASS ZM MATRICES
C      BY CALLING SUBROUTINES ELM303 AND ELM3, THEN ASSEMBLES THEM INTO
C      GLOBAL MATRICES AS SK = K - (RKAPA1**2)*M , WHERE
C
C          1           SIC 1
C      SK = 1   SII       1
C          1           SCC 1
C
C      INTEGER IVER(ITEL,7),IELMAT(ITEL),IELND(ITEL)
C      REAL X(ITNP),Y(ITNP),AMU1(NUMAT),AMU2(NUMAT),RHOS(NUMAT)
C      REAL ZK(7,7),ZM(7,7),XL(7),YL(7),SII(KI,KI),SIC(KI,KC),
.CSCC(KC,KC)
C      LOGICAL SWITCH
C      RKAPA2=RKAPA1**2
DO 10 I=1,KI
DO 11 J=1,KI
11 SII(I,J)=0.
10 CONTINUE
DO 15 I=1,KI
DO 16 J=1,KC
16 SIC(I,J)=0.
15 CONTINUE
DO 18 I=1,KC
DO 18 J=1,KC
18 SCC(I,J)=0.
DO 20 L=1,ITEL
MATYP=IELMAT(L)
G1=AMU1(MATYP)

```

```
G2=AMU2(MATYP)
RHO=RHOS(MATYP)
NEN=IELND(L)
DO 30 I=1,NEN
XL(I)=X(IVER(L,I))
YL(I)=Y(IVER(L,I))
30 CONTINUE
C CONSTANT STRAIN TRIANGLE (CST):3 NODES ONLY.
IF (NEN.GT.4) GO TO 111
CALL ELMS03(XL,YL,G1,G2,RHO,ZK,ZM)
GO TO 200
C CALCULATES ZK AND ZM FOR 6-NODE TRIANGLE OR 7-NODE QUADRILATERAL
C
111 CALL ELMS(XL,YL,NEN,G1,G2,RHO,ZK,ZM)
200 DO 41 M=1,NEN
IROW=IVER(L,M)
DO 42 N=1,NEN
ICOL=IVER(L,N)
TEMP=ZK(M,N)-RKAPA2*ZM(M,N)
IF(IROW.GT.KI) GO TO 300
IF (ICOL.GT.KJ) GO TO 121
SII(IROW,ICOL)=SII(IROW,ICOL)+TEMP
GO TO 300
121 ICOI1=ICOI-KI
SIC(IROW,ICOI1)=SIC(IROW,ICOI1)+TEMP
300 CONTINUE
42 CONTINUE
41 CONTINUE
20 CONTINUE
IF(SWITCH)PRINT 400
400 FORMAT(' ',2X,'$SPRINT SII FOR CHECK$',//)
IF(SWITCH) PRINT 401,SII
IF(SWITCH) PRINT 402
402 FORMAT(' ',2X,'$SPRINT SIC FOR CHECK$',//)
IF(SWITCH) PRINT 401,SIC
401 FORMAT(' ',2X,8G16.6)
RETURN
END
SUBROUTINE ELMS03(XL,YL,G1,G2,RHO,ZK,ZM)
C CALCULATES ELEMENTAL STIFFNESS AND MASS MATRICES,
C ZK AND ZM, FOR CST.
C
REAL XL(7),YL(7),ZK(7,7),ZM(7,7),D(2)
REAL R(2,3),PR(2,3),RTDB(3,3)
D(1)=G1
D(2)=G2
A1=XL(3)-XL(2)
A2=XL(1)-XL(3)
A3=XL(2)-XL(1)
B1=YL(2)-YL(3)
B2=YL(3)-YL(1)
B3=YL(1)-YL(2)
```

```

AREA=(A3*B2-A2*B3)/2.
B(1,1)=B1
B(1,2)=B2
B(1,3)=B3
B(2,1)=A1
B(2,2)=A2
B(2,3)=A3
C      CALCULATES  DR=D*B
DO 10 I=1,2
DO 11 J=1,3
11 DB(I,J)=D(I)*B(I,J)
10 CONTINUE
C      CALCULATES  BTDB=BT*DR
DO 20 I=1,3
DO 21 J=1,3
BTDB(I,J)=0.
DO 22 K=1,2
22 BTDB(I,J)=BTDB(I,J)+B(K,I)*DR(K,J)
21 CONTINUE
20 CONTINUE
C=AREA*RHO/6.
DO 31 M=1,3
DO 32 N=1,3
IF (N.NE.M) DTFMP=C/2.
IF (N.EQ.M) DTEMP=C
ZK(M,N)= RTDB(M,N)/(4.*AREA)
32 ZM(M,N)=DTEMP
31 CONTINUE
RETURN
END
SUBROUTINE FLMS(XL,YL,NFN,G1,G2,RHO,ZF,ZM)
C      CALCULATES ELEMENTAL STIFFNESS AND MASS MATRICES,ZF AND ZM,
C      FOR 6-NODE TRIANGLE AND 7-NODE QUADRILATERAL.
C
REAL XL(7),YL(7),ZK(7,7),ZM(7,7),SG(9),TG(9),WT(9)
REAL SHP(3,7),D(2),DB(2,7),BTDB(7,7)
DO 1 I=1,NFN
DO 1 J=1,NFN
ZK(I,J)=0.
1 ZM(I,J)=0.
CALL PGAUSS(SG,TG,WT)
C      PERFORMS 9-POINTS GAUSS INTEGRATION.
C
DO 100 N=1,9
IF (NEN.EQ.7) GO TO 111
CALL SHAPF6(SG(N),TG(N),XL,YL,XSJ,SHP)
GO TO 121
111 CALL SHAPF7(SG(N),TG(N),XL,YL,XSJ,SHP)
121 DV=XSJ*WT(N)
D(1)=G1*D
D(2)=G2*D

```

```
DO 10 I=1,2
DO 11 J=1,NEN
11 DB(I,J)=D(I)*SHP(I,J)
10 CONTINUE
DO 31 I=1,NEN
DO 32 J=1,NEN
BTDB(I,J)=0.
DO 33 K=1,2
33 BTDB(I,J)=BTDB(I,J)+SHP(K,I)*DB(K,J)
32 CONTINUE
31 CONTINUE
DV=XSJ*WT(N)*RHO
DO 41 I=1,NEN
DO 42 J=1,NEN
42 ZM(I,J)=ZM(I,J)+DV*SHP(3,I)*SHP(3,J)
41 CONTINUE
DO 51 J=1,NEN
DO 52 J=1,NEN
52 ZK(I,J)=ZK(I,J)+BTDB(I,J)
51 CONTINUE
100 CONTINUE
RETURN
END
SUBROUTINE PGAUSS(SG,TG,WT)
C
C      SG AND TG ARE 9-GAUSS POINTS,WT CORRESPONDING WEIGHTS.
C
REAL SG(9),TG(9),WT(9)
G=SORT(0.6)
SG(1)= -G
SG(2)= G
SG(3)= G
SG(4)= -G
SG(5)= 0.
SG(6)= G
SG(7)= 0.
SG(8)= -G
SG(9)= 0.
TG(1)= -G
TG(2)= -G
TG(3)= G
TG(4)= G
TG(5)= -G
TG(6)= 0.
TG(7)= G
TG(8)= 0.
TG(9)= 0.
W1=25./81.
W2=40./81.
W3=64./81.
DO 22 I=1,4
WT(I)=W1
I1=I+4
WT(I1)=W2
```

```

22 CONTINUE
WT(9)= W3
RETURN
END
SUBROUTINE SHAPF6(S,T,XL,YL,XSJ,SHP)
C
C   6-NODE TRIANGLE DEGENERATED FROM 8-NODE QUADRILATERAL.
C
REAL XL(7),YL(7),SHP(3,7),XS(2,2)
SHP(3,1)= 0.5*S*(S-1.)
SHP(3,2)= 0.25*(1.+S)*(1.-T)*(S-T-1.)
SHP(3,3)= 0.25*(1.+S)*(1.+T)*(S+T-1.)
SHP(3,4)= 0.5*(1.-S*S)*(1.-T)
SHP(3,5)= 0.5*(1.+S)*(1.-T*T)
SHP(3,6)= 0.5*(1.-S*S)*(1.+T)
C S-DERIVATIVE
SHP(1,1)= S-0.5
SHP(1,2)= 0.25*(1.-T)*(2.*S-T)
SHP(1,3)= 0.25*(1.+T)*(2.*S+T)
SHP(1,4)= -S*(1.-T)
SHP(1,5)= 0.5*(1.-T*T)
SHP(1,6)= -S*(1.+T)
C T-DERIVATIVE
SHP(2,1)= 0.
SHP(2,2)= 0.25*(1.+S)*(-S+2.*T)
SHP(2,3)= 0.25*(1.+S)*(S+2.*T)
SHP(2,4)= -0.5*(1.-S*S)
SHP(2,5)= -(1.+S)*T
SHP(2,6)= 0.5*(1.-S*S)
DO 201 J=1,2
XS(1,J)=0.
XS(2,J)=0.
DO 202 K=1,6
XS(1,J)= XS(1,J)+XL(K)*SHP(J,K)
202 XS(2,J)= XS(2,J)+YL(K)*SHP(J,K)
201 CONTINUE
XSJ= XS(1,1)*XS(2,2)-XS(1,2)*XS(2,1)
DO 300 I=1,6
TEMP=(XS(2,2)*SHP(1,I)-XS(2,1)*SHP(2,I))/XSJ
SHP(2,I)= (-XS(1,2)*SHP(1,I)+XS(1,1)*SHP(2,I))/XSJ
300 SHP(1,I)= TEMP
RETURN
END
SUBROUTINE SHAPF7(S,T,XL,YL,XSJ,SHP)
C   7- NODE QUADRILATERAL.
REAL XL(7),YL(7),XS(2,2),SHP(3,7)
C SHAPE-FUNCTIONS.
SHP(3,1)= -0.25*S*(1.-S)*(1.-T)
SHP(3,2)= 0.25*(1.+S)*(1.-T)*(S-T-1.)
SHP(3,3)= 0.25*(1.+S)*(1.+T)*(S+T-1.)
SHP(3,4)= -0.25*S*(1.-S)*(1.+T)
SHP(3,5)= 0.5*(1.-S*S)*(1.-T)
SHP(3,6)= 0.5*(1.+S)*(1.-T*T)
SHP(3,7)= 0.5*(1.-S*S)*(1.+T)

```

```

C S-DERIVATIVES.
SHP(1,1)= -0.25*(1.-T)*(1.-2.*S)
SHP(1,2)= 0.25*(1.-T)*(2.*S-T)
SHP(1,3)= 0.25*(1.+T)*(2.*S+T)
SHP(1,4)= -0.25*(1.+T)*(1.-2.*S)
SHP(1,5)= -S*(1.-T)
SHP(1,6)= 0.5*(1.-T*T)
SHP(1,7)= -S*(1.+T)
C T-DERIVATIVES.
SHP(2,1)= 0.25*S*(1.-S)
SHP(2,2)= 0.25*(1.+S)*(-S+2.*T)
SHP(2,3)= 0.25*(1.+S)*(S+2.*T)
SHP(2,4)= -0.25*S*(1.-S)
SHP(2,5)= -0.5*(1.-S*S)
SHP(2,6)= -(1.+S)*T
SHP(2,7)= 0.5*(1.-S*S)
C           1 XS(1,1)  XS(2,1)  1
C      FORM JACOBIAN =  1                   1
C           1 XS(1,2)  XS(2,2)  1
DO 201 J=1,2
XS(1,J)= 0.
XS(2,J)= 0.
DO 202 K=1,7
XS(1,J) = XS(1,J)+XL(K)*SHP(J,K)

202 XS(2,J)=XS(2,J)+YL(K)*SHP(J,K)

201 CONTINUE
XSJ=XS(1,1)*XS(2,2)-XS(1,2)*XS(2,1)
DO 300 I=1,7
TEMP=(XS(2,2)*SHP(1,T)-XS(2,1)*SHP(2,I))/XSJ
SHP(2,I)=(-XS(1,2)*SHP(1,I)+XS(1,1)*SHP(2,I))/XSJ
300 SHP(1,T)= TEMP
RETURN
END
SUBROUTINE WCMAT(WC,ANGLEC,WCINV,FC,WAREA,WC2,SWITCH)
C
C THIS SUBROUTINE FORMS BOUNDARY LOAD MATRIX :WC! FOR EACH
C COS~:(2N-2)*THETA~! AND SIN~:(2N-1)*THETA~!, WHERE THETA IS AN
C ANGLE ON C. IT ALSO FINDS THE INVERSE WCINV.
C KC=NUMBER OF NODES ON C MUST BE EVEN NUMBER.
C
REAL WC(KC,KC),ANGLEC(KC),WAREA(KC),WCINV(KC,KC),WC2(KC,KC)
LOGICAL SWITCH
DO 10 I=1,KC
DO 20 J=1,KC,2
L=J-1
M=J
N=J+1
TERM1=L*ANGLEC(I)
TERM2=M*ANGLEC(I)
WC(I,M)=COS(TERM1)
WC(I,N)=SIN(TERM2)
20 CONTINUE

```

```
10 CONTINUE
  IF(SWITCH) PRINT 200
  IF(SWITCH) PRINT 201,WC
200 FORMAT(' ',2X,'$SPRINT WC FOR CHECK$',/)
201 FORMAT(' ',2X,8G16.6)
C   COPY WC INTO WC2. WC2 WILL BE DESTROYED.
  DO 90 I=1,KC
  DO 91 J=1,KC
  91 WC2(I,J)=WC(I,J)
  90 CONTINUE
C   INVFRWC2=WC THROUGH IMSL.
  KPP=KC
  N=KPP
  IA=KPP
  IDGT=0
  CALL LINVIF(WC2,N,IA,WCINV,IDL,WARFA,IER)
  IF(SWITCH) PRINT 202
  IF(SWITCH) PRINT 201,WCINV
202 FORMAT(' ',2X,'$SPRINT WCINV FOR CHECK$',/)
  RETURN
END
SUBROUTINE WIMAT(SII,SIC,WI,WC,KI,KC,ITNP,WARFA,SWITCH)
C THIS SUBROUTINE CALCULATES WI(=W AT INTERIOR NODES) DUE TO
C BOUNDARY LOADS WC FROM EQUATION SII*WI=-SIC*WC THROUGH IMSL.
C IT ALSO ADDS UP WI AND WC TO FORM WN OF SIZE(ITNP*KC).
C
  REAL SII(KI,KI),SIC(KI,KC),WI(ITNP,KC),WC(KC,FC)
  REAL WAREA(KI)
  LOGICAL SWITCH
  DO 10 I=1,ITNP
  DO 10 J=1,KC
10 WI(I,J)=0.
  DO 15 I=1,KI
  DO 15 L=1,KC
  DO 15 J=1,KC
15 WI(I,L)=WI(I,L)-SIC(I,J)*WC(J,L)
  DO 21 I=1,KI
  DO 21 J=1,KC
21 SIC(I,J)=WI(I,J)
  IF(SWITCH) PRINT 200
  IF(SWITCH) PRINT 201,VI
  IF(SWITCH) PRINT 202
202 FORMAT(' ',2X,'$SPRINT SIC FOR CHECK$',//)
  IF(SWITCH) PRINT 201,SIC
  M=KC
  N=KI
  IA=KI
  IDG=0
C   CALLS IMSL SUBROUTINE
  CALL LEQTIF(SII,M,N,IA,SIC,IDL,WARFA,IER)
C   SII IS DESTROYED.
  IF(SWITCH) PRINT 202
  IF(SWITCH) PRINT 201,SIC
  DO 51 I=1,KI
```

```

DO 52 J=1,KC
52 WI(I,J)=SIC(I,J)
51 CONTINUE
  DO 53 I=1,KC
    I1=KI+I
    DO 54 J=1,KC
54 WI(I1,J)=WC(I,J)
53 CONTINUE
  IF(SWITCH)PRINT 200
  IF(SWITCH) PRINT 201, WI
200 FORMAT(' ',2X,'$PRINT WI FOR CHECK$',/)
201 FORMAT(' ',2X,8G16.6)
      RETURN
      END
      SUBROUTINE WDERC1(WN,K,KP,WDER,ANGLEC,IVER,X,Y,ITNP,
     .ITEL,ISTFLC,IENDFL,G1C,G2C,SWITCH)
C
C      CALCULATES THE MATRIX WDER=RADIAL DERIVATIVE OF WN ON C.
C      KP=KC AND K=KI.
C
      INTEGER IOO(3),IPP(3),IOO(3),IVER(ITEL,7)
      REAL WN(ITNP,KP),WDER(KP,KP),ANGLEC(KP),C(3),X(ITNP),Y(ITNP)
      LOGICAL SWITCH
      ISNPC=K+1
      LNPC=K+KP
      DO 10 I=1,KP
      DO 10 J=1,KP
10 WDER(I,J)=0.

C
C      FOR EACH COLUMN OF WN--FIND DERIVATIVE.
C
      DO 20 I=1,KP
      DO 30 L=ISTFLC,IENDFL
        IOO(1)=IVFR(L,1)
        IPP(1)=IVER(L,2)
        IOO(1)=IVER(L,3)
        IOO(2)=IPP(1)
        IPP(2)=IOO(1)
        IOO(2)=IOO(1)
        IOO(3)=IPP(2)
        IPP(3)=IOO(2)
        IOO(3)=IOO(2)
        MM=IPP(1)
        NN=IOO(1)
        DO 40 M=MM,NN
          MMK=M-K
          ANGLE=ANGLEC(MMK)
          COSINE=COS(ANGLE)*G2C
          SINE=SIN(ANGLE)*G1C
          DO 50 N=1,3
            IRR=IOO(N)
            ISS=IPP(N)
            ITT=IOO(N)
            SA22=X(IRR)-X(ITT)

```

```
SA33=X(ISS)-X(IRR)
SB22=Y(ITT)-Y(IRR)
SB33=Y(IRR)-Y(ISS)
AREA2=SA33*SB22-SA22*SP33
C(N)=(((Y(ISS)-Y(ITT))*SINE)+((X(ITT)-X(ISS))*COSINF))/AREA2
50 CONTINUE
N1=100(1)
N2=IPP(1)
N3=100(1)
TEMP=C(1)*WN(N1,I)+C(2)*WN(N2,I)+C(3)*WN(N3,I)
IF(M.NE.ISNPC.OR.M.NE.LNPC) TEMP=TEMP/2.
J=M-K
WDER(J,I)=WDER(J,I)+TEMP
40 CONTINUE

30 CONTINUE
20 CONTINUE
IF(SWITCH) PRINT 400
400 FORMAT(' ',2X,'$PRINT WDER FOR CHECK$',//)
IF(SWITCH) PRINT 401,WDER
401 FORMAT(' ',2X,8G16.6)
RETURN
END
//GO.FT02F001 DD DSN=CHOW.DA1.NEWDATA,UNIT=SYSDA,
//           SPACE=(TRK,(10,5)),DCB=(BLKSIZE=6080,LFCL=80,
//           RECFM=FB),DISP=(NEW,KEEP),VOL=SFR=WORK04
//GO.FT01F001 DD *
```

```

//WONG JOE ',,,C=0,L=10,T=30','CHOW',MSGLEV=(1,1)
// EXFC FORTXCLG,OPT=2,NMAP=NOMAP,P=D,AD=DIL4,
//      CSIZE=512K,LSIZE=512K,SIZE=512K,PARM.LKFD='SIZE=(512K,124K)'
//FORT.SYSIN DD *
C   PROGRAM SHHALF2(INPUT,OUTPUT,TAPE2)
C   CONTOUR C MUST BE SEMI-CIRCLE AT Y=0.
C   KC MUST BE EVEN NUMBER.
C   NOTATIONS:KI=NODFS INSIDE C.ITFL=TOTAL NO.
C   OF ELEMENTS.ISTELC AND IENEL=STARTING AND ENDING
C   ELEMENT NO. ON C FOR INTEGRATION.NKAPPA=NO. OF
C   KAPPAS CALLED RKAPPA(I).NCAMA=NO. OF INCIDENCE
C   ANGLES CALLED GAMMA(I).IELMAT(L)=MATERIAL PROPERTY
C   OF EACH ELEMENT L.IELND(L)=NEN=NO. OF NODES CONNECTED
C   TO EACH ELEMENT.IVER(L,IELND)=NODE NO. FOR EACH ELEMENT.

C   AMU1,AMU2,RHO=MATERIAL PROPERTIES.VN,WI,WC,W0=Z-DISPLACEMENTS
C   TOTAL,INTERIOR,ON C, AND INCIDENCE+REFLECTED.ZK AND RK=
C   ELEMENT AND GLOBAL STIFFNESS MATRICES.ZM AND FM=ELEMENTAL AND
C   GLOBAL MASS MATRICES.UMAT AND VMAT=INCIDENCE AND ITS DERIVATIVE
C   ON C.IOUTPR=SWITCH FOR PRINTING IN OUTER REGION,IF OUTER=0
C   NO PRINTING,IF IOUTPR.GT.0 READ NO. OF RP(I),THETA(I)
C   WHERE VALUES DESIRED.MTERM=KC+1.NUMAT=NO. OF MATERIAL PROPERTIES.
C

C   FOR INTERIOR WE ARE SOLVING REAL ARITHMETIC
C   PROBLEM WJ=-((S11)INVERSE)*S12*WC
C   S=RK-(KAPPA**2)*RM.ON C WE COLLOCATE TO SOLVE
C       **KII KIJ~~~*C~~*=~~UMAT~~*
C       **KJI KJJ~~~*A~~*=~~VMAT~~*, WHICH NEEDS COMPLEX ALGORITHM.C
C

LOGICAL SWITCH
INTEGER IPT1(20),IPT2(20)
REAL RKAPPA(20),GAMMA1(20),AMU1(6),AMU2(6),RHOS(6),X(167),Y(167),
ANGLEC(26),
WC(26,26),WCINV(26,26),WAREA(141),
WJ(167,26),WDER(26,26),R(26),
RP(24),THFTAV(24),BJ(27),BY(27)
COMPLEX UMAT(26),VMAT(26),HANL(27),HANLD(27),HDTOH(27),
FINAL(167),AOUT(26),W0(167),LRSIDF(26,26),RSIDF(26),RSIDF2(26),
HDTOHS(26,26),WSDIFF,WSCAT(167),VTOT(24),VSCAT2(24)
READ(2,*) KC,IOUTPR,ISCAT
READ(2,*) RKAPPA1,SWITCH,YLEN,ICOPY,VFRANG
READ(2,*) NGAMA,(GAMMA1(I),I=1,NGAMA)
RFAD(2,*) ITNP,MTERM
READ(2,*)(X(I),Y(I),I=1,ITNP)
READ(2,*)(ANGLEC(I),R(I),I=1,KC)
READ(2,*)(WC(I,J),WCINV(I,J),WDFP(I,J),I=1,KC),J=1,KC)
READ(2,*)(WI(I,J),I=1,ITNP),J=1,KC)
IF (IOUTPR.EQ.0) GO TO 206
READ(2,*) NPRPT,(RP(I),THFTAV(I),I=1,NPRPT)
206 CONTINUE
IF (ISCAT.EQ.0) GO TO 221
RFAD(2,*) NSCAT,(IPT1(I),IPT2(I),I=1,NSCAT)
221 CONTINUE
RC=R(1)

```

```
CALL HANKL1(RC,MTERM,HANL,HANLD,HDTOH,PKAPAI,BJ,BY,SWITCH)
DO 200 IGAMA=1,NGAMA
  GAMMA=GAMMA1(IGAMA)
  CALL MATUV1(X,Y,UMAT,VMAT,W0,ANGLEC,KC,ITNP,
  .GAMMA,PKAPAI,SWITCH)
  CALL SOLVE1(WDFR,WC,HANL,HDTOH,VMAT,UMAT,WGINV,KC,WI,
  .MTERM,ITNP,AOUT,FINAL,W0,WARFA,LRSIDE,RSIDE,RSIDE2,HDTOLS,
  .WSCAT,SWITCH)
  IF (IOUTPR.EQ.0) GO TO 210
  CALL OUTER(AOUT,PP,THFTAV,NPRPT,KC,PKAPAI,GAMMA,RJ,PY,WARFA,
  .HANL,WTOT,WSCAT2)
210 CONTINUE
  INNER=ITNP-KC
  PRINT 100,INNER,KC,ITNP
  DO 500 I=1,ICOPY
    CALL PRINT (RKAPAI,GAMMA,ITNP,KC,
  .FINAL,WSCAT,W0,AOUT,NPRPT,THFTAV,RP,WTOT,WSCAT2,ISCAT,
  .NSCAT,IPT1,IPT2,YLENG,Y,VFRANG)
500 CONTINUE
100 FORMAT('1',10(/)' ',50X,'DIFFRACTION OF PLANE SH-WAVFS'//
  .' ',57X,'IN A HALF SPACE'//'
  .' ',57X,'(MEI'S METHOD)',15(/)
  .' ',49X,36('*')//',51X,'NUMBER OF INNER NODES',4X,':',
  .I6//',51X,'NUMBER OF BOUNDARY NODES',1X,':',I6//'
  .' ',51X,'NUMBER OF TOTAL NODES',4X,':',I6//'
  .' ',49X,36('*'))
200 CONTINUE
  STOP
END
SUBROUTINE HANKL1(RC,MTERM,HANL,HANLD,HDTOH,PKAPAI,BJ,BY,SWITCH)
C FOP SEMI-CIRCLE OF RADIUS=RC, THIS CALCULATES THE HANKEL
C FUNCTIONS AND ITS DERIVATIVES. ARGUMENT=RC*PKAPAI.
COMPLEX C1,HANL(MTERM),HANLD(MTERM),HDTOH(MTERM)
REAL BJ(MTERM),BY(MTERM)
LOGICAL SWITCH
Z=RC*PKAPAI
M=MTERM
C1=CMPLX(0.,1.)
CALL MMBSJN(Z,M,BJ)
CALL MMBSYN(Z,0,M,BY,IFP)
DO 10 N=1,M
10 HANL(N)=BJ(N)-C1*BY(N)
MM1=M-1
DO 20 N=1,MM1
NP1=N+1
HANL(N)=-RKAPAI*HANL(NP1)+(N-1)*HANL(N)/RC
20 HDTOH(N)=HANLD(N)/HANL(N)
HANLD(M)=CMPLX(0.,0.)
HDTOH(M)=CMPLX(0.,0.)
IF(SWITCH)PRINT 200
IF(SWITCH)PRINT 201,HANL
IF(SWITCH)PRINT 202
IF(SWITCH)PRINT 201,HANLD
IF(SWITCH)PRINT 203
```

```

      IF(SWITCH)PRINT 201,FDTOR
200 FORMAT(' ',2X,'$SPRINT HANL FOR CHECK$',/)
201 FORMAT(' ',2X,8G16.6)
202 FORMAT(' ',2X,'$SPRINT HANLD FOR CHECK$',/)
203 FORMAT(' ',2X,'$SPRINT HDTON FOR CHECK$',/)
      RETURN
      END
      SUBROUTINE MATUV1(X,Y,UMAT,VMAT,W0,ANGLEC,KC,ITNP,GAMMA,RKAPAL,
     .                      SWITCH)
C
C      CALCULATES W0=(WINC.+WREFLECTED) AT ALL NODAL POINTS.
C      UMAT=(WINC.+WREFLECTED) AT POINTS ON C.
C      VMAT=RADIAL DERIVATIVE OF UMAT.
C
C      COMPLEX UMAT(KC),VMAT(KC),W0(ITNP),C1
C      REAL ANGLEC(KC),X(ITNP),Y(ITNP)
C      LOGICAL SWITCH
C      C1=CMPLX(0.,1.)
C      KI=ITNP-YC
C      DO 10 I=1,ITNP
C         TERM1=RKAPAL*SIN(GAMMA)
C         TERM2=TFPM1*X(I)
C         TERM3=RKAPAL*COS(GAMMA)
C         TFPN4=TERM3*Y(I)
C         W0(I)=2.*COS(TERM4)*CEXP(-C1*TERM2)
C         IF (I.LE.KI) GO TO 100
C         J=I-KI
C         THETA=ANGLEC(J)
C         UMAT(J)=W0(I)
C         VMAT(J)=-(2.*C1*TFPM1*COS(TERM4)*SIN(THETA)+2.*TERM3*SIN(TERM4)*
C         .COS(THETA))*CEXP(-C1*TERM2)
100    CONTINUE
10    CONTINUE
C      PRINT 200
C      PRINT 201,W0
      IF(SWITCH)PRINT 202
      IF(SWITCH)PRINT 201,UMAT
      IF(SWITCH)PPINT 203
      IF(SWITCH)PRINT 201,VMAT
C 200 FORMAT(' ',2X,'$SPRINT W0 FOR CHECK$',/)
201 FORMAT(' ',2X,8G16.6)
202 FORMAT(' ',2X,'$SPRINT UMAT FOR CHECK$',/)
203 FORMAT(' ',2X,'$SPRINT VMAT FOR CHECK$',/)
      RETURN
      END
      SUBROUTINE SOLVE1(KJI,KIJ,HANL,HDTOR,VMAT,UMAT,KIIINV,KP,
     .EN,MTERM,ITNP,AOUT,FINAL,W0,WARFA,LRSIDE,RSIDE,RSIDE2,HDTORH,
     .WSCAT,SWITCH)
C
C      SOLVES KIJ*C + KIJ*A = UMAT ,
C      KJI*C + KJJ*A = VMAT , WHERE KIJ=WC,KJI=WDER,
C      C=UNKNOWN COEFF. FOR WN,A ARE COEFF. FOR OUTFP EXPANSION
C      =AOUT.PROGRAM SOLVES FOR C AND THEN CALCULATES A.THEN IT
C      CALCULATES VTOTAL=FINAL(I) AND WSCATTERED=UTOTAL-W0.

```

```

C      KP=KC,KIIINV=WCINV.
C
C      REAL KJI(KP,KP),KII(KP,KP),KIIINV(KP,KP),WN(ITNP,KP),WAREA(KP)
C      COMPLEX WANI(MTERM),HDTOH(MTERM),VMAT(KP),UMAT(KP),LPSIDE(KP,KP)
C      COMPLEX RSIDE(KP),RSIDE2(KP),FINAL(ITNP),HDTOLS(KP,KP),AOUT(KP)
C      COMPLEX WSCAT(ITNP),W0(ITNP)
C      LOGICAL SWITCH
C      TRANSFER HDTOH TO A SQUARE MATRIX HDTOLS.
DO 1 I=1,KP
DO 2 J=1,KP
IF (I.EQ.J) GO TO 3
HDTOLS(I,J)=CMPLX(0.,0.)
GO TO 4
3 HDTOLS(I,J)=HDTOH(I)
4 CONTINUE
2 CONTINUE
1 CONTINUE
C      FORM LPSIDE=KII*HDTOLS AND RSIDE2=KIIINV*UMAT.
DO 10 I=1,KP
RSIDE2(I)=CMPLX(0.,0.)
DO 11 L=1,KP
LPSIDE(I,L)=CMPLX(0.,0.)
DO 12 J=1,KP
LPSIDE(I,L)=LPSIDE(I,L)+KII(I,J)*HDTOLS(J,L)
12 CONTINUE
RSIDE2(I)=RSIDE2(I)+KIIINV(I,L)*UMAT(L)
11 CONTINUE
10 CONTINUE
C      RSIDE=LPSIDE*PSIDE2
DO 20 I=1,KP
RSIDE(I)=CMPLX(0.,0.)
DO 21 L=1,KP
RSIDE(I)=PSIDE(I)+LPSIDE(I,L)*RSIDE2(L)
21 CONTINUE
20 CONTINUE
C      SUBTRACT LPSIDE FROM KJI TO FORM L.H.S.
C      SUBTRACT RSIDE FROM VMAT TO FORM R.H.S.
DO 30 I=1,KP
DO 31 J=1,KP
LPSIDE(I,J)=KJI(I,J)-LPSIDE(I,J)
31 CONTINUE
PSIDE(I)=VMAT(I)-RSIDE(I)
30 CONTINUE
IF(SWITCH)PRINT 400
IF(SWITCH)PRINT 401,LPSIDE
IF(SWITCH)PRINT 402
IF(SWITCH)PRINT 401,PSIDE
400 FORMAT(' ',2X,'$SPRINT LPSIDE FOR CHECK$',/)
401 FORMAT(' ',2X,8G16.6)
402 FORMAT(' ',2X,'$SPRINT PSIDE FOR CHECK$',/)
C      SOLVES :L.H.S.!*~:C~!= ~:R.H.S.~! THROUGH IMSL.
C      N=KP

```

```

IA=KP
M=1
IR=KP
IJOP=0
CALL LFOTIC(LPSIDE,N,IA,RSIDE,M,IR,IJOP,WAPFA,IER)
IF(SWITCH)PRINT 402
IF(SWITCH)PRINT 401,RSIDE
C   VFCTOR ~:C~! IS RETURNED IN RSIDE.
C   CALCULATE WTOTAL=TUE NODAL DISPLACEMENT CALLED FINAL=WN*C.
DO 50 I=1,ITNP
FINAL(I)=CMPLX(0.,0.)
DO 51 J=1,KP
FINAL(I)=FINAL(I)+WN(I,J)*PSIDE(J)
51 CONTINUE
50 CONTINUE
C   CALCULATES COEFF. A=AOUT FOR OUTER EXPANSION.
DO 200 I=1,KP
AOUT(I)=(RSIDE(I)-RSIDE2(I))/HANL(I)
200 CONTINUE
C   CALCULATE SCATTERED FIELD
DO 210 I=1,ITNP
WSCAT(I)=FINAL(I)-V0(I)
210 CONTINUE
RETURN
END
SUBROUTINE OUTER(AOUT,RP,THETAV,NPRPT,KC,RKAPAI,GAMMA,BJ,
BY,WAREA,HANL,WTOT,USCAT2)
C
C   IF JOUTPP.GT.0 THEN THIS SUBROUTINE IS ACTIVATED.
C   READ (RP,THETA) COORDS. OF NPRPT POINTS WHERE RESULTS ARE
C   DESIRED. PROGRAM GIVES TOTAL AND SCATTERED FIELD AT THESE POINTS
C
REAL RP(NPRPT),THETAV(NPRPT),WAREA(KC),BJ(KC),BY(KC)
COMPLEX AOUT(KC),HANL(KC),USCAT,WTOT(NPRPT),C1,USCAT2(NPRPT)
C1=CMPLX(0.,1.)
DO 10 I=1,NPRPT
ARG=RKAPAI*RP(I)
THFTA=THETAV(I)
CALL MMBSJN(ARG,KC,BJ)
CALL MMBSYN(ARG,0,KC,BY,IER)
DO 20 N=1,KC
20 HANL(N)=BJ(N)-C1*BY(N)
DO 30 J=1,KC,2
L=J-1
M=J
N=J+1
TERM1=L*THFTA
TERM2=M*THFTA
WAREA(M)=COS(TERM1)
30 WAREA(N)=SIN(TERM2)
USCAT2(I)=CMPLX(0.,0.)
DO 40 J=1,KC
USCAT2(I)=USCAT2(I)+HANL(J)*WAREA(J)*AOUT(J)
40 ABWSC=CABS(USCAT)

```

```
TERM1=RKAPA1*SIN(THETA)*SIN(GAMMA)
TERM2=RP(I)*TERM1
TERM3=RKAPA1*COS(THETA)*COS(GAMMA)
TERM4=RP(I)*TERM3
WTOT(I)=2.*COS(TERM4)*CEXP(-C1*TERM2)+WSCAT2(I)
10 CONTINUE
RETURN
END
SUBROUTINE MMBSJN(Z,MMM,BJ)
REAL BJ(MMM)
D=1.0D-10
DO 200 N=1,MMM
KK=N-1
PJ(N)=BESJ(Z,KK,D,IER)
200 CONTINUE
RETURN
END
REAL FUNCTION BESJ*8 (X, N, D, IER)
IMPLICIT RFAL*8(A-B,0-Z)
CFNFRIC
RFAL*8 X, D
BESJ = 0.
IF (N .GE. 0) GO TO 10
IER = 1
RETURN
10 IF (X .GT. 0) GO TO 20
IER = 2
RETURN
20 NTFST = 90+X/2
IF (X .LT. 15) NTFST = X*(10-X/3)+20
IF (N .LT. NTFST) GO TO 30
IER = 4
RETURN
30 IER = 0
N1 = N+1
BPFV = 0.0D0
MA = X+6
IF (X .GE. 5.) MA = 1.4*X+60./X
MB = N+INT(X)/4+2
MZERO = MAX0(MA, MB)
DO 50 M = MZERO, NTFST, 3
FM1 = 1.0D-28
FM = 0.0D0
ALPHA = 0.0D0
JT = 1
IF (N .EQ. M/2*2) JT = -1
M2 = M-2
DO 40 K = 1, M2
MK = M-K
BMK = 2.0D0*MK*FM1/X-FM
FM = FM1
FM1 = BMK
IF (MK-N .EQ. 1) BESJ = FMK
JT = -JT
```

```

S = 1+JT
40 ALPHA = ALPHA+BMK*S
    BMK = 2.0D0*FM1/X-FM
    IF (N .EQ. 0) BESJ = BMK
    ALPHA = ALPHA+BMK
    BESJ = BESJ/ALPHA

C     IF (ABS(BESJ-BPREV) .LE. ABS(D*BESJ)) RETURN
        IF (ABS(BESJ-BPREV) .LE. ABS(D*BESJ)) GO TO 55
50 BPREV = BESJ
    IEP = 3

55 IF (ABS(BESJ) .LE. 10.0D-30) BESJ = 0.0D0

    RETURN
END
SUBROUTINE PRINT (RKAPAI,CAMMA,ITNP,KC,
•FINAL,WSCAT,W0,AOUT,NPRPT,THETAV,FP,WTOT,WSCAT2,ISCAT,
•NSCAT,IPT1,IPT2,YLNG,Y,VERANG)
COMPLEX FINAL(ITNP),WSCAT(ITNP),W0(ITNP),AOUT(KC),
•WTOT(NPRPT),WSCAT2(NPRPT),WSDIFF
INTEGER IPT1(NSCAT),IPT2(NSCAT)
REAL THETAV(NPRPT),RP(NPRPT),Y(ITNP)

C
PRINT 50, RKAPAI,CAMMA,YLNG,VERANG
PRINT 100
DO 10 I=1,ITNP
ABWTOT=CABS(FINAL(I))
ABWSC=CABS(WSCAT(I))
ABW0=CABS(W0(I))
PRINT 110,I,FINAL(I),ABWTOT,WSCAT(I),ABWSC,W0(I),ABW0
10 CONTINUE
PRINT 120
PRINT 130,AOUT
PRINT 140
DO 20 I=1,NPRPT
ABWTOT=CABS(WTOT(I))
ABWSC=CABS(WSCAT2(I))
PRINT 150, I,RP(I),THETAV(I),WTOT(I),ABWTOT,WSCAT2(I),ABWSC
20 CONTINUE
IF (ISCAT .EQ. 0) GO TO 222
PRINT 160
PPINT 170
DO 30 IS=1,NSCAT
I1=IPT1(IS)
I2=IPT2(IS)
WSDIFF=WSCAT(I1)-WSCAT(I2)
ABW=CABS(WSDIFF)
APW1=ABW/(4.*YLNG*RKAPAI)
PRINT 180, I1,I2,Y(I1),WSDIFF,ABW,APW1
30 CONTINUE
222 CONTINUE
50 FORMAT('1',2X,'RKAPAI=',G10.3,2Y,'CAMMA=',G10.3,

```

```
.2X,'CRACK LENGTH=',G10.3,2X,'ANGLE FROM HORIZONTAL AXIS=',G10.3,
.2X,'**MEI'S METHOD**')
100 FORMAT('---',2X,'NODE NO.',4X,10(*),'TOTAL FIELD',
.9(*),10X,8(*),'SCATTERED FIELD',7(*),9X,
.8(*),'INCIDENCE FIELD',7(*)/
.' ',14X,'RFTF',9X,'IMTF',9X,'ARTF',9X,'RFSE',9X,'JMSF',
.9X,'ARSF',9X,'RFIF',9X,'IMIF',9X,'ARIF'//)
110 FORMAT(' ',4X,I6,9C13.5)
120 FORMAT('---',42X,'****AOUT = COEFFICIENT OF OUTER EXPANSION****')
130 FORMAT(' ',2X,8G16.6)
140 FORMAT('---',4X,'NODE NO.',32X,14(*),'TOTAL FIELD',14(*),
.8X,8(*),'SCATTERED FIELD',11(*),/ ',16X,'R',10X,'THETA',12X,
.'RFTF',12X,
.'IMTF',12X,'ARTF',12X,'RFSE',12X,'JMSF',12X,'ARSF',//)
150 FORMAT(' ',4X,I4,8C15.5)
160 FORMAT('---',25X,'****DIFFERENCE OF SCATTERED FIELD****')
170 FORMAT(' ',,'BETWEEN NODES',5X,'Y',8X,9(*),'DIFFERENCE',9(*),
.7X,
.'\DIFFERENCE\',5X,'DIFF BY 4KL'//)
180 FORMAT(' ',2X,2I5,2X,F9.5,2X,4G16.6)
      RETURN
      END
//GO.FT02F001 DD DSN=CHOW.DA1.NEWDATA,UNIT=SYSDA,
//           DISP=(OLD,KEEP),VOL=SER=WORK04
```

```

//WONG JOB ',,,T=10,L=2','KIN WONG'
// EXEC FORTXCC,SIZE=512K,P=D,PARM.GO=( 'EP=MAIN', 'SIZE=256K' ),
//      MAP=NOMAP
//FORT.SYSIN DD *
      INTEGER ITNP/10/, MTERM/20/
      REAL*8 GAMMA/0.0/, RS/1.0D0/,
*          TRY(8)/0.05,0.1,0.25,0.50,1.,2.,3.,5./
      REAL*8 HANX,ANGLES(10),ATER,RKAPA,BJ(20)
      COMPLEX*16 IMGG,REF(10),HANL(20),COEFA(19),
+          COEFB(19),SCAT(10)
      DO 10 J=1,8
      RKAPA=TRY(J)
      HANX=RKAPA*RS
      IMGG=(0.0D0,1.0D0)

C
      CALL COOR(ITNP,ANGLES)
      CALL INCREF(IMGG,RKAPA,RS,GAMMA,ANGLES,ITNP,REF)
      CALL HANKFL(HANX,MTERM,HANL,BJ,IMGG)
      CALL COEFF(HANL,BJ,ITNP,COEFA,COEFB,MTERM,HANX,GAMMA,IMGG)
      CALL SCATER(COEFA,COEFB,ANGLES,ITNP,SCAT,REF,HANL,MTERM,
*          RS,RKAPA,GAMMA)
10    CONTINUE
      STOP
      END
      SUBROUTINE COOR(ITNP,ANGLES)
      INTEGER ITNP
      REAL*8 ANGLES(ITNP),PI,DIV,RINC,RINCC
      PI=3.141592654
C DIV = ITNP -1 IF WORK WITH FMEI
      DIV=ITNP-1
C
      DIV=ITNP-2
      RINC=PI/DIV
      RINCC=0.0D0
      DO 10 J=1,ITNP
C THE FOLLOWING 3 CODE SHOULD BE DELETED IF WORK WITH FMEI
      ITNPM1=ITNP-1
      IF(J .EQ. 1 .OR. J .EQ. ITNPM1)RINC=PINC/2
      IF(J .NE. 1 .AND. J .NE. ITNPM1)RINC=PI/DIV
      ANGLES(J)=RINCC
      RINCC=RINCC+RINC
      ANGLES(J)=PI/2.0D0-ANGLES(J)
C
      PRINT 100,J,ANGLES(J)
100   FORMAT(' ',I4,'ANGLES',G10.3)
10    CONTINUE
      RETURN
      END
      SUBROUTINE INCREF(IMGG,RKAPA,RS,GAMMA,ANGLES,ITNP,REF)
      INTEGER ITNP
      REAL*8 RKAPA,RS,GAMMA,ANGLES(ITNP),TERM1,TERM2,ANGLE
      COMPLEX*16 IMGG,REF(ITNP)
      DO 10 J=1,ITNP
          ANGLE=ANGLES(J)
          TERM1=RKAPA*DSIN(GAMMA)*RS*DSIN(ANGLE)
          TERM2=RKAPA*DCOS(GAMMA)*RS*DCOS(ANGLE)

```

```

REF(J)=2.0D0*CDEXP(-IMGG*TERM1)*DCOS(TERM2)
C      PRINT 100,J,REF(J)
100  FORMAT(' ',I4,5X,'REF',2G20.5)
10    CONTINUE
      RETURN
END

SUBROUTINE HANKEL(HANX,MTERM,HANL,PJ,IMGG)
INTEGER MTERM
REAL*8 BJ(MTERM),BY,BESJ,BESY,D,HANX
COMPLEX*16 IMGG,HANL(MTERM)
D=1.0D-7
DO 10 J=1,MTERM
  JM1=J-1
  BJ(J)=BESJ(HANX,JM1,D,IER)
  BY=BESY(HANX,JM1,IER)
  HANL(J)=BJ(J)-IMGG*BY
C      PRINT 100,J,BJ(J),HANL(J)
100  FORMAT(' ',5X,I4,5X,'BJ',G20.10,5X,'HANL',2G20.10)
10    CONTINUE
      RETURN
END

SUBROUTINE COEFF(HANL,BJ,ITNP,COEFA,COEFB,MTERM,HANX,GAMMA,
+                      IMGG)
INTEGER ITNP,MTERM,NM1,N2M1,N2M2,N2M3,HNM1,HN2M1,HN2M2,
+                      HN2M3
REAL*8 BJ(MTERM),HANX,GAMMA
COMPLEX*16 HANL(MTERM),COEFA(ITNP),COEFB(ITNP),IMGG
COEFA(1)=-2.0D0*BJ(2)/HANL(2)
COEFB(1)=4.0D0*IMGG*DSIN(GAMMA)*(HANX*PJ(1)-BJ(2))/(
+                      (HANX*HANL(1)-HANL(2)))
DO 10 N=2,ITNP
  NM1=N-1
  N2M1=2*N-1
  N2M2=2*N-2
  N2M3=2*N-3
  HNM1=NW1+1
  HN2M1=N2M1+1
  HN2M2=N2M2+1
  HN2M3=N2M3+1
  COEFA(N)=-4.0D0*((-1)**NM1)*DCOS(N2M2*GAMMA)*
+                      ((HANX*BJ(HN2M3)-N2M2*BJ(HN2M2))/(
+                      (HANX*HANL(HN2M3)-N2M2*HANL(HN2M2))))
  COEFB(N)=4.0D0*IMGG*((-1)**NM1)*DSIN(N2M1*GAMMA)*
+                      ((HANX*BJ(HN2M2)-(N2M1)*BJ(HN2M1))/(
+                      (HANX*HANL(HN2M2)-(N2M1)*HANL(HN2M1))))
10    CONTINUE
      DO 20 N=1,ITNP
C      PRINT 200,N,COEFA(N),COEFB(N)
200  FORMAT(' ',I4,5X,'COEFA',2G10.3,5X,'COEFB',2G10.3)
20    CONTINUE
      RETURN
END

SUBROUTINE SCATER(COEFA,COEFB,ANGLES,ITNP,SCAT,REF,
+                      HANL,MTERM,RS,RKAPA,GAMMA)

```

```

INTEGEPE ITNP,N2M1,N2M2,HN2M1,HN2M2,MTERM
REAL*8 ANGLES(ITNP),ANGLE,AETEMP
COMPLEX*16 COFFA(ITNP),COEFA(ITNP),SCAT(ITNP),REF(ITNP),
+ HANL(MTERM),TEMP,TOTAL
DO 10 M=1,ITNP
    ANGLE=ANGLEFS(M)
    SCAT(M)=(0.0D0,0.0D0)
    DO 11 N=1,ITNP
        N2M1=2*N-1
        N2M2=2*N-2
        HN2M1=N2M1+1
        HN2M2=N2M2+1
        SCAT(M)=SCAT(M)+COEFA(N)*HANL(HN2M2)*DCOS(N2M2*ANGLE)+  

+ COEFA(N)*HANL(HN2M1)*DSIN(N2M1*ANGLE)
11    CONTINUE
C     PRINT 105,M,SCAT(M)
105   FORMAT(' ',I4,5X,'SCAT',2G20.10)
10    CONTINUE
    PRINT 1, RKAPA,GAMMA,RS
1    FORMAT('1','RKAPA=',G13.5,5X,'GAMMA=',G13.5,5X,'RS=',G13.5)
    PRINT 100
100   FORMAT('-'/'-',2X,'NODE NO.',4X,10('*'),'TOTAL FIELD',
.9('*'),10X,8('*'),'SCATTERED FIELD',7('*'),9X,
.8('*'),'INCIDENCE FIELD',7('*')/
. ',14X,'RETF',9X,'IMTF',9X,'ARTF',9X,'RESF',9X,'IMSF',
.9X,'ABSF',9X,'REIF',9X,'IMIF',9X,'ABIF'//)
    DO 20 M=1,ITNP
        TOTAL=REF(M)+SCAT(M)
        AETOT=CDABS(TOTAL)
        ABSCAT=CDABS(SCAT(M))
        AEREF=CDABS(REF(M))
    PRINT 200,M,TOTAL,AETOT,SCAT(M),ABSCAT,REF(M),AEREF
200   FORMAT(' ',4X,I6,9G13.5)
20    CONTINUE
    RETURN
END
REAL FUNCTION BESJ*8 (X, N, D, IER)
IMPLICIT REAL*8(A-H,O-Z)
GENERIC
REAL*8 X, D
BESJ = 0.
IF (N .GE. 0) GO TO 10
IER = 1
RETURN
10 IF (X .GT. 0) GO TO 20
IER = 2
RETURN
20 NTEST = 90+X/2
IF (X .LE. 15) NTEST = X*(10-X/3)+20
IF (N .LT. NTEST) GO TO 30
IER = 4
RETURN
30 IER = 0
N1 = N+1

```

```
BPREV = 0.0D0
MA = X+6
IF (X .GE. 5.) MA = 1.4*X+60./X
MB = N+INT(X)/4+2
MZERO = MAX0(MA, MB)
DO 50 M = MZERO, NTEST, 3
FM1 = 1.0D-28
FM = 0.0D0
ALPHA = 0.0D0
JT = 1
IF (M .EQ. M/2*2) JT = -1
M2 = M-2
DO 40 K = 1, M2
NK = M-K
BMK = 2.0D0*MK*FM1/X-FM
FM = FM1
FM1 = BMK
IF (MK-N .EQ. 1) BESJ = BMK
JT = -JT
S = 1+JT
40 ALPHA = ALPHA+BMK*S
BMK = 2.0D0*FM1/X-FM
IF (N .EQ. 0) BESJ = BMK
ALPHA = ALPHA+BMK
BESJ = BESJ/ALPHA

C      IF (ABS(BESJ-BPREV) .LE. ABS(D*BESJ)) RETURN
      IF (ABS(BESJ-BPREV) .LE. ABS(D*BESJ)) GO TO 55
50 BPREV = BESJ
IER = 3

55 IF (ABS(BESJ) .LE. 10.0D-30) BESJ = 0.0D0
      RETURN
END
REAL FUNCTION BESY*8 (X, N, IER)
IMPLICIT REAL*8(A-H,O-Z)
GENERIC
REAL*8 X
IF (N .LT. 0) GO TO 100
IER = 0
IF (X .LE. 0) GO TO 110
IF (X .LE. 4.) GO TO 10
T1 = 4.0/X
T2 = T1*T1
P0 = ((((-.0000037043*T2+.0000173565)*T2-.0000487613)*T2+.00017343
&)*T2-.001753062)*T2+.3989423
Q0 = ((((.0000032312*T2-.0000142078)*T2+.0000342468)*T2-
&.00000869791)*T2+.0004564324)*T2-.01246694
P1 = ((((.0000042414*T2-.0000200920)*T2+.0000580759)*T2-.000223203
&)*T2+.002921826)*T2+.3989423
Q1 = ((((-.0000036594*T2+.00001622)*T2-.0000398708)*T2+.0001064741
&)*T2-.0006390400)*T2+.03740084
```

```
A = 2.0/SQRT(X)
B = A*T1
C = X-.7853982
Y0 = A*P0*SIN(C)+B*Q0*COS(C)
Y1 = -A*P1*COS(C)+B*Q1*SIN(C)
GO TO 40
10 XX = X/2.
X2 = XX*XX
T = LOG(XX)+.5772157
SUM = 0.
TERM = T
Y0 = T
DO 20 L = 1, 15
IF (L .NE. 1) SUM = SUM+1./(L-1)
TERM = (TERM*(-X2)/L**2)*(1.-1./(L*(T-SUM)))
20 Y0 = Y0+TERM
TERM = XX*(T-.5)
SUM = 0.
Y1 = TERM
DO 30 L = 2, 16
SUM = SUM+1./(L-1)
FL1 = L-1.
TS = T-SUM
TERM = (TERM*(-X2)/(FL1*L))*((TS-.5/L)/(TS+.5/FL1))
30 Y1 = Y1+TERM
PI2 = .6366198
Y0 = PI2*Y0
Y1 = -PI2/X+PI2*Y1
40 IF (N .GT. 1) GO TO 60
IF (N .EQ. 0) GO TO 50
BESY = Y1
RETURN
50 BESY = Y0
RETURN
60 YA = Y0
YE = Y1
K = 1
70 T = 2*K/X
YC = T*YB-YA
IF (ABS(YC) .LE. 1.0E+70) GO TO 80
IER = 3
RETURN
80 K = K+1
IF (K .EQ. N) GO TO 90
YA = YB
YE = YC
GO TO 70
90 BESY = YC
RETURN
100 IER = 1
RETURN
110 IER = 2
RETURN
END
```

```

//WONG JOB ',,C=0,L=10,T=30', 'WONG', MSGLEVFL=(1,1)
// EXEC FORTXCLG,OPT=2,MAP=NOMAP,P=D,AD=DBL4,
//      CSIZE=512K,LSIZE=512K,SIZE=512K,PARM.LKFD='SIZE=(512K,124V)'
//FORT.SYSIN DD *
C      PROGRAM SHDEEP3(INPUT,OUTPUT,TAPE1,TAPE2)
C
C      HFPEIN CONTOUR C IS A CIRCLE. ALL THE COMMENTS OF SPHALF
C      APPLY. KC MUST BE AN EVEN INTEGER. IOUTER=0 IF OUTER EXPANSION
C      IS NOT REQUIRED. ISCAT=0 IF THE DIFFERENCE IN SCATTERED FIELD
C      IS NOT REQUIRED. IKIND=0 IF AUTOMATIC MESH GENERATOR USED.
C
C      REAL GAMMA1(10),AMU1(3),AMU2(3),RHOS(3)
C      REAL X(176),Y(176),YPH(176),ANGLEC(32),SII(144,144),
C      .SIC(144,32),WC(32,32),
C      .WARFA(144),WI(176,32),R(32),
C      .PP(17),THETAV(17)
C      INTEGER IVER(198,7),IFLMAT(198),IELND(198)
C      INTEGER IPT1(11),IPT2(11)
C      READ (1,*) KI,KC,ITEL,ISTELC,IENDEL,IOUTPR,NUMAT,ISCAT,
C      .IKIND
C      READ (1,*) RKAPA1,CRACK,ICOPY
C      READ (1,*) NGAMA,(GAMMA1(I),I=1,NGAMA)
C      READ (1,*) DEPTH,ALPHA
C      PRINT 400,KI,KC,ITEL,ISTELC,IENDEL,IOUTPR,NUMAT
C      PRINT 401,RKAPA1
C      PRINT 402,NGAMA,(GAMMA1(I),I=1,NGAMA)
C      PRINT 403,DEPTH,ALPHA
C      PRINT 404,ISCAT,IKIND
C
400 FORMAT(' ',2X,'KI = ',I4,2X,'KC = ',I4,2X,'ITEL = ',I4,
.2X,'ISTELC = ',I4,2X,'IFNDFL = ',I4,2X,'IOUTPR = ',
.I4,2X,'NUMAT = ',I4//)
401 FORMAT(' ',2X,'RKAPA1 = ',G14.4//)
402 FORMAT(' ',2X,'NGAMA = ',I4,2X,'GAMMAS= :',10F9.4//)
403 FORMAT(' ',2X,'DEPTH = ',F15.5,2X,'ALPHA = ',F15.5//)
404 FORMAT(' ',2X,'ISCAT = ',I5,2X,'IKIND = ',I5//)
C
ITNP=KI+KC
KCH=KC/2
MTERM=KC+1
MTFRM1=KCH+1
MTFRM2=KCH+2
DO 600 I=1,ITEL
DO 600 J=1,7
600 IVER(I,J)=0
IF (IKIND.EQ.0) GO TO 251
CALL COORD3(X,Y,YPH,ITNP,ALPHA,DEPTH)
GO TO 252
251 CALL COORD4(X,Y,YPH,ITNP,DEPTH)
252 CALL VFCAL(IVER,IFLMAT,IELND,ITEL)
CALL MATRYL(AMU1,AMU2,RHOS,NUMAT)
CALL ANGLE3(X,Y,R,ANGLEC,ITNP,KC)
CALL KANDM4(X,Y,ITNP,ITEL,IVER,IFLMAT,IELND,AMU1,
.AMU2,RHOS,NUMAT,SII,SIC,KI,KC,RKAPA1)
CALL WCMAT4(WC,ANGLEC,KC)
CALL WIMAT(SII,SIC,WI,WC,KI,KC,ITNP,WARFA)

```

```

      WRITE(2,*) KI,ITFL,ISTELC,IFNDFL
      WRITE(2,*) ((IVFR(I,J),I=1,ITFL),J=1,7)
      WRITE(2,*) KC,IOUTPR,ISCAT
      WRITE(2,*) RKAPAI,DEPTH,CRACK,ICOPY
      WRITE(2,*) NGAMA,(GAMMA1(I),I=1,NGAMA)
      WRITE(2,*) ITNP,KCH,MTEFM,MTEPM1,MTEPM2
      WRITE(2,*) (X(J),Y(I),YPH(I),I=1,ITNP)
      WRITE(2,*) (ANGLEC(I),R(I),I=1,KC)
      WRITE(2,*) ((VC(I,J),I=1,KC),J=1,KC)
      WRITE(2,*) ((WI(I,J),I=1,ITNP),J=1,KC)
      IF (IOUTPR.EQ.0) GO TO 205
      READ(1,*) NPPPT,(RP(I),THETAV(I),I=1,NPPPT)
      PRINT 406,(RP(I),THETAV(I),I=1,NPPPT)
      WRITE(2,*) NPPPT,(RP(I),THETAV(I),I=1,NPPPT)
205 CONTINUE
      IF (ISCAT.EQ.0) GO TO 221
      READ(1,*) NSCAT,(IPT1(J),IPT2(I),I=1,NSCAT)
      PRINT 405,NSCAT,(IPT1(I),IPT2(I),I=1,NSCAT)
405 FORMAT(' ',2X,'NSCAT = ',I4,2X,'NODE PATES: ',20I4//)
      WRITE(2,*) NSCAT,(IPT1(I),IPT2(I),I=1,NSCAT)
221 CONTINUE
406 FORMAT(' ',2X,'$ RP,THETA ARRAYS:=',10F9.4//)
      STOP
      END
      SUBROUTINE COORD3(X,Y,YPH,ITNP,ALPHAC,II)
C
C      READS AND PRINTS X,Y COORDS OF ALL NODE POINTS, YPH=Y+II.
C      ALPHA IS CLOCKWISE RIGID BODY ROTATION OF ENTIRE GRID SYSTEM.
C
      REAL X(ITNP),Y(ITNP),YPH(ITNP)
      PRINT 200
      DO 10 J=1,ITNP
      READ(1,*) X(J),Y(J)
      PRINT 101,J,X(J),Y(J)
      XTEMP=X(J)*COS(ALPHAC)-Y(J)*SIN(ALPHAC)
      YTEMP=X(J)*SIN(ALPHAC)+Y(J)*COS(ALPHAC)
      X(J)=XTEMP
      Y(J)=YTEMP
10     YPH(J)=Y(J)+II
      PRINT 201
      DO 15 J=1,ITNP
15     PRINT 102,J,X(J),Y(J),YPH(J)
101    FORMAT(' ',4X,I6,2G16.6)
102    FORMAT(' ',4X,I6,3G16.6)
200    FORMAT(' ',4X,'NODE NO.',5X,'X-COORD',10X,'Y-COORD'//)
201    FORMAT(' ',4X,'NODE NO.',5X,'Y-COORD',10X,'Y-COORD',10X,
     .'Y+DEPTH-COORD'//)
      RETURN
      END
      SUBROUTINE COORD4(X,Y,YPH,ITNP,II)
C
C      AUTOMATICALLY GENRATES MESH FOR CONCENTRIC CIRCLES,
C      CALCULATES X,Y AND Y+II=YPH COORDINATES. RADV=RADIUS OF
C      THE CIRCLE,ARGV = INITIAL ARGUMENTS IN DEGREES ON THAT

```

```

C      CIRCLE,NCIRC = NO. OF CIRCLES. ITNP MUST BE = 4*NPOINT
C      WHERE NPOINT = NO.OF POINTS ON EACH CIRCLE.
C
C      DATA PI/3.14159265/
C      REAL X(ITNP),Y(ITNP),YPH(ITNP),RADV(5),ARGV(5)
C      READ(1,*) NCIRC,(RADV(I),ARGV(I),I=1,NCIRC)
C      PRINT 400,NCIRC,(RADV(I),ARGV(I),I=1,NCIRC)
400 FORMAT(' ',2X,'NCIRC = ',I4,2X,'RADIUS AND ARGUMENT = ',
.10F9.5//)
NPOINT=ITNP/NCIRC
DZ=2.*PI/NPOINT
PRINT 201
DO 100 I=1,NCIRC
RAD=RADV(I)
ARC=ARGV(I)*PI/180.
NADD=(I-1)*NPOINT
DO 110 J=1,NPOINT
J1=J+NADD
X(J1)=RAD*COS(ARC)
Y(J1)=RAD*SIN(ARC)
YPH(J1)=Y(J1)+P
PRINT 202, J1,X(J1),Y(J1),YPH(J1)
110 ARC=ARC+DZ
100 CONTINUE
201 FORMAT(' ',4X,'NODE NO.',5X,'X-COORD',10X,'Y-COORD',10X,
.'(Y+P)-COORD'//)
202 FORMAT(' ',4X,I6,3G16.6)
RETURN
END
SUBROUTINE VVERCAL(IVFP,IFLMAT,IFLND,ITFL)
C
C      READS AND PRINTS ELEMENT NO. ITS MATERIAL TYPE AND
C      NO. OF NODES CONNECTED TO EACH ELEMENT
C
INTEGER IVFE(ITFL,7),IFLMAT(ITFL),IFLND(ITFL)
PRINT 200
DO 10 I=1,ITFL
READ(1,*) IFLMAT(I),IDUM,(IVER(L,J),J=1,IDUM)
IFLND(I)=IDUM
PRINT 201,L,IFLMAT(I),IFLND(I),(IVER(L,J),J=1,TDUM)
10 CONTINUE
201 FORMAT(' ',4X,I8,8X,I8,8X,I8,8X,7I8)
200 FORMAT(' ',4X,'ELEM NO.',5X,'MATERIAL TYPE',5X,
.'NODES PER ELEMENT',20X,'N-O-D-E-S',/)
RETURN
END
SUBROUTINE MATRYI(AMU1,AMU2,RHOS,NUMAT)
C      READS SETS OF MATERIAL PROPERTIES.
REAL AMU1(NUMAT),AMU2(NUMAT),RHOS(NUMAT)
PRINT 200
DO 10 I=1,NUMAT
READ(1,*) AMU1(I),AMU2(I),RHOS(I)
PRINT 201,I,AMU1(I),AMU2(I),RHOS(I)

```

```

10 CONTINUE
201 FORMAT(' ',5X,I6,3G16.6)
200 FORMAT(' ',2X,'MATERIAL NO.',5X,'C1',15X,'C2',15X,'RHO',/)
      RETURN
      END
      SUBROUTINE ANGLE3(X,Y,R,ANGLEC,ITNP,KC)
C
C      CALCULATES R=SORT(X**2+Y**2),ANGLEC=ARCTAN(X/Y)=THETA
C      AT POINTS ON C ONLY.
      REAL X(ITNP),Y(ITNP),ANGLEC(KC),P(KC)
      DATA PI/3.141592654/
      PRINT 299
      KI=ITNP-KC
      DO 200 I=1,KC
      J=I+KI
      CE=X(J)
      ATEP=Y(J)
      IF(X(J).EQ.0..AND.Y(J).EQ.0.) GO TO 80
      R(I)=SQRT(X(J)**2+Y(J)**2)
      IF (CE) 10,20,30
10   IF (ATEP) 40,50,60
60   ANGLEC(I)=ATAN2(CE,ATEP)
      GO TO 300
50   ANGLEC(I)=PI/2.
      GO TO 300
40   AATER=ABS(ATEP)
      ANGLEC(I)=PI/2.+ATAN2(AATER,CE)
      GO TO 300
20   IF (ATEP) 70,80,90
90   ANGLEC(I)=0.
      GO TO 300
80   R(I)=0.
      ANGLEC(I)=0.
      GO TO 300
70   ANGLEC(I)=PI
      GO TO 300
10   ACE=ABS(CE)
      IF (AFTER) 100,110,120
120  ANGLEC(I)=-ATAN2(ACE,AFTER)+2.*PI
      GO TO 300
110  ANGLEC(I)=3.*PI/2.
      GO TO 300
100  AATER=ABS(ATEP)
      ANGLEC(I)=3.*PI/2.-ATAN2(AATER,ACE)
300  CONTINUE
      PRINT 201,I,J,X(J),Y(J),R(I),ANGLEC(I)
200  CONTINUE
201 FORMAT(' ',5X,I6,5X,I6,4G16.6)
299 FORMAT(' ',2X,'SERIAL NO.',5X,'NODE NO.',8X,'X-COORD',
      .'Y-COORD',12X,'R',10X,'THETA',/)
      RRETURN
      END
      SUBROUTINE RANDM4(X,Y,ITNP,ITEL,IVER,IFLMAT,IFLND,AMU1,
      .AMU2,RHOS,NUMAT,SII,SIC,KI,KC,RKAPAI)

```

```

C
C      CALCULATES INDIVIDUAL ELEMENT STIFFNESS ZK AND MASS ZM MATRICES
C      BY CALLING SUBROUTINES ELMS03 AND ELMS, THEN ASSEMBLES THEM INTO
C      GLOBAL MATRICES AS SK = K - (RKAPA1**2)*M , WHERE
C          1      SIC 1
C          SK = 1 SII      1
C          1      SCC 1
C
C      INTEGER IVER(ITFL,7),IFLMAT(ITFL),IFLND(ITFL)
C      REAL X(ITNP),Y(ITNP),AMU1(NUMAT),AMU2(NUMAT),RHOS(NUMAT)
C      REAL ZK(7,7),ZM(7,7),XL(7),YL(7),SII(KI,KI),SIC(KI,KC)
C      RKAPA2=RKAPA1**2
C      DO 10 I=1,KI
C      DO 11 J=1,KI
C 11 SII(I,J)=0.
C 10 CONTINUE
C      DO 15 I=1,KI
C      DO 16 J=1,KC
C 16 SIC(I,J)=0.
C 15 CONTINUE
C      DO 20 L=1,ITFL
C      MATYP=IFLMAT(L)
C      G1=AMU1(MATYP)
C      G2=AMU2(MATYP)
C      RHO=RHOS(MATYP)
C      NEN=IFLND(L)
C      DO 30 I=1,NEN
C      XL(I)=X(IVER(L,I))
C      YL(I)=Y(IVER(L,I))
C 30 CONTINUE
C      CONSTANT STRAIN TRIANGLE (CST):3 NODES ONLY.
C      IF (NEN.GT.4) GO TO 111
C      CALL ELMS03(XL,YL,G1,G2,RHO,ZK,ZM)
C      GO TO 200
C
C      CALCULATES ZK AND ZM FOR 6-NODE TRIANGLE OR 7-NODE QUADRILATERAL
C
C 111 CALL ELMS(XL,YL,NEN,G1,G2,RHO,ZK,ZM)
C 200 DO 41 M=1,NEN
C      IROW=IVER(L,M)
C      DO 42 N=1,NEN
C      ICOL=IVFR(L,N)
C      TEMP=ZK(M,N)-RKAPA2*ZM(M,N)
C      IF(IROW.GT.KI) GO TO 300
C      IF (ICOL.GT.KI) GO TO 121
C      SII(IROW,ICOL)=SII(IROW,ICOL)+TEMP
C      GO TO 300
C 121 ICOL1=ICOL-KI
C      SIC(IROW,ICOL1)=SIC(IROW,ICOL1)+TEMP
C 300 CONTINUE
C 42 CONTINUE
C 41 CONTINUE
C 20 CONTINUE
C      PRINT 400

```

```

400 FORMAT(' ',2X,'$SPRINT SII FOR CHECKSS',//)
C      PRINT 401,SII
C      PRINT 402
402 FORMAT(' ',2X,'$SPRINT SIC FOR CHECKSS',//)
C      PRINT 401,SIC
401 FORMAT(2X,8G16.6)
      RETURN
      END
      SUBROUTINE ELMS03(XL,YL,G1,G2,RHO,ZK,ZM)
C
C      CALCULATES ELEMENTAL STIFFNESS AND MASS MATRICES,
C      ZK AND ZM, FOR CST.
C
      REAL XL(7),YL(7),ZK(7,7),ZM(7,7),D(2)
      REAL B(2,3),DB(2,3),BTDB(3,3)
      D(1)=G1
      D(2)=G2
      A1=XL(3)-XL(2)
      A2=XL(1)-XL(3)
      A3=XL(2)-XL(1)
      B1=YL(2)-YL(3)
      B2=YL(3)-YL(1)
      B3=YL(1)-YL(2)
      AREA=(A3*B2-A2*B3)/2.
      B(1,1)=B1
      B(1,2)=B2
      B(1,3)=B3
      B(2,1)=A1
      B(2,2)=A2
      B(2,3)=A3
C      CALCULATES DB=D*B
      DO 10 I=1,2
      DO 11 J=1,3
11  DB(I,J)=D(I)*B(I,J)
10  CONTINUE
C      CALCULATES BTDB=BT*D*B
      DO 20 I=1,3
      DO 21 J=1,3
        BTDB(I,J)=0.
      DO 22 K=1,2
22  BTDB(I,J)=BTDB(I,J)+B(K,I)*DB(K,J)
21  CONTINUE
20  CONTINUE
      C=AREA*RHO/6.
      DO 31 N=1,3
      DO 32 M=1,3
        IF (N.NE.M) DTEMP=C/2.
        IF (N.EQ.M) DTEMP=C
        ZF(M,N)= BTDB(M,N)/(4.*AREA)
32  ZM(M,N)=DTEMP
31  CONTINUE
      RETURN
      END
      SUBROUTINE ELMS(XL,YL,NFN,G1,G2,RHO,ZK,ZM)

```

```

C
C      CALCULATES ELEMENTAL STIFFNESS AND MASS MATRICES,ZK AND ZM,
C      FOR 6-NODE TRIANGLE AND 7-NODE QUADRILATERAL.
C
C      REAL XL(7),YL(7),ZK(7,7),ZM(7,7),SC(9),TG(9),WT(9)
C      REAL SPP(3,7),P(2),DR(2,7),BTDB(7,7)
C      DO 1 I=1,NEN
C      DO 1 J=1,NEN
C      ZK(I,J)=0.
1   ZM(I,J)=0.
C      CALL  PCAUSS(SC,TG,WT)
C
C      PERFORMS 9-POINTS GAUSS INTEGRATION.
C
C      DO 100 N=1,9
C      IF (NEN.EQ.7) GO TO 111
C      CALL SHAPF6(SC(N),TG(N),XL,YL,XSJ,SHP)
C      GO TO 121
C
111 CALL SHAPF7(SC(N),TG(N),XL,YL,XSJ,SPP)
121 DV=XSJ*WT(N)
      D(1)=G1*D
      D(2)=G2*D
      DO 10 I=1,2
      DO 11 J=1,NEN
11   DB(I,J)=D(I)*SPP(I,J)
10   CONTINUE
      DO 31 I=1,NEN
      DO 32 J=1,NEN
      BTDB(I,J)=0.
      DO 33 K=1,2
33   BTDB(I,J)=BTDB(I,J)+SHP(K,I)*DR(K,J)
32   CONTINUE
31   CONTINUE
      DV=XSJ*WT(N)*RHO
      DO 41 I=1,NEN
      DO 42 J=1,NEN
42   ZM(I,J)=ZM(I,J)+DV*SPP(3,I)*SPP(3,J)
41   CONTINUE
      DO 51 I=1,NEN
      DO 52 J=1,NEN
52   ZK(I,J)=ZK(I,J)+BTDB(I,J)
51   CONTINUE
100  CONTINUE
      RETURN
      END
      SUBROUTINE PCAUSS(SC,TG,WT)
C
C      SG AND TG ARE 9-GAUSS POINTS,WT CORRESPONDING WEIGHTS.
C
      REAL SG(9),TG(9),WT(9)
      G=SQRT(0.6)
      SC(1)= -G
      SC(2)= G

```

```

SG(3)= G
SG(4)= -G
SG(5)= 0.
SG(6)= G
SG(7)= 0.
SG(8)= -G
SG(9)= 0.
TG(1)= -G
TG(2)= -G
TG(3)= G
TG(4)= G
TG(5)= -G
TG(6)= 0.
TG(7)= G
TG(8)= 0.
TG(9)= 0.
W1=25./81.
W2=40./81.
W3=64./81.
DO 22 I=1,4
WT(I)=W1
I1=I+4
WT(I1)=W2
22 CONTINUE
WT(9)= W3
RETURN
END
SUBROUTINE SHAPF6(S,T,XL,YL,XSJ,SHP)
C
C   6-NODE TETRAHEDRON DEGENERATED FROM 8-NODE QUADRILATERAL.
C
REAL XL(7),YL(7),SHP(3,7),XS(2,2)
SHP(3,1)= 0.5*S*(S-1.)
SHP(3,2)= 0.25*(1.+S)*(1.-T)*(S-T-1.)
SHP(3,3)= 0.25*(1.+S)*(1.+T)*(S+T-1.)
SHP(3,4)= 0.5*(1.-S*S)*(1.-T)
SHP(3,5)= 0.5*(1.+S)*(1.-T*T)
SHP(3,6)= 0.5*(1.-S*S)*(1.+T)
C   S-DERIVATIVE
SHP(1,1)= S-0.5
SHP(1,2)= 0.25*(1.-T)*(2.*S-T)
SHP(1,3)= 0.25*(1.+T)*(2.*S+T)
SHP(1,4)= -S*(1.-T)
SHP(1,5)= 0.5*(1.-T*T)
SHP(1,6)= -S*(1.+T)
C   T-DERIVATIVE
SHP(2,1)= 0.
SHP(2,2)= 0.25*(1.+S)*(-S+2.*T)
SHP(2,3)= 0.25*(1.+S)*(S+2.*T)
SHP(2,4)= -0.5*(1.-S*S)
SHP(2,5)= -(1.+S)*T
SHP(2,6)= 0.5*(1.-S*S)
DO 201 J=1,2
XS(1,J)=0.

```

```

XS(2,J)=0.
DO 202 K=1,6
XS(1,J)= XS(1,J)+XL(K)*SHP(J,K)
202 XS(2,J)= XS(2,J)+YL(K)*SHP(J,K)
201 CONTINUE
XSJ= XS(1,1)*XS(2,2)-XS(1,2)*XS(2,1)
DO 300 I=1,6
TEMP=(XS(2,2)*SHP(1,I)-XS(2,1)*SHP(2,I))/XSJ
SHP(2,I)= (-XS(1,2)*SHP(1,I)+XS(1,1)*SHP(2,I))/XSJ
300 SHP(1,I)= TEMP
RETURN
END
SUBROUTINE SHAPF7(S,T,XL,YL,XSJ,SHP)
C 7- NODE QUADRILATERAL.
REAL XL(7),YL(7),XS(2,2),SHP(3,7)
C SHAPF-FUNCTIONS.
SHP(3,1)= -0.25*S*(1.-S)*(1.-T)
SHP(3,2)= 0.25*(1.+S)*(1.-T)*(S-T-1.)
SHP(3,3)= 0.25*(1.+S)*(1.+T)*(S+T-1.)
SHP(3,4)= -0.25*S*(1.-S)*(1.+T)
SHP(3,5)= 0.5*(1.-S*S)*(1.-T)
SHP(3,6)= 0.5*(1.+S)*(1.-T*T)
SHP(3,7)= 0.5*(1.-S*S)*(1.+T)
C S-DERIVATIVES.
SHP(1,1)= -0.25*(1.-T)*(1.-2.*S)
SHP(1,2)= 0.25*(1.-T)*(2.*S-T)
SHP(1,3)= 0.25*(1.+T)*(2.*S+T)
SHP(1,4)= -0.25*(1.+T)*(1.-2.*S)
SHP(1,5)= -S*(1.-T)
SHP(1,6)= 0.5*(1.-T*T)
SHP(1,7)= -S*(1.+T)
C T-DERIVATIVES.
SHP(2,1)= 0.25*S*(1.-S)
SHP(2,2)= 0.25*(1.+S)*(-S+2.*T)
SHP(2,3)= 0.25*(1.+S)*(S+2.*T)
SHP(2,4)= -0.25*S*(1.-S)
SHP(2,5)= -0.5*(1.-S*S)
SHP(2,6)= -(1.+S)*T
SHP(2,7)= 0.5*(1.-S*S)
C           1 XS(1,1)  XS(2,1)  1
C      FORM JACOBIAN =   1           1
C           1 XS(1,2)  XS(2,2)  1
DO 201 J=1,2
XS(1,J)= 0.
XS(2,J)= 0.
DO 202 K=1,7
XS(1,J)= XS(1,J)+XL(K)*SHP(J,K)
202 XS(2,J)= XS(2,J)+YL(K)*SHP(J,K)
201 CONTINUE
XSJ=XS(1,1)*XS(2,2)-XS(1,2)*XS(2,1)
DO 300 I=1,7
TEMP=(XS(2,2)*SHP(1,I)-XS(2,1)*SHP(2,I))/XSJ

```

```
SHP(2,I)=(-XS(1,2)*SHP(1,I)+XS(1,1)*SHP(2,I))/XSJ
300 SHP(1,I)= TEMP
      RETURN
      END
      SUBROUTINE WCMAT4(WC,ANGLEC,KC)
C      THIS SUBROUTINE FORMS THE BOUNDARY LOAD MATRIX :WC! FOR EACH
C      COS(NT(I)) AND SIN(NT(J)), WHERE T(I)= ANGLE ON C. IT ALSO
C      FINDS THE INVERSE OF WC = WCINV.
C
C      KC MUST BE AN EVEN NUMBER, KCH = KC/2
      REAL WC(KC,KC),ANGLEC(KC)
      KCH=KC/2
      DO 10 I=1,KC
      DO 20 J=1,KCH
      JM1=J-1
      KCHPJ=KCH+J
      TEFM1=JM1*ANGLEC(I)
      TEFM2=J*ANGLEC(I)
      WC(I,J)=COS(TEFM1)
20    WC(I,KCHPJ)=SIN(TEFM2)
10    CONTINUE
      RETURN
      END
      SUBROUTINE WIIMAT(SII,SIC,WI,WC,KI,KC,ITNP,WAREA)
C      THIS SUBROUTINE CALCULATES WI(=W AT INTERIOR NODES) DUE TO
C      BOUNDARY LOADS WC FROM EQUATION SII*WI=-SIC*WC THROUGH IMSL.
C      IT ALSO ADDS UP WI AND WC TO FORM WN OF SIZE(ITNP*KC).
C
      REAL SII(KI,VI),SIC(KI,KC),WI(ITNP,KC),WC(KC,KC)
      REAL WAREA(KI)
      DO 10 I=1,ITNP
      DO 10 J=1,KC
10    WI(I,J)=0.
      DO 15 I=1,KI
      DO 15 L=1,KC
      DO 15 J=1,KC
15    WI(I,L)=WI(I,L)-SIC(I,J)*WC(J,L)
      DO 21 I=1,KI
      DO 21 J=1,KC
21    SIC(I,J)=WI(I,J)
C      PRINT 200
C      PRINT 201,VI
C      PRINT 202
202  FORMAT(' ',2X,'$SPRINT SIC FOR CHECK$',//)
C      PRINT 201,SIC
      M=KC
      N=KI
      IA=KI
      IDG=0
C      CALLS IMSL SUBROUTINE
      CALL LFOTIF(SII,M,N,IA,SIC,IDG,WAREA,IER)
C      SII IS DESTROYED.
C      PRINT 202
C      PRINT 201,SIC
```

```
DO 51 I=1,KI
DO 52 J=1,KC
52 WI(I,J)=SIC(I,J)
51 CONTINUE
    DO 53 I=1,KC
        I1=KI+I
        DO 54 J=1,KC
54 WI(I1,J)=WC(I,J)
53 CONTINUE
C      PRINT 200
C      PRINT 201,WT
200 FORMAT(' ',2X,'$PPINT WI FOR CHECK$',/)
201 FORMAT(' ',2X,8G16.6)
      RETURN
      END
//GO.FT02F001 DD DSN=KCWONG.D1,NEUDATA,UNIT=SYSDA,
//                      SPACE=(TRK,(10,5)),DCB=(BLKSIZE=6080,LRECL=80,
//                      RECFM=FB),DISP=(NEW,KEEP),VOL=SER=WORK04
//GO.FT01F001 DD *
```

```

//WONG JOR ', , ,C=0,L=10,T=30', 'WONG', MSGLEVFL=(1,1)
// EXEC FORTXCLG,OPT=2,MAP=NOMAP,P=D,AD=DPL4,
//      CSIZE=512K,LSIZF=512K,SIZE=512F,PARM.LFFD='SIZF=(512K,124P)'
//FORT.SYSIN DD *
C      PROGRAM SHDEEP4(INPUT,OUTPUT,TAPF2)
      INTEGFR IPT1(11),IPT2(11)
      REAL GAMMA1(10),AMU1(3),AMU2(3),PHOS(3)
      REAL X(176),Y(176),YPH(176),ANGLEC(32),WCINV(32,32),
      .WAREA(144),WI(176,32),WDFR(32,32),R(32),FC(32,32),UC2(32,32),
      .BJ(33),BY(33),BJDER(33),RP(17),THETAV(17)
      COMPLEX UMAT(32),VMAT(32),FINAL(176),AOUT(32),
      .WO(176),KIJ(32,32),KJJ(32,32),PKH(33),
      .HN(18),HNDER(18),STORE1(32),STORE2(32,32),
      .LRSIDE(32,32),RSIDE(32),RSIDF1(32),WSDIFF,AMULT(32),
      .WSCAT(176),WSCAT1(32),WSCAT2(32)
      DIMENSION IVER(198,7)
      READ(2,*) KI,ITFL,ISTELC,IENDFL
      READ(2,*) ((IVER(I,J),I=1,ITFL),J=1,7)
      READ(2,*) FC,IOUTPP,ISCAT
      READ(2,*) RKAPA1,DEPTH,CRACK,ICOPY
      READ(2,*) NGAMA,(GAMMA1(I),I=1,NGAMA)
      READ(2,*) ITNP,KCH,NTERM,MTEPM1,MTEPM2
      READ(2,*) (X(I),Y(I),YPH(I),I=1,ITNP)
      READ(2,*) (ANGLEC(I),R(I),I=1,FC)
      READ(2,*) ((WC(I,J),J=1,FC),I=1,FC)
      READ(2,*) ((WI(I,J),J=1,ITNP),I=1,FC)
      IF (IOUTPP.EQ.0) GO TO 206
      READ(2,*) NPRPT,(PP(I),THETAV(I),I=1,NPPPT)
206 CONTINUE
      IF (ISCAT.EQ.0) GO TO 221
      READ(2,*) NSCAT,(IPT1(I),IPT2(I),I=1,NSCAT)
221 CONTINUE
      CALL WCINV4(WC,FC,WCINV,WAREA,WC2)
      CALL WDFRC3(WI,KI,FC,WDFP,ANGLEC,IVER,X,Y,
      .ITNP,ITFL,ISTELC,IENDFL)
      CALL HANKL3(PKAPA1,NTERM,DEPTH,HKH,BJ,BY)
      CALL FORM3(R,ANGLEC,HKH,KIJ,KJJ,KC,MTEPM,KCH,MTEPM2,
      .RKAPA1,BJ,BY,BJDER,HN,HNDER,RSIDE,AMULT)
      DO 200 JGAMA=1,NGAMA
      GAMMA=GAMMA1(JGAMA)
      CALL MATUV3(X,YPH,UMAT,VMAT,WO,ANGLEC,FC,
      .ITNP,GAMMA,RKAPA1)
      CALL SOLVE2(WDFR,KIJ,KJJ,WCINV,VMAT,UMAT,WI,AOUT,
      .FINAL,WO,FC,ITNP,STORE1,STORE2,RSIDE,RSIDF,
      .RSIDE1,WAREA,WSCAT)
      IF (IOUTPP.EQ.0) GO TO 210
      CALL OUTER3(AOUT,PP,THETAV,NPRPT,FC,KCH,RKAPA1,GAMMA,HKH,
      .MTEPM,MTEPM2,HN,RSIDF,BJ,BY,DEPTH,AMULT,RSIDE1,DEPTH,
      .WSCAT1,WSCAT2)
210 CONTINUE
      PRINT 100,KI,FC,ITNP
      DO 500 I=1,ICOPY
      CALL PRINT(RKAPA1,GAMMA,DEPTH,CRACK,ITNP,NPRPT,FC,
      .NSCAT,WSCAT,FINAL,WO,WSCAT1,WSCAT2,RSIDF1,AOUT,PP,
      .RSIDE1,RSIDE,RSIDF,RSIDE2,RSIDE3,RSIDE4,RSIDE5,RSIDE6,RSIDE7,RSIDE8,RSIDE9,RSIDE10,RSIDE11,RSIDE12,RSIDE13,RSIDE14,RSIDE15,RSIDE16,RSIDE17,RSIDE18,RSIDE19,RSIDE20,RSIDE21,RSIDE22,RSIDE23,RSIDE24,RSIDE25,RSIDE26,RSIDE27,RSIDE28,RSIDE29,RSIDE30,RSIDE31,RSIDE32,RSIDE33,RSIDE34,RSIDE35,RSIDE36,RSIDE37,RSIDE38,RSIDE39,RSIDE40,RSIDE41,RSIDE42,RSIDE43,RSIDE44,RSIDE45,RSIDE46,RSIDE47,RSIDE48,RSIDE49,RSIDE50,RSIDE51,RSIDE52,RSIDE53,RSIDE54,RSIDE55,RSIDE56,RSIDE57,RSIDE58,RSIDE59,RSIDE60,RSIDE61,RSIDE62,RSIDE63,RSIDE64,RSIDE65,RSIDE66,RSIDE67,RSIDE68,RSIDE69,RSIDE70,RSIDE71,RSIDE72,RSIDE73,RSIDE74,RSIDE75,RSIDE76,RSIDE77,RSIDE78,RSIDE79,RSIDE80,RSIDE81,RSIDE82,RSIDE83,RSIDE84,RSIDE85,RSIDE86,RSIDE87,RSIDE88,RSIDE89,RSIDE90,RSIDE91,RSIDE92,RSIDE93,RSIDE94,RSIDE95,RSIDE96,RSIDE97,RSIDE98,RSIDE99,RSIDE100,RSIDE101,RSIDE102,RSIDE103,RSIDE104,RSIDE105,RSIDE106,RSIDE107,RSIDE108,RSIDE109,RSIDE110,RSIDE111,RSIDE112,RSIDE113,RSIDE114,RSIDE115,RSIDE116,RSIDE117,RSIDE118,RSIDE119,RSIDE120,RSIDE121,RSIDE122,RSIDE123,RSIDE124,RSIDE125,RSIDE126,RSIDE127,RSIDE128,RSIDE129,RSIDE130,RSIDE131,RSIDE132,RSIDE133,RSIDE134,RSIDE135,RSIDE136,RSIDE137,RSIDE138,RSIDE139,RSIDE140,RSIDE141,RSIDE142,RSIDE143,RSIDE144,RSIDE145,RSIDE146,RSIDE147,RSIDE148,RSIDE149,RSIDE150,RSIDE151,RSIDE152,RSIDE153,RSIDE154,RSIDE155,RSIDE156,RSIDE157,RSIDE158,RSIDE159,RSIDE160,RSIDE161,RSIDE162,RSIDE163,RSIDE164,RSIDE165,RSIDE166,RSIDE167,RSIDE168,RSIDE169,RSIDE170,RSIDE171,RSIDE172,RSIDE173,RSIDE174,RSIDE175,RSIDE176,RSIDE177,RSIDE178,RSIDE179,RSIDE180,RSIDE181,RSIDE182,RSIDE183,RSIDE184,RSIDE185,RSIDE186,RSIDE187,RSIDE188,RSIDE189,RSIDE190,RSIDE191,RSIDE192,RSIDE193,RSIDE194,RSIDE195,RSIDE196,RSIDE197,RSIDE198,RSIDE199,RSIDE200,RSIDE201,RSIDE202,RSIDE203,RSIDE204,RSIDE205,RSIDE206,RSIDE207,RSIDE208,RSIDE209,RSIDE210,RSIDE211,RSIDE212,RSIDE213,RSIDE214,RSIDE215,RSIDE216,RSIDE217,RSIDE218,RSIDE219,RSIDE220,RSIDE221,RSIDE222,RSIDE223,RSIDE224,RSIDE225,RSIDE226,RSIDE227,RSIDE228,RSIDE229,RSIDE230,RSIDE231,RSIDE232,RSIDE233,RSIDE234,RSIDE235,RSIDE236,RSIDE237,RSIDE238,RSIDE239,RSIDE240,RSIDE241,RSIDE242,RSIDE243,RSIDE244,RSIDE245,RSIDE246,RSIDE247,RSIDE248,RSIDE249,RSIDE250,RSIDE251,RSIDE252,RSIDE253,RSIDE254,RSIDE255,RSIDE256,RSIDE257,RSIDE258,RSIDE259,RSIDE260,RSIDE261,RSIDE262,RSIDE263,RSIDE264,RSIDE265,RSIDE266,RSIDE267,RSIDE268,RSIDE269,RSIDE270,RSIDE271,RSIDE272,RSIDE273,RSIDE274,RSIDE275,RSIDE276,RSIDE277,RSIDE278,RSIDE279,RSIDE280,RSIDE281,RSIDE282,RSIDE283,RSIDE284,RSIDE285,RSIDE286,RSIDE287,RSIDE288,RSIDE289,RSIDE290,RSIDE291,RSIDE292,RSIDE293,RSIDE294,RSIDE295,RSIDE296,RSIDE297,RSIDE298,RSIDE299,RSIDE200,RSIDE201,RSIDE202,RSIDE203,RSIDE204,RSIDE205,RSIDE206,RSIDE207,RSIDE208,RSIDE209,RSIDE2010,RSIDE2011,RSIDE2012,RSIDE2013,RSIDE2014,RSIDE2015,RSIDE2016,RSIDE2017,RSIDE2018,RSIDE2019,RSIDE2020,RSIDE2021,RSIDE2022,RSIDE2023,RSIDE2024,RSIDE2025,RSIDE2026,RSIDE2027,RSIDE2028,RSIDE2029,RSIDE20210,RSIDE20211,RSIDE20212,RSIDE20213,RSIDE20214,RSIDE20215,RSIDE20216,RSIDE20217,RSIDE20218,RSIDE20219,RSIDE20220,RSIDE20221,RSIDE20222,RSIDE20223,RSIDE20224,RSIDE20225,RSIDE20226,RSIDE20227,RSIDE20228,RSIDE20229,RSIDE20230,RSIDE20231,RSIDE20232,RSIDE20233,RSIDE20234,RSIDE20235,RSIDE20236,RSIDE20237,RSIDE20238,RSIDE20239,RSIDE20240,RSIDE20241,RSIDE20242,RSIDE20243,RSIDE20244,RSIDE20245,RSIDE20246,RSIDE20247,RSIDE20248,RSIDE20249,RSIDE202410,RSIDE202411,RSIDE202412,RSIDE202413,RSIDE202414,RSIDE202415,RSIDE202416,RSIDE202417,RSIDE202418,RSIDE202419,RSIDE202420,RSIDE202421,RSIDE202422,RSIDE202423,RSIDE202424,RSIDE202425,RSIDE202426,RSIDE202427,RSIDE202428,RSIDE202429,RSIDE202430,RSIDE202431,RSIDE202432,RSIDE202433,RSIDE202434,RSIDE202435,RSIDE202436,RSIDE202437,RSIDE202438,RSIDE202439,RSIDE202440,RSIDE202441,RSIDE202442,RSIDE202443,RSIDE202444,RSIDE202445,RSIDE202446,RSIDE202447,RSIDE202448,RSIDE202449,RSIDE202450,RSIDE202451,RSIDE202452,RSIDE202453,RSIDE202454,RSIDE202455,RSIDE202456,RSIDE202457,RSIDE202458,RSIDE202459,RSIDE202460,RSIDE202461,RSIDE202462,RSIDE202463,RSIDE202464,RSIDE202465,RSIDE202466,RSIDE202467,RSIDE202468,RSIDE202469,RSIDE202470,RSIDE202471,RSIDE202472,RSIDE202473,RSIDE202474,RSIDE202475,RSIDE202476,RSIDE202477,RSIDE202478,RSIDE202479,RSIDE202480,RSIDE202481,RSIDE202482,RSIDE202483,RSIDE202484,RSIDE202485,RSIDE202486,RSIDE202487,RSIDE202488,RSIDE202489,RSIDE202490,RSIDE202491,RSIDE202492,RSIDE202493,RSIDE202494,RSIDE202495,RSIDE202496,RSIDE202497,RSIDE202498,RSIDE202499,RSIDE2024100,RSIDE2024110,RSIDE2024120,RSIDE2024130,RSIDE2024140,RSIDE2024150,RSIDE2024160,RSIDE2024170,RSIDE2024180,RSIDE2024190,RSIDE2024200,RSIDE2024210,RSIDE2024220,RSIDE2024230,RSIDE2024240,RSIDE2024250,RSIDE2024260,RSIDE2024270,RSIDE2024280,RSIDE2024290,RSIDE2024300,RSIDE2024310,RSIDE2024320,RSIDE2024330,RSIDE2024340,RSIDE2024350,RSIDE2024360,RSIDE2024370,RSIDE2024380,RSIDE2024390,RSIDE2024400,RSIDE2024410,RSIDE2024420,RSIDE2024430,RSIDE2024440,RSIDE2024450,RSIDE2024460,RSIDE2024470,RSIDE2024480,RSIDE2024490,RSIDE2024500,RSIDE2024510,RSIDE2024520,RSIDE2024530,RSIDE2024540,RSIDE2024550,RSIDE2024560,RSIDE2024570,RSIDE2024580,RSIDE2024590,RSIDE2024600,RSIDE2024610,RSIDE2024620,RSIDE2024630,RSIDE2024640,RSIDE2024650,RSIDE2024660,RSIDE2024670,RSIDE2024680,RSIDE2024690,RSIDE2024700,RSIDE2024710,RSIDE2024720,RSIDE2024730,RSIDE2024740,RSIDE2024750,RSIDE2024760,RSIDE2024770,RSIDE2024780,RSIDE2024790,RSIDE2024800,RSIDE2024810,RSIDE2024820,RSIDE2024830,RSIDE2024840,RSIDE2024850,RSIDE2024860,RSIDE2024870,RSIDE2024880,RSIDE2024890,RSIDE2024900,RSIDE2024910,RSIDE2024920,RSIDE2024930,RSIDE2024940,RSIDE2024950,RSIDE2024960,RSIDE2024970,RSIDE2024980,RSIDE2024990,RSIDE20241000,RSIDE20241100,RSIDE20241200,RSIDE20241300,RSIDE20241400,RSIDE20241500,RSIDE20241600,RSIDE20241700,RSIDE20241800,RSIDE20241900,RSIDE20242000,RSIDE20242100,RSIDE20242200,RSIDE20242300,RSIDE20242400,RSIDE20242500,RSIDE20242600,RSIDE20242700,RSIDE20242800,RSIDE20242900,RSIDE20243000,RSIDE20243100,RSIDE20243200,RSIDE20243300,RSIDE20243400,RSIDE20243500,RSIDE20243600,RSIDE20243700,RSIDE20243800,RSIDE20243900,RSIDE20244000,RSIDE20244100,RSIDE20244200,RSIDE20244300,RSIDE20244400,RSIDE20244500,RSIDE20244600,RSIDE20244700,RSIDE20244800,RSIDE20244900,RSIDE20245000,RSIDE20245100,RSIDE20245200,RSIDE20245300,RSIDE20245400,RSIDE20245500,RSIDE20245600,RSIDE20245700,RSIDE20245800,RSIDE20245900,RSIDE20246000,RSIDE20246100,RSIDE20246200,RSIDE20246300,RSIDE20246400,RSIDE20246500,RSIDE20246600,RSIDE20246700,RSIDE20246800,RSIDE20246900,RSIDE20247000,RSIDE20247100,RSIDE20247200,RSIDE20247300,RSIDE20247400,RSIDE20247500,RSIDE20247600,RSIDE20247700,RSIDE20247800,RSIDE20247900,RSIDE20248000,RSIDE20248100,RSIDE20248200,RSIDE20248300,RSIDE20248400,RSIDE20248500,RSIDE20248600,RSIDE20248700,RSIDE20248800,RSIDE20248900,RSIDE20249000,RSIDE20249100,RSIDE20249200,RSIDE20249300,RSIDE20249400,RSIDE20249500,RSIDE20249600,RSIDE20249700,RSIDE20249800,RSIDE20249900,RSIDE202410000,RSIDE202411000,RSIDE202412000,RSIDE202413000,RSIDE202414000,RSIDE202415000,RSIDE202416000,RSIDE202417000,RSIDE202418000,RSIDE202419000,RSIDE202420000,RSIDE202421000,RSIDE202422000,RSIDE202423000,RSIDE202424000,RSIDE202425000,RSIDE202426000,RSIDE202427000,RSIDE202428000,RSIDE202429000,RSIDE202430000,RSIDE202431000,RSIDE202432000,RSIDE202433000,RSIDE202434000,RSIDE202435000,RSIDE202436000,RSIDE202437000,RSIDE202438000,RSIDE202439000,RSIDE202440000,RSIDE202441000,RSIDE202442000,RSIDE202443000,RSIDE202444000,RSIDE202445000,RSIDE202446000,RSIDE202447000,RSIDE202448000,RSIDE202449000,RSIDE202450000,RSIDE202451000,RSIDE202452000,RSIDE202453000,RSIDE202454000,RSIDE202455000,RSIDE202456000,RSIDE202457000,RSIDE202458000,RSIDE202459000,RSIDE202460000,RSIDE202461000,RSIDE202462000,RSIDE202463000,RSIDE202464000,RSIDE202465000,RSIDE202466000,RSIDE202467000,RSIDE202468000,RSIDE202469000,RSIDE202470000,RSIDE202471000,RSIDE202472000,RSIDE202473000,RSIDE202474000,RSIDE202475000,RSIDE202476000,RSIDE202477000,RSIDE202478000,RSIDE202479000,RSIDE202480000,RSIDE202481000,RSIDE202482000,RSIDE202483000,RSIDE202484000,RSIDE202485000,RSIDE202486000,RSIDE202487000,RSIDE202488000,RSIDE202489000,RSIDE202490000,RSIDE202491000,RSIDE202492000,RSIDE202493000,RSIDE202494000,RSIDE202495000,RSIDE202496000,RSIDE202497000,RSIDE202498000,RSIDE202499000,RSIDE2024100000,RSIDE2024110000,RSIDE2024120000,RSIDE2024130000,RSIDE2024140000,RSIDE2024150000,RSIDE2024160000,RSIDE2024170000,RSIDE2024180000,RSIDE2024190000,RSIDE2024200000,RSIDE2024210000,RSIDE2024220000,RSIDE2024230000,RSIDE2024240000,RSIDE2024250000,RSIDE2024260000,RSIDE2024270000,RSIDE2024280000,RSIDE2024290000,RSIDE2024300000,RSIDE2024310000,RSIDE2024320000,RSIDE2024330000,RSIDE2024340000,RSIDE2024350000,RSIDE2024360000,RSIDE2024370000,RSIDE2024380000,RSIDE2024390000,RSIDE2024400000,RSIDE2024410000,RSIDE2024420000,RSIDE2024430000,RSIDE2024440000,RSIDE2024450000,RSIDE2024460000,RSIDE2024470000,RSIDE2024480000,RSIDE2024490000,RSIDE2024500000,RSIDE2024510000,RSIDE2024520000,RSIDE2024530000,RSIDE2024540000,RSIDE2024550000,RSIDE2024560000,RSIDE2024570000,RSIDE2024580000,RSIDE2024590000,RSIDE2024600000,RSIDE2024610000,RSIDE2024620000,RSIDE2024630000,RSIDE2024640000,RSIDE2024650000,RSIDE2024660000,RSIDE2024670000,RSIDE2024680000,RSIDE2024690000,RSIDE2024700000,RSIDE2024710000,RSIDE2024720000,RSIDE2024730000,RSIDE2024740000,RSIDE2024750000,RSIDE2024760000,RSIDE2024770000,RSIDE2024780000,RSIDE2024790000,RSIDE2024800000,RSIDE2024810000,RSIDE2024820000,RSIDE2024830000,RSIDE2024840000,RSIDE2024850000,RSIDE2024860000,RSIDE2024870000,RSIDE2024880000,RSIDE2024890000,RSIDE2024900000,RSIDE2024910000,RSIDE2024920000,RSIDE2024930000,RSIDE2024940000,RSIDE2024950000,RSIDE2024960000,RSIDE2024970000,RSIDE2024980000,RSIDE2024990000,RSIDE20241000000,RSIDE20241100000,RSIDE20241200000,RSIDE20241300000,RSIDE20241400000,RSIDE20241500000,RSIDE20241600000,RSIDE20241700000,RSIDE20241800000,RSIDE20241900000,RSIDE20242000000,RSIDE20242100000,RSIDE20242200000,RSIDE20242300000,RSIDE20242400000,RSIDE20242500000,RSIDE20242600000,RSIDE20242700000,RSIDE20242800000,RSIDE20242900000,RSIDE20243000000,RSIDE20243100000,RSIDE20243200000,RSIDE20243300000,RSIDE20243400000,RSIDE20243500000,RSIDE20243600000,RSIDE20243700000,RSIDE20243800000,RSIDE20243900000,RSIDE20244000000,RSIDE20244100000,RSIDE20244200000,RSIDE20244300000,RSIDE20244400000,RSIDE20244500000,RSIDE20244600000,RSIDE20244700000,RSIDE20244800000,RSIDE20244900000,RSIDE20245000000,RSIDE20245100000,RSIDE20245200000,RSIDE20245300000,RSIDE20245400000,RSIDE20245500000,RSIDE20245600000,RSIDE20245700000,RSIDE20245800000,RSIDE20245900000,RSIDE20246000000,RSIDE20246100000,RSIDE20246200000,RSIDE20246300000,RSIDE20246400000,RSIDE20246500000,RSIDE20246600000,RSIDE20246700000,RSIDE20246800000,RSIDE20246900000,RSIDE20247000000,RSIDE20247100000,RSIDE20247200000,RSIDE20247300000,RSIDE20247400000,RSIDE20247500000,RSIDE20247600000,RSIDE20247700000,RSIDE20247800000,RSIDE20247900000,RSIDE20248000000,RSIDE20248100000,RSIDE20248200000,RSIDE20248300000,RSIDE20248400000,RSIDE20248500000,RSIDE20248600000,RSIDE20248700000,RSIDE20248800000,RSIDE20248900000,RSIDE20249000000,RSIDE20249100000,RSIDE20249200000,RSIDE20249300000,RSIDE20249400000,RSIDE20249500000,RSIDE20249600000,RSIDE20249700000,RSIDE20249800000,RSIDE20249900000,RSIDE202410000000,RSIDE202411000000,RSIDE202412000000,RSIDE202413000000,RSIDE202414000000,RSIDE202415000000,RSIDE202416000000,RSIDE202417000000,RSIDE202418000000,RSIDE202419000000,RSIDE202420000000,RSIDE202421000000,RSIDE202422000000,RSIDE202423000000,RSIDE202424000000,RSIDE202425000000,RSIDE202426000000,RSIDE202427000000,RSIDE202428000000,RSIDE202429000000,RSIDE202430000000,RSIDE202431000000,RSIDE202432000000,RSIDE202433000000,RSIDE202434000000,RSIDE202435000000,RSIDE202436000000,RSIDE202437000000,RSIDE202438000000,RSIDE202439000000,RSIDE202440000000,RSIDE202441000000,RSIDE202442000000,RSIDE202443000000,RSIDE202444000000,RSIDE202445000000,RSIDE202446000000,RSIDE202447000000,RSIDE202448000000,RSIDE202449000000,RSIDE202450000000,RSIDE202451000000,RSIDE202452000000,RSIDE202453000000,RSIDE202454000000,RSIDE202455000000,RSIDE202456000000,RSIDE202457000000,RSIDE202458000000,RSIDE202459000000,RSIDE202460000000,RSIDE202461000000,RSIDE202462000000,RSIDE202463000000,RSIDE202464000000,RSIDE202465000000,RSIDE202466000000,RSIDE202467000000,RSIDE202468000000,RSIDE202469000000,RSIDE202470000000,RSIDE202471000000,RSIDE202472000000,RSIDE202473000000,RSIDE202474000000,RSIDE202475000000,RSIDE202476000000,RSIDE202477000000,RSIDE202478000000,RSIDE202479000000,RSIDE202480000000,RSIDE202481000000,RSIDE202482000000,RSIDE202483000000,RSIDE202484000000,RSIDE202485000000,RSIDE202486000000,RSIDE202487000000,RSIDE202488000000,RSIDE202489000000,RSIDE202490000000,RSIDE202491000000,RSIDE202492000000,RSIDE202493000000,RSIDE202494000000,RSIDE202495000000,RSIDE202496000000,RSIDE202497000000,RSIDE202498000000,RSIDE202499000000,RSIDE2024100000000,RSIDE2024110000000,RSIDE2024120000000,RSIDE2024130000000,RSIDE2024140000000,RSIDE2024150000000,RSIDE2024160000000,RSIDE2024170000000,RSIDE2024180000000,RSIDE2024190000000,RSIDE2024200000000,RSIDE2024210000000,RSIDE2024220000000,RSIDE2024230000000,RSIDE2024240000000,RSIDE2024250000000,RSIDE2024260000000,RSIDE2024270000000,RSIDE2024280000000,RSIDE2024290000000,RSIDE2024300000000,RSIDE2024310000000,RSIDE2024320000000,RSIDE2024330000000,RSIDE2024340000000,RSIDE2024350000000,RSIDE2024360000000,RSIDE2024370000000,RSIDE2024380000000,RSIDE2024390000000,RSIDE2024400000000,RSIDE2024410000000,RSIDE2024420000000,RSIDE2024430000000,RSIDE2024440000000,RSIDE2024450000000,RSIDE2024460000000,RSIDE2024470000000,RSIDE2024480000000,RSIDE2024490000000,RSIDE2024500000000,RSIDE2024510000000,RSIDE2024520000000,RSIDE2024530000000,RSIDE2024540000000,RSIDE2024550000000,RSIDE2024560000000,RSIDE2024570000000,RSIDE2024580000000,RSIDE2024590000000,RSIDE2024600000000,RSIDE2024610000000,RSIDE2024620000000,RSIDE2024630000000,RSIDE2024640000000,RSIDE2024650000000,RSIDE2024660000000,RSIDE2024670000000,RSIDE2024680000000,RSIDE2024690000000,RSIDE2024700000000,RSIDE2024710000000,RSIDE2024720000000,RSIDE2024730000000,RSIDE2024740000000,RSIDE2024750000000,RSIDE2024760000000,RSIDE2024770000000,RSIDE2024780000000,RSIDE2024790000000,RSIDE2024800000000,RSIDE2024810000000,RSIDE2024820000000,RSIDE2024830000000,RSIDE2024840000000,RSIDE2024850000000,RSIDE2024860000000,RSIDE2024870000000,RSIDE2024880000000,RSIDE2024890000000,RSIDE2024900000000,RSIDE2024910000000,RSIDE2024920000000,RSIDE2024930000000,RSIDE2024940000000,RSIDE2024950000000,RSIDE2024960000000,RSIDE202497000000
```

```

      .     THETAV,IPT1,IPT2,YPH,ISCAT)
500  CONTINUE
100  FORMAT('1',10(/)' ',50X,'DIFFRACTION OF PLANE SH-WAVES'//
      ',57X,'IN A HALF SPACE'//
      ',57X,'(MEI'S METHOD)',15(/)
      ',49X,36('*')//',51X,'NUMBER OF INNER NODES',4X,':',
      ,I6//',51X,'NUMBER OF BOUNDARY NODES',1X,':',I6//,
      ',51X,'NUMBER OF TOTAL NODES',4X,':',I6//'
      ',49X,36('*'))
200  CONTINUE
      STOP
      END
      SUBROUTINE WCINV4(WC,KC,WCINV,WAREA,WC2)
      REAL WC(KC,KC),WAREA(KC),WCINV(KC,KC),WC2(KC,KC)
C      COPY WC INTO WC2.  WC2 WILL BE DESTROYED.
C      PRINT 200
200  FORMAT(' ',2X,'$SPRINT WC FOR CHECK$$'//)
C      PRINT 201,WC
201  FORMAT(' ',2X,8G16.6)
      DO 90 I=1,KC
      DO 90 J=1,KC
90  WC2(I,J)=WC(I,J)
C      INVERT WC2 = WC USING IMSL ROUTINE
      KPP=KC
      N=PWP
      IA=KPP
      IDGT=0
      CALL LINV1F(WC2,N,IA,WCINV,IDLGT,WAREA,IFP)
C      PRINT 202
202  FORMAT(' ',2X,'$SPRINT WCINV FOR CHECK$$'//)
C      PRINT 201,WCINV
      RETURN
      END
      SUBROUTINE WDERC3(WN,K,KP,WDER,ANGLEC,IVER,X,Y,ITNP,
      ,ITEL,ISTELC,IFNDEL)
C
C      CALCULATES THE MATRIX WDER=RADIAL DERIVATIVE OF WN ON C.
C      KP=KC AND K=KT.
C
      INTEGER IOO(3),IPP(3),IOO(3),IVER(ITEL,7)
      REAL WN(ITNP,KP),WDER(KP,KP),ANGLEC(KP),C(3),X(ITNP),Y(ITNP)
      DO 10 I=1,KP
      DO 10 J=1,KP
10  WDER(I,J)=0.
C
C      FOR EACH COLUMN OF WN--FIND DEPIVATIVE.
C
      DO 20 I=1,KP
      DO 30 L=ISTELC,IEDEL
      IOO(1)=IVER(L,1)
      IPP(1)=IVER(L,2)
      IOO(1)=IVER(L,3)
      IOO(2)=IPP(1)
      IPP(2)=IOO(1)

```

```

I00(2)=I00(1)
I00(3)=IPP(2)
IPP(3)=I00(2)
I00(3)=I00(2)
DO 40 MI=1,2
M=IPP(MI)
MMK=M-K
ANGLE=ANGLEC(MMK)
COSINE=COS(ANGLE)
SINE=SIN(ANGLE)
DO 50 N=1,3
IPP=I00(N)
ISS=IPP(N)
ITT=I00(N)
SA22=X(IRR)-X(ITT)
SA33=X(ISS)-X(IRR)
SB22=Y(ITT)-Y(IPP)
SB33=Y(IRR)-Y(ISS)
AREA2=SA33*SB22-SA22*SB33
C(N)=(((Y(ISS)-Y(ITT))*SINE)+((X(ITT)-Y(ISS))*COSINE))/AREA2
50 CONTINUE
N1=I00(1)
N2=IPP(1)
N3=I00(1)
TEMP=C(1)*WN(N1,1)+C(2)*WN(N2,1)+C(3)*WN(N3,1)
TEMP=TEMP/2.
J=M-K
WDFP(J,I)=WDFP(J,I)+TEMP
40 CONTINUE

30 CONTINUE
20 CONTINUE
C      PRINT 400
400 FORMAT(' ',2X,'$SPRINT WDFP FOR C'FCKSS$',//)
C      PRINT 401,WDFP
401 FORMAT(' ',2X,8G16.6)
RETURN
END
SUBROUTINE HANKL3(RKAPAI,MTERM,H,UKH,BJ,BY)
C
C      CALCULATES HANKEL FUNCTION OF ARGUMENT = 2*RKAPAI*H,
C      WHERE H = DFPTH.
C
REAL BJ(MTERM),BY(MTERM)
COMPLEX CJ,HKH(MTERM)
DATA CJ/(0.,1.)/
M=MTERM
Z=2.*RKAPAI*H
CALL MMBSJN(Z,M,BJ)
CALL MMBSYN(Z,0,M,BY,IER)
DO 20 N=1,M
20 UKH(N)=BJ(N)+CJ*BY(N)
C      PRINT 400
C      PRINT 401,UKH

```

```

400 FORMAT(' ',2X,'$SPRINT HKH FOR CHECK$',/)
401 FORMAT(' ',2X,8G16.6)
    RETURN
    END
    SUBROUTINE FORM3(R,ANGLEC,HKH,KIJ,KJJ,KC,MTERM,KCH,
    •MTERM2,RKAPAI,BJ,RY,BJDER,HN,HNDER,V,AMULT)
C
C   THIS SUBROUTINE FORMS :KIJ!=FUNCTIONS EVALUATED AT KC
C   POINTS ON C,AND :KJJ!=RADIAL DERIVATIVE OF :KIJ! FOR
C   OUTFR EXPANSION.CALLS THE SUBROUTINE AID.
C
    REAL R(KC),ANGLEC(KC),BJ(MTERM2),RY(MTERM2),
    •RKAPAI(MTERM2)
    COMPLEX C1,HKH(MTERM),HN(MTERM2),HNDER(MTERM2),
    •KIJ(KC,KC),KJJ(KC,KC),V(KC),AMULT(KC)
    MTERM1=KCH+1
    KCHM1=KCH-1
    C1=CMPLX(0.,1.)
    RC=R(1)
    Z=PC*RKAPAI
    CALL MMBSJN(Z,MTERM2,BJ)
    CALL MMPSYM(Z,0,MTER2,RY,TFR)
    DO 20 N=1,MTERM2
20  HN(N)=BJ(N)+C1*RY(N)
    DO 30 N=1,MTERM1
    NP1=N+1
    HNDEP(N)=-PKAPAI*IN(NP1)+(N-1)*HN(N)/RC
30  BJDFR(N)=-PKAPAI*RI(NP1)+(N-1)*BJ(N)/RC
    HNDFR(MTERM2)=CMPLX(0.,0.)
    BJDER(MTERM2)=0.
    DO 10 I=1,KC
    THETA=ANGLEC(I)
    CALL AID3(HN,BJ,HKH,THETA,V,MTERM,MTERM2,KCH,KC)
    DO 40 J=1,KC
40  KIJ(I,J)=V(J)
    CALL AID3(HNDER,BJDER,HKH,THETA,V,MTERM,MTERM2,VCP,KC)
    DO 50 J=1,KC
50  KJJ(I,J)=V(J)
10  CONTINUE
    DO 60 J=1,KC
60  AMULT(J)=KIJ(I,J)
    DO 70 J=1,KC
    DO 75 I=1,KC
      KIJ(I,J)=KIJ(I,J)/AMULT(J)
75  KJJ(I,J)=KJJ(I,J)/AMULT(J)
70  CONTINUE
C     PRINT 399
C     PRINT 401,AMULT
399 FORMAT(' ',2X,'$ SPRT AMULT FOR CHECK $$',/)
C     PRINT 400
C     PRINT 401,KIJ
C     PRINT 402
C     PRINT 401,KJJ
400 FORMAT(' ',2X,'$ SPRT KIJ FOR CHECK$$',/)

```

```
402 FORMAT(' ',2X,'$ PRINT KJJ FOR CHECK$',/)  
401 FORMAT(' ',2X,8G16.6)  
    RETURN  
    END  
    SUBROUTINE ATD3(HN1,BJ1,HKH,THETA,V,MTERM,MTERM2,KCH,KC)  
C  
C      PERFORMS THE SUMMATION FOR THE INTERIOR EXPANSION.  
C  
    REAL BJ1(MTERM2)  
    COMPLEX HN1(MTERM2),V(KC),HKH(MTERM),SUM1  
    KCUM1=KCH-1  
    DO 40 J=1,KCH  
    N=J-1  
    SUM1=CMPLX(0.,0.)  
    DO 50 M=1,KCUM1  
    NPM1=N+M+1  
    NMM=N-M  
    NM1=NMM+1  
    NMMA=IABS(NMM)  
    NMMA1=NMMA+1  
    MT=(-1)**M  
    M1=M+1  
    APC=M*THETA  
    IF (NMM) 60,70,70  
70  SUM1=SUM1+MT*(HKH(NPM1)+MT*HKH(NM1))*BJ1(M1)*COS(APC)  
    GO TO 50  
60  SUM1=SUM1+MT*(HKH(NPM1)+MT*((-1)**NMMA)*  
     .HKH(NMMA1))*BJ1(M1)*COS(APC)  
50  CONTINUE  
40  V(J)=((-1)**N)*HN1(J)*COS(N*THETA)+HKH(J)*BJ1(1)+SUM1  
    DO 140 N=1,KCH  
    NKCH=N+KCH  
    NJ=N+1  
    SUM1=CMPLX(0.,0.)  
    DO 150 M=1,KCH  
    NPM1=N+M+1  
    NMM=N-M  
    NM1=NMM+1  
    NMMA=IABS(NMM)  
    NMMA1=NMMA+1  
    MT=(-1)**M  
    MT1=(-1)**(M-1)  
    M1=M+1  
    APC=M*THETA  
    IF (NMM) 160,170,170  
170  SUM1=SUM1+MT1*(HKH(NPM1)-MT*HKH(NM1))*  
     .BJ1(M1)*SIN(APC)  
    GO TO 150  
160  SUM1=SUM1+MT1*(HKH(NPM1)-MT*((-1)**NMMA)*  
     .HKH(NMMA1))*BJ1(M1)*SIN(APC)  
150  CONTINUE  
140  V(NKCH)=SUM1+((-1)**(N-1))*HN1(N1)*SIN(N*THETA)  
    RETURN  
    END
```

```

SUBROUTINE MATUV3(X,Y,UMAT,VMAT,W0,ANGLEC,KC,ITNP,GAMMA,RKAPA1)
C
C   CALCULATES W0=(WINC.+WREFLECTED) AT ALL NODAL POINTS.
C   UMAT=(WINC.+WREFLECTED) AT POINTS ON C.
C   VMAT=RADIAL DERIVATIVE OF UMAT.
C
COMPLEX UMAT(KC),VMAT(KC),W0(ITNP),C1
REAL ANGLEC(KC),X(ITNP),Y(ITNP)
C1=CMPLX(0.,1.)
KI=ITNP-KC
DO 10 I=1,ITNP
TERM1=-RKAPA1*SIN(GAMMA)
TERM2=TERM1*X(I)
TERM3=RKAPA1*COS(GAMMA)
TERM4=TERM3*Y(I)
W0(I)=2.*COS(TERM4)*CEXP(-C1*TERM2)
IF (I.LE.KI) GO TO 100
J=I-KI
THETA=ANGLEC(J)
UMAT(J)=W0(I)
VMAT(J)=-(2.*C1*TERM1*COS(TERM4)*SIN(THETA)+2.*TERM3*SIN(TERM4)*
.COS(THETA))*CEXP(-C1*TERM2)
100 CONTINUE
10 CONTINUE
C   PPTNT 200
C   PRTNT 201,W0
C   PPTNT 202
C   PRINT 201,UMAT
C   PRINT 203
C   PPTNT 201,VMAT
200 FORMAT(' ',2X,'$SPRINT W0 FOR CHECKSS',/)
201 FORMAT(' ',2X,8G16.6)
202 FORMAT(' ',2X,'$SPRINT UMAT FOR CHECKSS',/)
203 FORMAT(' ',2X,'$SPRINT VMAT FOR CHECKSS',/)
RETURN
END
SUBROUTINE SOLVE2(KIJ,KIJ,KJJ,KIIINV,VMAT,UMAT,WN,AOUT,
.FINAL,W0,KC,ITNP,STORE1,STORE2,LRSIDE,RSIDE,RSIDE1,WARFA,
.WSCAT)
C
C   SOLVES KII*C +KIJ*A = UMAT ----DISPLACEMENT
C   KJI*C +KJJ*A = VMAT ----NORMAL DERIVATIVE,
C   WHERE KII=WC,KJI=WDPE,C=UNKNOWN COEFF. FOR WN,
C   A=AOUT=UNKNOWN COEFF. OF OUTER EXPANSION.SOLVES FOR AOUT
C   FIRST AND THEN FOR C.CALCULATES WTOT. AND WSCATTERED.
C
REAL KIJ(KC,KC),KIIINV(KC,KC),WN(ITNP,KC)
REAL WARFA(KC)
COMPLEX KIJ(KC,KC),KJJ(KC,KC),UMAT(KC),VMAT(KC),W0(ITNP),
.FINAL(ITNP),AOUT(KC),STORE1(KC),STORE2(KC,KC),
.LRSIDE(KC,KC),RSIDE(KC),RSIDE1(KC),WSCAT(ITNP)
C
STORE1=KIIINV*UMAT
STORE2=KIIINV*KIJ
DO 10 I=1,KC

```

```

STORE1(I)=CMPLX(0.,0.)
DO 11 J=1,KC
11 STORE1(I)=STORE1(I)+KIIINV(I,J)*UMAT(J)
10 CONTINUE
DO 20 I=1,KC
DO 20 J=1,KC
STORE2(I,J)=CMPLX(0.,0.)
DO 21 K=1,KC
21 STORE2(I,J)=STORE2(I,J)+KIIINV(I,K)*VTK(J,K)
20 CONTINUE
C   LRSIDE = VJJ - KJI*KIIINV*KIJ
DO 30 I=1,KC
DO 30 J=1,KC
LPSIDE(I,J)=CMPLX(0.,0.)
DO 31 K=1,KC
31 LRSIDE(I,J)=LRSIDE(I,J)+KJI(I,K)*STORE2(K,J)
30 CONTINUE
DO 40 I=1,KC
DO 40 J=1,KC
40 LPSIDE(I,J)=VJJ(I,J)-LRSIDE(I,J)
C   R.H.S. CALLED TEMPORARILY AOUT=VMAT-KJT*KIIINV*UMAT
DO 50 I=1,KC
RSIDE(I)=CMPLX(0.,0.)
DO 51 J=1,KC
51 RSIDE(I)=RSIDE(I)+VTK(I,J)*STORE1(J)
50 AOUT(I)=VMAT(I)-RSIDE(I)
C   SOLVES :LRSIDE!~:AOUT~! = ~:R.H.S.~!, THROUGH TMSL.
N=KC
IA=KC
M=1
IB=KC
IJOR=0
CALL LEQTC(LRSIDE,N,IA,AOUT,M,IR,IJOB,LAREA,IER)
C   DESIRED SOLUTION RETURNS IN AOUT=A, THE COFF.
C   COFFS. C ARE NOW CALCULATED AS RSIDE(I).
DO 100 I=1,KC
RSIDE1(I)=CMPLX(0.,0.)
DO 110 J=1,KC
110 RSIDE1(I)=RSIDE1(I)+STORE2(I,J)*AOUT(J)
100 RSIDE(I)=STORE1(I)-RSIDE1(I)
C   CALCULATES UTOTAL=FINAL(I)=VN*C.
DO 120 I=1,ITNP
FINAL(I)=CMPLX(0.,0.)
DO 130 J=1,KC
130 FINAL(I)=FINAL(I)+VN(I,J)*RSIDE(J)
120 CONTINUE
C   CALCULATES SCATTERED FIELD.
DO 210 I=1,ITNP
WSCAT(I)=FINAL(I)-W0(I)
210 CONTINUE
DO 151 I=1,KC
151 AOUT(I)=-AOUT(I)
RETURN
END

```

SUBROUTINE OUTER3(AOUT,RP,THETAV,NPRPT,KC,KCH,RKAPAI,
.GAMMA,HKH,MTERM,MTERM2,HN,V,BJ,BY,I,AMULT,RSIDE1,HDFP,
.WSCAT1,WSCAT2)

C
C IF LOUTPR.GT.0, THEN THIS SUBROUTINE IS ACTIVATED.
C

COMPLEX AOUT(KC),HKH(MTERM),HN(MTERM2),V(KC),C1,
.WSCAT1(NPRPT),USCAT2(NPRPT),RSIDE1(NPRPT),AMULT(KC)
REAL BJ(MTERM2),BY(MTERM2),RP(NPRPT),THETAV(NPRPT)
C1=CMPLX(0.,1.)
DO 10 I=1,NPRPT
THETA=THETAV(I)
RAD=HDFP/COS(THETA)
RP(I)=ARS(RAD)
Z=RKAPAI*RP(I)
CALL MMBSJN(Z,MTERM2,BJ)
CALL MMESYN(Z,0,MTERM2,BY,IFR)
DO 20 N=1,MTERM2
20 HN(N)=BJ(N)+C1*FY(N)
CALL ATD3(HN,BJ,HKH,THETA,V,MTERM,MTERM2,KCH,KC)
WSCAT1(I)=CMPLX(0.,0.)
DO 40 J=1,KC
40 WSCAT1(I)=WSCAT1(I)+V(J)*AOUT(J)/AMULT(J)
DO 140 J=1,KC
N=J-1
140 V(J)=((-1)**N)*2.*HN(J)*COS(N*THETA)
DO 150 N=1,KC
NKCH=N+KC1
N1=N+1
NM1=N-1
150 V(NKCH)=((-1)**NM1)*2.*HN(N1)*SIN(N*THETA)
WSCAT2(I)=CMPLX(0.,0.)
DO 160 J=1,KC
160 WSCAT2(I)=WSCAT2(I)+V(J)*AOUT(J)/AMULT(J)
TERM1=-RKAPAI*SIN(THETA)*SIN(GAMMA)
TERM2=RP(J)*TERM1
TERM3=RKAPAI*COS(GAMMA)
TERM4=TERM3*(RP(J)*COS(THETA)+I)
RSIDE1(I)=2.*COS(TERM4)*CEXP(-C1*TERM2)
10 CONTINUE
DO 180 J=1,KC
180 AOUT(J)=AOUT(J)/AMULT(J)
PFTURN
END

SUBROUTINE MMBSJN(Z,MM,BJ)
PFTAL BJ(MM)
D=1.0D-10
DO 200 N=1,MM
KK=N-1
BJ(N)=BESJ(Z,KK,D,IFR)
200 CONTINUE
RETURN
END

REAL FUNCTION BFSJ*8 (X, N, D, IFR)

```
IMPLICIT REAL*8(A-H,O-Z)
GENERIC
REAL*8 X, D
BFSJ = 0.
IF (N .GE. 0) GO TO 10
IEP = 1
RETURN
10 IF (X .GT. 0) GO TO 20
IEP = 2
RETURN
20 NTEST = 90+X/2
IF (X .LE. 15) NTEST = X*(10-X/3)+20
IF (N .LT. NTEST) GO TO 30
IEP = 4
RETURN
30 IEP = 0
N1 = N+1
BPREV = 0.0D0
MA = X+6
IF (X .GE. 5.) MA = 1.4*X+60./X
MB = N+INT(X)/4+2
MZERO = MAX0(MA, MB)
DO 50 M = MZERO, NTEST, 3
FM1 = 1.0D-28
FM = 0.0D0
ALPHA = 0.0D0
JT = 1
IF (M .EQ. M/2*2) JT = -1
M2 = M-2
DO 40 K = 1, M2
MK = M-K
BMK = 2.0D0*MF*FM1/X-FM
FM = FM1
FM1 = BMK
IF (MK-N .EQ. 1) BESJ = BMK
JT = -JT
S = 1+JT
40 ALPHA = ALPHA+RMK*S
BMK = 2.0D0*FM1/X-FM
IF (N .EQ. 0) BESJ = BMK
ALPHA = ALPHA+RMK
BFSJ = BESJ/ALPHA
C     IF (ABS(BESJ-BPREV) .LE. ABS(D*BFSJ)) RETURN
      IF (ABS(BESJ-BPREV) .LE. ABS(D*BESJ)) GO TO 55
50 BPREV = BESJ
IEP = 3
55 IF (ABS(BESJ) .LE. 10.0D-30) BFSJ = 0.0D0
      RETURN
END
SUBROUTINE PRINT(RKAPAI,GAMMA,DEPTH,CRACK,ITNP,
```

```

*          NPPRPT,KC,NSCAT,USCAT,FINAL,W0,WSCAT1,
*          WSCAT2,RSIDE1,AOUT,RP,THETAV,IPT1,IPT2,YPH,ISCAT)
COMPLEX FINAL(ITNP),WSCAT(ITNP),W0(ITNP),WSCAT1(NPPRPT),
*          WSCAT2(NPPRPT),FSIDE1(NPPRPT),AOUT(KC),WSDIFF
REAL THETAV(NPPRPT),RP(NPPRPT),YPH(ITNP)
INTEGER IPT1(NSCAT),IPT2(NSCAT)
PPINT 100,RKAPAL,GAMMA,DEPTHI,CRACK
PPINT 110
DO 10 I=1,ITNP
ARWSC=CABS(WSCAT(I))
ABUTOT=CABS(FINAL(I))
ABW0=CABS(W0(I))
PPINT 120,I,FINAL(I),ABUTOT,USCAT(I),ARWSC,W0(I),ABW0
10  CONTINUE
PRINT 130
DO 20 I=1,NPPRPT
ABUSC1=CABS(WSCAT1(I))
ABUSC2=CABS(WSCAT2(I))
PPINT 140,I,RP(I),THETAV(I),USCAT1(I),ABUSC1,USCAT2(I),ABUSC2
20  CONTINUE
PRINT 150
DO 30 I=1,NPPRPT
ABWSC=CABS(FSIDE1(I))
PRINT 160,I,RP(I),THETAV(I),FSIDE1(I),ABWSC
30  CONTINUE
PRINT 170
PRINT 180,AOUT
IF(ISCAT .EQ. 0)GO TO 222
PRINT 190
PRINT 200
DO 40 IS=1,NSCAT
I1=IPT1(IS)
I2=IPT2(IS)
WSDIFF=WSCAT(I1)-WSCAT(I2)
ABV=CABS(WSDIFF)
ABW1=ABV/(4.*CRACK*RKAPAL)
PPINT 210,I1,I2,YPH(I1),WSDIFF,ABV,ABW1
40  CONTINUE
222 CONTINUE
100 FORMAT('1'//2X,'RKAPAL=',G10.3,2X,'GAMMA=',G10.3,
.2X,'DEPTHI=',G10.3,2X,'CRACK=',G10.3,
.2X,'**BY MET'S METHOD----DFEP**')
110 FORMAT('-'/'-',2X,'NODE NO.',4X,10('*'),'TOTAL FIELD',
.9(*'),10X,8('*'),'SCATTERED FIELD',7('*'),9X,
.8('*'),'INCIDENCE FIELD',7('*')/
.14X,'RFTF',9X,'INTF',9X,'APTF',9X,'RFSE',9X,'IMSF',
.9X,'APSE',9X,'REIF',9X,'IMIF',9X,'ABIF'//)
120 FORMAT(' ',4X,I6,9G13.5)
130 FORMAT(' '//10X,'NODE NO.',28X,'SCATTERED FIELD',30X,
.'SCATTERED FIELD',//',16X,'R',10X,'THETA',12X,
.'PFAL',12X,'IMAG',12X,'ABSL',12X,'PFAL',12X,
.'IMAG',12X,'APSL',//)
140 FORMAT(' ',4X,I4,8G15.5)
150 FORMAT(' ',10X,'NODE NO.',28X,'INCIDENCE FIELD',//',16X,
.
```

```
'R',10X,'THETA',12X,'RREAL',12X,'IMAG',12X,'ABSL',//)
160 FORMAT(' ',4X,I4,5G15.5)
170 FORMAT(' ',2X,-----ACUT=COEFFICIENTS OF OUTER EXPANSION--'//)
180 FORMAT(' ',2X,8G16.6)
190 FORMAT(' '-'/-',25X,'*****DIFFERENCE OF SCATTERED FIELD*****'//)
200 FORMAT(' ','BETWEEN NODES',5X,'Y',8X,9('*'),'DIFFERENCE',9('*'),
.7X,
.'\DIFFERENCE\',5X,'DIFF BY 4KL'//)
210 FORMAT(' ',2X,2I5,2X,F9.5,2X,4G16.6)
      RETURN
      END
//GO.FT02F001 DD DSN=KCWONG.D1,NEUDATA,UNIT=SYSDA,
//                  DISP=(OLD,KEEP),VOL=SEP=WORK04
```